DOCTOR OF SCIENCES

Self-organised Aggregation in Swarms of Robots with Informed Robots

FIRAT, Ziya

Award date:
2023

Awarding institution:
University of Namur

Self-organised Aggregation in Swarms of Robots with Informed Robots

Author:
Ziya Firat

Promoteur:
Dr. Elio Tuci
Co-Promoteur:
Dr. Eliseo Ferrante

July 14, 2023

Word count: ten thousand and four

Abstract

Self-organised aggregation is a decision-making process ubiquitous in nature whereby agents gather all around the same area, without relying on global information, global communication, or any kind of centralised information or decision. In addition to being a widely studied behaviour in swarm robotics systems, it is also one of its most fundamental building blocks. Indeed, many problems in swarm robotics require the swarm to gather in order to develop more complex group response.

We introduced the concept of informed robots in the context of self-organised aggregation, and we studied how informed robots impact the aggregation dynamics. Informed robots are members of the swarm that have been informed a priori about the aggregation site to stop on, in an environment that offers multiple sites for aggregation. Apart from the preference on the site on which to aggregate, the behaviour of informed robots will be controlled by exactly the same mechanisms of non-informed robots. The roles of informed robots is to influence the aggregation dynamics, in a very indirect way, since none of the robots has any means to discriminate informed from non-informed robots.

In the first research contribution illustrated in chapter 4, We carry out our work with a series of simulation experiments on different scenarios represented by a circular arena containing two to four aggregation sites. In the simplest possible scenario, the arena is characterized by two aggregating areas colored with black and white. The objective of the swarm is to form a single aggregate on the black site. Only informed (knowledgeable) robots are programmed to avoid stopping in the white area. Both the black and white space are equally good resting places for all the other robots of the pack. In the experiment, we provide an analysis of cluster dynamics leading to the formation of a single cluster. Also, for each scenario, we analyze how the dynamics of the collection process depends on the proportion of informed robots. We also show what happens when no robot in the swarm is informed. The analysis of the model's parameters leads to a deeper understanding of the relationships between environmental features and agents' exploration strategies. We show how these relationships bear upon the emergence of a single aggregate and how they interfere by amplifying or by reducing the effects of informed robots on the group aggregation process.

In the second research contribution, illustrated in chapter 5, we discuss an analytical model which looks at the possibility to use the concept of informed individuals to allow the swarm to distribute on different aggregation sites according to relative proportions of different types of informed robots in the swarm. The analysis of the model shows that the designer capability to exploit informed individuals to control how the swarm aggregates depends on the environmental conditions. For intermediate values of the site carrying capacity, a small minority of informed individuals is able to guide the dynamics as desired by the designer. We also show that the larger the site carrying capacity the larger the total proportion of informed individuals required to lead the swarm to the desired distribution of individuals between the two sites.

The third research contribution illustrated in chapter 6, instead of focusing exclusively on the formation of a single aggregate, we discuss how to design a swarm of robots capable of generating aggregation dynamics that can correspond to a variety of final distributions of the robots to the available aggregation sites. We discuss the promising results of a set of simulations that systematically consider a variety of experimental conditions. The results with simulated robots are validate with physical kilobot robots.

Dedication and acknowledgements

First of all, I would like to thank my research advisor, Dr. Elio Tuci. It gave me the opportunity and supported me throughout my research years. Thank you for helping me achieve my goals in my remote work and home experiments during the pandemic. He inspired me a lot during my PhD. I would like to thank my supervisor, Dr. Eliseo Ferrante, who guided me in my doctoral study and supported me when I needed it. I am grateful for his help in preparing the necessary conditions and providing the robots in my experiments. Many thanks to Judhi Prasetyo and Raina Zakir from Middlesex University for their support in the use and modification of physical kilobot robots. They were very helpful in preparing and installing the arena and programmed IR LEDs that move the robots away from the arena walls. I would also like to thank Yannick Gillet for his analytical model studies in proving our work. Thanks also to Nicolas Cambier for his support. Special thanks to my wife Ela and my children Ahmet and Ali for the difficulties they faced as they were busy conducting this thesis with me. Many thanks to Ms Jinny Hayman for reviewing chapters 2,3 and 7 for spelling, grammar, punctuation and syntax errors, as well as general consistency and flow and use of English. Finally, I would like to thank my family and friends for their support and motivation. And here I would like to thank everyone whose names I forgot to write.

Author's declaration

I declare that the work in this dissertation was carried out in accordance with the requirements of the University's Regulations and Code of Practice for Research Degree Programmes and that it has not been submitted for any other academic award. Except where indicated by specific reference in the text, the work is the candidate's own work. Work done in collaboration with, or with the assistance of, others, is indicated as such. Any views expressed in the dissertation are those of the author.

SIGNED: ..... DATE: .....

TABLE OF CONTENTS

List of Tables

Table **Page**

List of Figures

Figure **Page**

CHAPTER 1

INTRODUCTION

Swarm robotics is a sub-domain of a larger research area dedicated to the design and control of multi-robot systems (Şahin 2004, Brambilla et al. 2013). Swarm robotics is characterised by the following distinctive elements: i) the use of distributed embodied control, that is, each robot has is own on-board control system in charge of determining the robot's behaviour; ii) local perception, that is, each robot can sense and communicate only within a given range using sensors and actuators mounted on its body; iii) the use of indirect communication: given that the robots of a swarm are "anonymous", any single agent can not selectively choose a specific message receiver, but rather communicate implicitly through modification of the environment in which they operate. The latter can be done by emitting sound or by generating other types of signal that are eventually detected by other agents.

One of the main building blocks in swarm robotics is collective decision-making; that is, the ability to make a collective decision without any centralised leadership, but only via local interaction and communication. Several types of collective behaviours can be seen as instances of collective decision making (see Valentini et al. 2017, 2016*a*), including collective motion where robots have to agree on a common direction of motion, and aggregation where robots have to agree on a common location in the environment (see Garnier et al. 2005, 2008*a*, Bayindir & Şahin 2009, Correll & Martinoli 2011, Gauci, Chen, Li, Dodd & Groß 2014). Indeed, aggregation is often a necessity for many swarm robotic systems as it is a prerequisite for other cooperative behaviours (Dorigo et al. 2004, Tuci et al. 2018).

In this chapter, we present the original contributions of this thesis and the corresponding scientific publications. The contents of this thesis are based upon a number of research articles that we published. In Section 1.1, we list these articles and highlight their contributions to the contents of this thesis. In Section 1.2, we conclude by describing how the chapters of this thesis are organized.

1.1 Original contributions and related publications

We explore the aggregation dynamics generated by the principle of attraction between individuals in a novel setting. We introduce the concept of "informed robots" which are robots that are a priori informed on which site they need to stop. Apart from the additional capacity to avoid stopping on undesired aggregation sites, informed robots behave exactly like any other robot in the swarm. As designers, we hypothesise that the effect of informed robots is to stir the aggregation dynamics towards a specific site chosen by the experimenter among those available to the robots. The effects of informed individuals on group dynamics has been recently investigated in biology to account for the motion of collective systems, such as birds and fishes. In a seminal study illustrated in (Couzin et al. 2005), the authors study collective decision making in the context of collective motion looking at what happens when *informed individuals*[1] are introduced. These special individuals have a preferred direction of motion and they bias the collective decision in that direction. The rest of the swarm does not have any preferred direction of motion, nor is able to recognise informed individuals. The authors show that the accuracy of the group motion towards the direction known by the informed agents increases asymptotically as the proportion of informed individuals increases. Moreover, the authors show that larger the group, the smaller the proportion of informed individuals needed to guide the group with a given accuracy.

In swarm robotics, the framework of informed individuals has been studied mainly in the context of collective motion (Celikkanat & Şahin 2010, Ferrante et al. 2012, 2014). Inspired by these works, we study the effect of informed individuals in the context of self-organised aggregation. Different from the aggregation studies mentioned above, and analogously to the studies performed within collective motion (Couzin et al. 2005), in this thesis we introduce informed robots in the context of self-organised aggregation, and we study how they impact the aggregation dynamics. The role of informed robots is to influence the aggregation dynamics in a very indirect way since none of the robots has any means to discriminate informed robots from non-informed robots.

- Firat Z., Ferrante E., Cambier N., Tuci E., "Self-organised aggregation in swarms of robots with informed robots", the 7^{th} International Conference on the Theory and Practice of Natural Computing (TPNC), Dublin, Ireland, D. Fagan, C. Martín-Vide, M. O'Neill, M.A. Vega-Rodríguez (Eds), Springer, pp 49-60, 2018 Firat et al. (2018)

- Firat Z., Ferrante E., Gillet Y., Tuci E., "On self-organised aggregation dynamics in swarms of robots with informed robots", Neural Computing and Applications, 32(17), 13825-13841, 10.1007/s00521-020-04791-0, 2020 Firat, Ferrante, Gillet & Tuci (2020).

[1] Informed individuals are also referred to as implicit leaders in (Couzin et al. 2005). The term "implicit" signifies that these individuals do not have the right, due to social status or kinship, to lead the group. Thus, they are not recognised as leaders by the group mates. Nevertheless, informed individuals behave as they were "leaders" by trying to influence the behaviour of the group by locally interacting with the group mates.

The first study listed above was presented at the international conference. The second study was published in an international journal. In the above listed papers, we have contributed to the wider agenda of studying the role of implicit leader in the context of collective decision making. First, we have focused on self-organised aggregation in the simplest possible scenario whereby two symmetrical but differently coloured sites are present. We considered a swarm of robots divided in two sets: informed robots, that possess extra information on which site the swarm has to aggregate, and non-informed robots which do not possess this extra information. In the first study, we run experiments using the ARGoS simulator in which we varied the proportion of informed robots from 0% to 100%. Our results show that, in absence of informed robots, robots can either split between the two sites, or break the symmetry randomly by aggregating in one of them. As soon as informed robots are introduced, the symmetry is instead immediately broken and increasingly more robots aggregate on the black site. When at least 50% of the robots are informed, the entire swarm aggregates on the black site, for all swarm sizes we have considered. We have also shown that the speed and accuracy of convergence is also strongly affected by the proportion of informed robots.

In the second paper, we have focused on self-organised aggregation in scenarios that feature two types of aggregation sites: a site coloured in black and a site coloured in white. The circular arena's floor where the robots operate is coloured in grey. We studied three different scenarios: two symmetrical scenarios, in which either two or four aggregation sites are available in the environment, and an asymmetrical scenario in which three aggregation sites are available. In the symmetric scenario, the two types of aggregation site (the black and the white) are equally represented. In the asymmetric scenario, one type of aggregation site (the white) is twice as much represented than the other type of site. In all scenarios, the robots are required to form a single aggregate, on a black site. We considered a swarm of robots divided in two sets: informed robots, that possess extra information on which site the swarm has to aggregate. Therefore, they selectively avoid to stop on any white site. Non-informed robots do not possess this extra information. Therefore, they are equally likely to stop on a white and on a black site according to the mechanisms of the finite state machine that controls their behaviour. The objective of this study is to look at whether and eventually which proportion of informed robots is required to direct the aggregation process toward a pre-defined type of site (i.e., the black) among those available in the environment.

- Gillet Y., Ferrante E., Firat Z., Tuci E., "Guiding aggregation dynamics in a swarm of agents via informed individuals: an analytical study", Proceedings of the 2019 Conference on Artificial Life, Newcastle upon Tyne, UK, MIT proceedings, 31, 590-597, 2019 Gillet et al. (2019)

In the above-listed paper presented at an international conference, we introduced a mathematical ordinary differential equations model that is inspired by the one proposed by Amé et al.

(2006). We performed an analytical study of self-organised aggregation in presence of two distinctive aggregation sites, one black and one white. We consider a swarm of agents characterised by the presence of informed individuals, that is agents that are able to recognise the colour and therefore discriminate between the two sites. Our model considers sub-populations of informed individuals, distinguishing between those that prefer the white and those that prefer the black site. Each type of informed individuals never rests on the non-preferred site. From an engineering perspective, when designing self-organised systems engaged in aggregation tasks, we would like to use informed individuals to guide the self-organised aggregation dynamics.

- Firat Z., Ferrante E., Zakir R., Prasetyo J., Tuci E., Group-size Regulation in Self-organised Aggregation via Informed Individuals in Robot Swarms, Proc of the 12th Int. Conf. on Swarm Intelligence (ANTS), Springer LNCS, Barcelona, Spain, In Press, 2020.

The above article was published at an international conference. In this paper, we have shown that the aggregation dynamics of a swarm of robots can be controlled using the system heterogeneity. In this self-organised aggregation scenario, with a swarm of robots required to operate in an arena with two aggregation sites, the system heterogeneity is represented by informed robots; that is, agents that selectively avoid a type of aggregation site (i.e., the black/white site) to systematically rest on the other type of site (i.e., the white/black site). The results of our simulations indicate that with a small pro-portion of informed robots a designer can effectively control the way in which an entire swarm distribute on the two aggregation sites. This is because the size of the robots' aggregates at each site tends to match the relative proportion of the two different types of informed robots characterising the swarm. We have also performed few preliminary tests with physical robots to test the effectiveness of the PFSM discussed.

1.2 Dissertation outline

The rest of the dissertation is organized as follows.

In Chapter 2, We present the background of this thesis. We present the concept of swarm robotics and especially design methods and analysis methods used in self-organized aggregation and other swarm robotics studies.

In Chapter 3, we describe swarm robotics state of the art and discuss literature on collective behaviours. We also introduce the problem of self organized aggregatio.

In Chapter 4, we illustrate the first scientific contribution of this thesis. We describes the self-organised aggregation method used. We present the experimental setup and we illustrate how we study the effect of informed robots. We presents the results of the three experiments with simulated robots. We introduced a mathematical ordinary differential equations model. We performed an analytical study of self-organised aggregation in presence of two distinctive aggregation sites, one black and one white. Finally, we discuss the significance of our results for the swarm robotics community, and we point to interesting future directions of work.

In Chapter 5, we introduce a mathematical ordinary differential equations model that is inspired by the one proposed by Amé et al. (2006). We performed an analytical study of self-organised aggregation in presence of two distinctive aggregation sites, one black and one white

In Chapter 6, we show that the aggregation dynamics of a swarm of robots can be controlled using the system heterogeneity. The results of our simulations indicate that with a small proportion of informed robots a designer can effectively control the way in which an entire swarm distribute on the two aggregation sites.

In Chapter 7, concludes the dissertation with a summary of the main contributions and with several proposals for future research directions.

Finally, in Appendix A, we describe the simulated and physical robot platforms used in this thesis.

CHAPTER 2

METHODOLOGY IN SWARM ROBOTICS

In this chapter, we introduce the context in which the research described in this thesis has been carried out. In Section 2.1, we briefly introduce the concepts of swarm robotics in general and describe the research scope of robotic systems. In Section 2.2, we present the literature on design methods and classify the available methods for designing robot swarms by dividing them into manual design methods and automatic design methods. In Section 2.3, we discuss and classify the analytical literature on two different levels: the microscopic level and the macroscopic level. We conclude with an overview of how analysis with physical robots is conducted. Finally, in section 2.4, we introduce the concepts of homogeneous and heterogeneous swarms and illustrate some of the most relevant research work carried out using these two different types of artificial swarms.

2.1 Swarm robotics

Swarm robotics has been defined as "the study of how a large number of relatively simple physically embodied agents can be designed such that a desired collective behaviour emerges from the local interactions among the agents and between the agents and the environment" (Sahin et al. 2008). Swarm robotics studies the design of collective behaviors in groups of autonomous robots (see Brambilla et al. 2013). It takes inspiration from studies of social insects and other social animals in which simple individuals are able to exhibit superior collective intelligence when working in groups (Bonabeau, Dorigo, Marco, Theraulaz et al. 1999). The overall goal is to design systems that are robust, scalable, and flexible like their natural counterparts (Brambilla et al. 2013).

*"**Robustness** is the ability to cope with the loss of individuals. In social animals, robustness is promoted by redundancy and the absence of a leader. **Scalability** is the ability to perform*

well with different group sizes. The introduction or removal of individuals does not result in a drastic change of the performance of a swarm. In social animals, scalability is promoted by local sensing and communication. ***Flexibility*** *is the ability to cope with a broad spectrum of different environments and tasks. In social animals, flexibility is promoted by redundancy, simplicity of the behaviors and mechanisms such as task allocation"* (Brambilla et al. 2013).

To achieve robustness, scalability, and flexibility, swarm robotics relies on the application of the following principles: i) the absence of external infrastructure and a reliance on on-board sensing and computation only; ii) the use of local perception and communication (that is, each robot can sense and communicate only within a given range via on-board devices); and iii) the process of self-organization, from microscopic behaviors and individual interactions to macroscopic complex collective behaviors.

Research in swarm robotics generally focuses on the design of individual control mechanisms underpinning a desired collective response, which emerges in a self-organized way from the interactions of system components (i.e., the robots and their environment, see Brambilla et al. 2013). Examples of such collective responses are area coverage (Hauert et al. 2008), chain formation (Sperati et al. 2011*a*), collective decision-making and task partitioning (Montes de Oca et al. 2011, Pini et al. 2011, Tuci & Rabérin 2015), cooperative transport (Alkilabi et al. 2017*b*), and collective motion (Ferrante et al. 2014).

Swarm robotics stems from swarm intelligence, which is a discipline that studies the processes used by simple (natural and artificial) individuals to self-organize and to produce complex and fascinating behaviors (Bonabeau, Dorigo & Theraulaz 1999, Dorigo et al. 2007). Social insects make decisions using a process known as collective decision making in a decentralized way. A collective decision, sometimes called a consensus decision, results from a process in which all members of a group choose the same option from two or more alternatives. Well-known examples of collective decisions are decisions made by bee swarms when choosing the best nest location from among several candidates (Seeley 2010) and by ant colonies when choosing the shortest path from their nest to a food source (Goss et al. 1989).

Collective decision making is the ability to make a collective decision via local interaction and communication only (Valentini et al. 2017). It is an important collective response which has been extensively studied in swarm robotics. Collective decision making can take several forms, and it can be studied either explicitly (Valentini et al. 2017, 2016*a*) or implicitly in other collective behaviors such as collective motion (i.e., decisions on a common direction of motion) and aggregation (i.e., decisions on a common location for gathering in the environment). Two factors that can synergistically or antagonistically influence collective decision making process are asymmetries in the environment, or the active modulation performed by all or some of the swarm members (Valentini et al. 2017). In a seminal study on collective decision making, Couzin et al. (2005) studied collective motion models in the presence of so-called *implicit leaders* or *informed individuals*, who direct the collective action in the desired direction. The rest of the

swarm does not possess a preferred direction of motion, nor is it able to recognize informed individuals. The main results of this study are that even a minority of informed individuals is able to guide the swarm in the desired direction, and that larger groups can obtain equal levels of accuracy with a smaller proportion of informed individuals.

As in the study of animal groups (Couzin et al. 2005), in swarm robotics the framework of informed individuals has been studied mainly in the context of collective motion (Celikkanat & Şahin 2010, Ferrante et al. 2012, 2014). Recently, this framework has been ported to another collective behavior, namely self-organized aggregation (Firat et al. 2018, Firat, Ferrante, Gillet & Tuci 2020, Gillet et al. 2019). Self-organized aggregation is an inherently ubiquitous decision making process (Camazine 2003). In a self-organized aggregation process, agents gather around the same area without relying on global information, global communication, or any centralized information or decision. Self-organized aggregation (Correll & Martinoli 2011, Gauci, Chen, Li, Dodd & Groß 2014, Bayindir & Şahin 2009) is inspired by the biological study of cockroaches, where probabilistic models have been proposed (Deneubourg et al. 2002, Jeanson et al. 2005*a*). In those biological studies, Deneubourg et al. (2002) investigated how the probability of an ant entering or leaving a shelter depends on the size of the shelter, and they found a function to modulate that work. In addition, by examining cockroach clumping behavior, they calculated the probabilities of joining and leaving, modeling the functions by observing two different shelter visits. Their models have been adapted and implemented on distributed robotic systems (Garnier et al. 2005, 2008*a*, Gauci, Chen, Li, Dodd & Groß 2014). Besides being a further example of collective decision making, aggregation is a basic building block for other cooperative behaviors (Dorigo et al. 2004, Tuci et al. 2018). Self-organized aggregation can take place in environments that are completely homogeneous (except for boundaries and potential obstacles) where no perceivable special locations, called sites or shelters, are present, and thus robots are required to aggregate anywhere (Cambier et al. 2018*b*). Alternatively, as is the case in the current study, the sites where robots are required to aggregate can be specific areas in the environment that can be clearly perceived by all or some of the robots (Garnier et al. 2009*a*, Campo et al. 2010*b*).

2.2 Control design methods in swarm robotics

In this section, we categorize existing methods for designing robot swarms into manual design methods and automated design methods. Manual design methods are used to design and develop robot swarms based on human design, creativity, and expertise. Automated design methods refer to computationally intensive processes where an algorithm automatically develops the desired robot swarm. Below, we discuss manual design methods and automated design methods, explaining the general principles and their relative advantages and disadvantages.

2.2.1 Manual design methods

Manual design methods are a set of control structures in which a swarm designer directly generates the individual behavioral rules that specify which actions each robot has to make in response to specific sensory stimulation. The most commonly used manually designed control structure is the finite state machine, that is, a system made of simple behavioral building blocks, called states. Each state refers to a specific action such as “random walk”, “obstacle avoidance”. The set of all states represents the behavioral repertoire of the robot. The finite state machine also consists of a series of rules that regulate the transition from one state to another. These transitions can be triggered by external events, such as the presence of an obstacle that induces the robot to switch from a random walk state to an obstacle avoidance state, or by internal events such as the robot’s proprioception of its battery level that may induce it to switch from a random walk state to a “move back to the nest” state.

Another common manual design control structure is the probabilistic finite state machine (PFSM) (Minsky 1967). With a PFSM, the transitions between states, such as the transition between probability of leaving and probability of joining a site, are governed by probabilistic rules (Firat et al. 2018).In our work, each robot is controlled by a PFSM and we use three states: random walk ($\mathscr{RW}$), stay ($\mathscr{S}$), and leave ($\mathscr{L}$). This model was inspired by social insects such as ants (Bonabeau et al. 1997) and cockroaches (Amé et al. 2006). PFSMs have been used to perform collective behaviors including chain formation (Nouyan et al. 2008), task-allocation (Labella et al. 2006), and aggregation (Soysal & Sahin 2005). In this study, aggregation behavior is achieved with a PFSM that consists of four basic states/behaviors: obstacle avoidance, approach, repel, and wait. Schmickl et al. (2006) conducted a study inspired by the trophallactic interactions of honey bees (The mouth-to-mouth transfer of liquid food between adult animals), called collective perception, which they compared with the other used technical solution which is ‘hop-count’-based strategies in swarm robotics. Hop-count is smaller than or equal its own hop-count navigates towards a neighbor. If more than one neighbor has the same low hop-count, the robot calculates its direction by averaging the vectors towards these neighbors (Payton et al. 2001). They also worked on a bio-inspired approach that had to demonstrate its advantages in a volatile environment and developed a PFSM with three states: random walk, approach, and wait. There are several advantages to using PFSMs: PFSMs are easy to read, understand, and analyze; actions and conditions can be easily combined in a structured way; the modularity of PFSMs encourages reuse of improved behaviors; and PFSMs can be used recursively, generating behaviors that consist of sub-behaviors.

A different manual design method is virtual physics, in which each robot is considered a virtual particle, and other robots or the environment are considered interacting virtual forces. Khatib (1986) used virtual forces to avoid obstacles with real-time robot operations. Collision avoidance can be effectively distributed between different control levels, allowing real-time robot operations in a complex environment. Khatib (1986) applied this general obstacle avoidance problem to the

robot arm mechanism and used visual sensing for real-time collision avoidance demonstrations on moving obstacles. Reif & Wang (1999) defined artificial force laws between pairs of robot groups. They presented a preliminary study on the application of potential fields to distributed autonomous multi-robot control. They developed a method called social potential fields, using the reverse force laws by combining both attraction and repulsion between pairs of robots or groups of robots. The force laws can be different and reflect "social relations" between robots. The motion of a single robot is controlled by the resulting artificial force exerted by other robots and other components of the system. With computer simulations, they showed that the method could yield interesting and useful behaviors among robots. The virtual physics-based method used different collective behaviors such as pattern formation. Spears et al. (2004) introduced the framework of "physicomimetics" that established scientific principles and was motivated by natural laws of physics. They presented a general artificial physics framework for distributed control of vehicle swarms, based on Newtonian physics and the natural laws approach of distributed physics. The framework has been implemented to create a variety of both static and dynamic multi-agent entities and behaviors. Theoretical analyses of system phase transition and system potential energy have been provided, facilitating deeper system understanding and predictability analysis. Maxim et al. (2009) developed a novel chain formation algorithm that is rooted in physics, with the aim of making the virtual cable self-organize and repair itself when the line of sight between the robots is lost. There are also studies on collective exploration conducted by Howard et al. (2002) and on coordinated motion conducted by Reynolds (1987).

An alternative manual design method proposed by Bachrach et al. (2010) is the Proto spatial computing language. Swarm behaviors written in Proto can be built simply to generate robustness and scalable behaviors from the system components. Beal (2004) introduced amorphous computing, which addresses the problem of controlling millions of spatially distributed unreliable devices that communicate only with close neighbors. Beal (2004) developed a system that would compile in a high-level description language for desired global behaviors and developed code that runs the desired global behavior locally. They also programmed it in amorphous media language, where the system could cover the entire environment with a single connected communication network. This so-called amorphous media language is an example of how behavior can be programmed using amorphous media abstraction. Berman et al. (2009) developed a stochastic optimization method for design of task allocation behavior. They explored this approach in ant-inspired behaviors that caused the robots to converge to the better of the two sites, or to split between the two sites at a certain rate. Using several new optimization methods, they focused on optimizing the speed at which robots switched between tasks for rapid convergence to the desired allocation. Hamann & Wörn (2008) used statistical Langevin and Fokker-Planck equations in their studies of collective swarm behavior.

2.2.2 Automatic design methods

Automated design methods automatically generate robot behaviors and evaluate the performance of a robot's behavior at the individual and swarm levels. Evolutionary robotics is a very powerful approach to designing swarms of robots that solves the problem of collective behavior. It uses a combination of evolutionary computation techniques to find the best set of parameters for the robot/s control system, and is inspired by Darwinian principles of natural selection based on the concepts of genetic inheritance, genetic variability, and random mutation. Artificial evolution explores the space of parameters randomly until the best solution is found (see Holland et al. 1992, Goldberg & Holland 1988). Very frequently, evolutionary computation is used to design artificial neural network types of robot controllers. Evolutionary robotics consists of a combination of evolutionary computing and artificial neural networks. Initially, a random population of genotypes is generated. In evolutionary computing methods, a genotype is usually a string of bits or real numbers that encodes a potential solution to a given problem. In evolutionary robotics, the genotype specifies the characteristics of a robotic system that should be able to display a desired behavior (Trianni & Nolfi 2011). Each individual is then evaluated according to its performance or "fitness" of the genotype, and the fitness score is used to select genotypes. The basic principle of the selection strategy is that the better the individual, the higher its chance of becoming a parent. This is the process that determines which solutions are to be preserved and which deserve to be destroyed. Selection mechanisms include roulette wheel selection, rank selection, tournament selection, steady state selection, Boltzmann selection, and elitism selection. The roulette wheel is a relatively simple selection technique in which all chromosomes in the population are placed according to their fitness values, and a roulette wheel segment is assigned that is proportional to the size of the individual fitness. The virtual roulette wheel is rotated, and the individual it is standing on is selected. This process is repeated until the desired number of individuals has been selected. In this process, individuals with high fitness are more likely to be selected for the next generation. In the proportional roulette wheel technique, individuals are selected with a probability directly proportional to their fitness value. Rank selection sorts the population from the best fitness values to the worst fitness values. Each chromosome has a probability to be selected that is generated based on its ranking. In other words, each individual (or chromosome) in the population is assigned a numerical ranking based on fitness, and selection is based on that ranking rather than on differences in fitness. Tournament selection runs tournaments among individuals chosen at random, generating selection pressure by adjusting the tournament size. The winner of the tournament is the individual with the highest fitness of all the tournament contenders and is added to the mating pool. Steady state selection is used to ensure that most of the chromosomes survive into future generations. Some good chromosomes are used in each new offspring formation. The defective chromosomes are removed, and new offspring take their place. In this way, the rest of the population survives until the next generation. In each generation, several good chromosomes with high fitness are selected to produce a new offspring. Then some

bad chromosomes with low fitness are removed and new offspring are placed in their place. The rest of the population survives to the next generation. Boltzmann selection controls the ever-changing temperature selection rate according to a preset program. When the temperature is high, the selection pressure is low. As the temperature is lowered, it gradually increases the selection pressure, thus allowing the genetic algorithm to move closer to the best part of the search space while maintaining an appropriate degree of diversity.Elitism is to arrange the chromosomes in descending order of fitness values and then apply selection for both chromosomes in the arranged set. This means that there is no chance of applying Genetic Algorithm between weak and strong chromosomes. Elitism is a type of selection in which the best individual is passed on to the next generation without any change. The purpose of this selection is to arrange the chromosomes in descending order according to their fitness values and then to apply selection with both chromosomes in the edited set (Yadav & Sohal 2017).

Genotypes produce the next generation of individuals by mutation or crossover. The crossover operator functions primarily in the search for information accessible through the search field, which inadvertently improves the behavior of genetic algorithms. Mutation is a secondary operator that functions to change the genes of the offspring. The search algorithm is based on the principle that some or all of the genetic changes applied to the selected genotypes will produce genotypes of higher fitness and will become increasingly effective in generating the mechanisms needed by the robots to achieve the desired goal.

Evolutionary robotics methods are especially useful in swarm robotics, where they can be applied to control design for autonomous robots. Evolutionary swarm robotics is a computationally expensive process. Therefore, due to the time required and the risk of damaging the robots, evolution is run in simulation environments rather than directly on physical robots. Some examples of evolutionary robotics techniques applied to group behaviors have been published by Quinn et al. (2003), who studied the evolution of coordinated motion in a group of three simulated and physical robots. Using only four infrared proximity sensors, they allowed the robots to move as far as possible from their original position without losing contact with each other. Dorigo et al. (2004) developed an evolutionary swarm robotics technique with a self-organized aggregation task. The robots started in an arena in random locations and at the end of the experiment were all gathered in one place. Alkilabi et al. (2018) developed a study in which a certain number of robots were required to push a heavy enough cuboid object from its starting position toward a nest area.

Reinforcement learning is a method that select the behavior of agents and how they interact with the environment using a reward function. This learning strategy is based on so-called rewards and punishments. This interaction measures the performance of the robot's individual behaviors by receiving positive and negative feedback from the environment (Wolpert & Tumer 1999). Q-learning and temporal difference learning are two common reinforcement learning methods. Q-learning learns the usefulness of performing actions in situations, whereas temporal

difference learning learns the benefit of being in situations themselves. Reinforcement learning methods are inspired by dynamic programming concepts and define formulas for updating expected utilities and using them for state space exploration. Hüttenrauch et al. (2017) investigated deep reinforcement leaning with deep Q-learning techniques. They showed how global state information can be used with a Q-learning function, with actors basing their decisions on locally perceived information only. Deep reinforcement learning is a combination of deep learning with reinforcement learning Mnih et al. (2015). It became a normative approach to artificial intelligence and has received a lot of attention from the research community.

Other automatic design methods that are different than evolutionary robotics or reinforcement learning have been developed by Li et al. (2004). Their work developed stick-pull experiments to measure specialization in collaborative swarm systems. Specialization is a concept that includes both diversity and adaptation. Ferrante, Duéñez-Guzmán, Turgut & Wenseleers (2013) proposed a novel automated design method on grammatical evolution (GESwarm) for collective behaviors in foraging case studies. Francesca et al. (2014) investigated a new approach in a PFSM automatically generated by an optimization algorithm.

2.3 Control design models in swarm robotics

In this section, we summarize the main available control design models at the individual and collective levels. At the individual level, the *microscopic model* includes the characteristics of single individuals and the interactions between them. At the collective level, the *macroscopic model* includes the characteristics of the swarm as a whole. The development of these models to analyze swarms of robots at both levels of separation is a topic that requires further research. Modeling the interaction of microscopic and macroscopic is very difficult due to the nature of self-organizing systems. Below, we describe and discuss *microscopic* and *macroscopic* models.

2.3.1 Microscopic models

Microscopic models are computationally intense computer simulations in which the physical properties of the robots and of the environment are modeled in a relatively accurate way. Microscopic modeling focuses on mathematically modeling each robot and its interactions. In this method, the behavior of robots is defined as states and robot–robot and robot–environment transitions. Microscopic models enable very detailed investigation of a swarm. However, to define the behavior of a swarm, it is necessary to repeat the definition of a single robot according to the number of robots in the swarm. This results in a model with many components that are computationally difficult to handle. Therefore, microscopic models are analyzed using a computer simulator (Brambilla et al. 2013).

The probabilistic microscopic model is widely used in swarm robotics. The probability of each state transition between robot actions is calculated based on the time limit of the model at each

model step by systematic experiments performed on robots (Bayindir & Şahin 2007). Martinoli & Easton (2003) and Martinoli et al. (2004) performed a PFSM and demonstrated a microscopic model showing that transitions depend on the probabilities of one robot interacting with another robot and the environment. In chapter 4, we performed experimental results with more control over the microscopic self-organizing aggregation model, showing that informed individuals drive dynamics in a wide range of environmental conditions.

2.3.2 Macroscopic models

Macroscopic models are computationally light analytical tools such as ordinary and stochastic differential equations, chemical reaction networks, and Langevin and Fokker–Planck equations. Macroscopic models are generally used to explore the parameter space to get an initial idea of the system dynamics without considering the physics of the swarm-environment model. We used a macroscopic model in our analysis of the aggregation dynamics (see chapter 5). The results of the macro model were used to develop micro-models in which the "macro" dynamics of mathematical models are reproduced by designing low-level individual control and interaction mechanisms that guide simulated and physical robots.

Macroscopic models are the most common model used for the analysis of robot swarms. This system behavior is defined with difference equations such as ordinary differential equations (ODE) which are used to define the time evolution of the behavior of the robot swarm. Amé et al. (2006) studied a mathematical ODE model, and in Gillet et al. (2019), we drew on their model for our PFSM work. Rate and differential equations are a very powerful technique for analyzing a swarm of robots

In one of the other macroscopic models, Hamann & Wörn (2008) adapted Langevin and Fokker–Planck equations from the statistical physics literature to the swarm robotics community.. In some studies, classical control and stability theory has been used to provide the characteristics of the swarm. Liu et al. (2003) and Gazi & Passino (2005) developed a mathematical model for an m-dimensional stability analysis with a fixed communication topology and a one-dimensional discrete-time asynchronous swarm. Soysal & Şahin (2006) also modeled the final aggregate distributions predicted by the macroscopic model.

2.4 Characteristic approaches in swarm robotics

This section provides different characterization of swarm robotics system approaches. It divides the scope of current multi-robot studies into two parts: homogeneous groups of robots (where robots share the same control algorithm, including the same threshold value) and heterogeneous groups of robots (in which each robot is assigned a different controller).

2.4.1 Homogeneous Swarms

A homogeneous swarm uses the same control software, and all jobs are the same as for other robots and can be interchangeable; only the robot's historical interaction with the environment can lead to specialized behaviors (Dorigo et al. 2021). Jeanson & Weidenmüller (2014) studied individuals in a natural colony to understand how individual behavior changes physically and behaviorally and how inter-individual variability is modulated to take advantage of division of labor, homeostasis, and colony fitness in social insects.

Wang & Rubenstein (2020) presented a distributed algorithm in which all robots move to the target location and can shape the desired image quickly and without collision, executed on a group of up to 1024 simulated robots and a swarm of 100 physical robots. Berman et al. (2009) worked on a scalable approach to dynamically allocate a homogeneous swarm of robots to multiple tasks that can be optimized for rapid convergence to a target distribution subject to a constraint on idle passes in equilibrium. Kalantar & Zimmer (2007) examined large underwater autonomous robot formations to explore the ocean surface, dividing the control and coordination strategy into two non-overlapping clusters, namely the boundary and the interior. This decision making is based entirely on local knowledge of individual robots. Wang & Rubenstein (2021) tried to verify position estimates of homogeneous robots obtained with the proposed decentralized algorithm, using physical and simulated experiments with algorithms that allowed them to align according to the patterns designed.

Heterogeneous and homogeneous swarm differences are sometimes difficult to define. For example, a swarm may be homogeneous at time zero but become heterogeneous over time. This is usually what happens in robots controlled by a dynamic neural network or in a probabilistic control where individual probabilities can change with robot experience. (Ampatzis et al. 2009) presented the results of an evolutionary methodology for the design of control strategies for self-assembled robots. The control method they proposed for the physical connection of two homogeneous robots is the distribution of roles between gripper (the robot that grips) and grippee (the robot that receives the grip). However, behavioral heterogeneity emerges with the interaction of robots.

2.4.2 Heterogeneous Swarms

The idea of heterogeneity in a swarm is that the behavior of swarm members has predetermined roles. Heterogeneity is considered essential for giving these collectives behavioral flexibility, adaptability to new circumstances, and resilience to external disturbances. Honey bees provide an example (see Seeley 1982, for example): the fact that a bee undertakes different tasks at different times in its life can be interpreted as a form of heterogeneous behavior.

Dorigo et al. (2013) developed the Swarmanoid project, which uses the heterogeneity and complementary of robot types to perform complex tasks. In the project, three foot-bot robots are mounted around a hand-bot robot, and they are used for collective transport. An eye-bot attached

to the ceiling has a view of the environment and can transmit necessary information about the environment to the robots.

Kengyel et al. (2015) investigated heterogeneous behaviors in swarms of agents, predefining static roles in a specific part of a swarm. Heterogeneous swarms outperformed homogeneous swarms in the predetermined behavior for the selected aggregation scenario. The selection of behaviors was inspired by results from biological experiments with juvenile bees. In our own work, we have studied heterogeneous swarm behaviors with a small proportion of informed robots, enabling a designer to effectively control the entire swarm distributed on the two aggregation sites (Firat, Ferrante, Zakir, Prasetyo & Tuci 2020). Pinciroli & Beltrame (2016) presented a new programming language designed for heterogeneous robot swarms. They applied a mixed paradigm for bottom-up and top-down approaches in robot swarms, describing a compositional and predictable approach to improving and implementing a general language that can express the most common swarm behaviors. Prasetyo et al. (2019) studied the best-of-n problem in a dynamic environment where two option properties can change abruptly over time. They used two adaptation mechanisms to deal with dynamic site qualities: stubborn agents, who do not change their opinion, and spontaneous changers, who are likely to change their opinion at random.

O'Grady et al. (2009) adapted the cockroach collection model by dynamic application of control group size regulation. They demonstrated a new self-organized cooperative operation between flying and ground-based robots. Their system was implemented in a simulator system and represented in a mathematical analysis. Garnier et al. (2009*b*) indicated self-organized aggregation behavior in simulated heterogeneous environment robotic experiments with two aggregation sites of the *Blattella germanica cockroach*. They also demonstrated self-organized processing used as an aggregation site selection mechanism for groups of autonomous mini-robots.

CHAPTER 3

STATE OF THE ART

In this chapter, in Section 3.1, we discuss the literature on collective behaviors, concluding with a discussion of the current limits of swarm robotics. In Section 3.2, we introduce the literature on self-organizing aggregation in collective behavior, in which a plethora of studies have been carried out on biological systems and a wide array of swarms of robots have been implemented.

3.1 Collective behaviors

Research in swarm robotics generally focuses on the design of individual control mechanisms underpinning a desired collective response which emerges in a self-organized way from the interactions of system components (i.e., the robots and their environment) (Brambilla et al. 2013, Schranz et al. n.d., Hamann 2018). Examples of such collective responses are area coverage (Hauert et al. 2008), chain formation (Sperati et al. 2011*a*), collective decision-making and task partitioning (Montes de Oca et al. 2011, Pini et al. 2011, Tuci & Rabérin 2015), cooperative transport (Alkilabi et al. 2017*b*), aggregation (Correll & Martinoli 2011, Gauci, Chen, Li, Dodd & Groß 2014, Bayindir & Şahin 2009), and collective motion (Ferrante et al. 2012). In addition, Schranz et al. (n.d.) worked to motivate future research and engineering activities by providing a comprehensive list of available platforms, projects, and products as a starting point for applied research in swarm robotics. They collected, categorized, and displayed varies types of spatial organization, navigation, and decision making (Hamann 2018).

Collective behaviors are categorized as spatial organization (aggregation, pattern formation, chain formation, object cluster and morphogenesis), navigation (collective exploration, coordinated motion, collective transport), collective decision making (consensus achievement, task allocation), and other. In this section, we present a review of the main collective behaviors studied in the

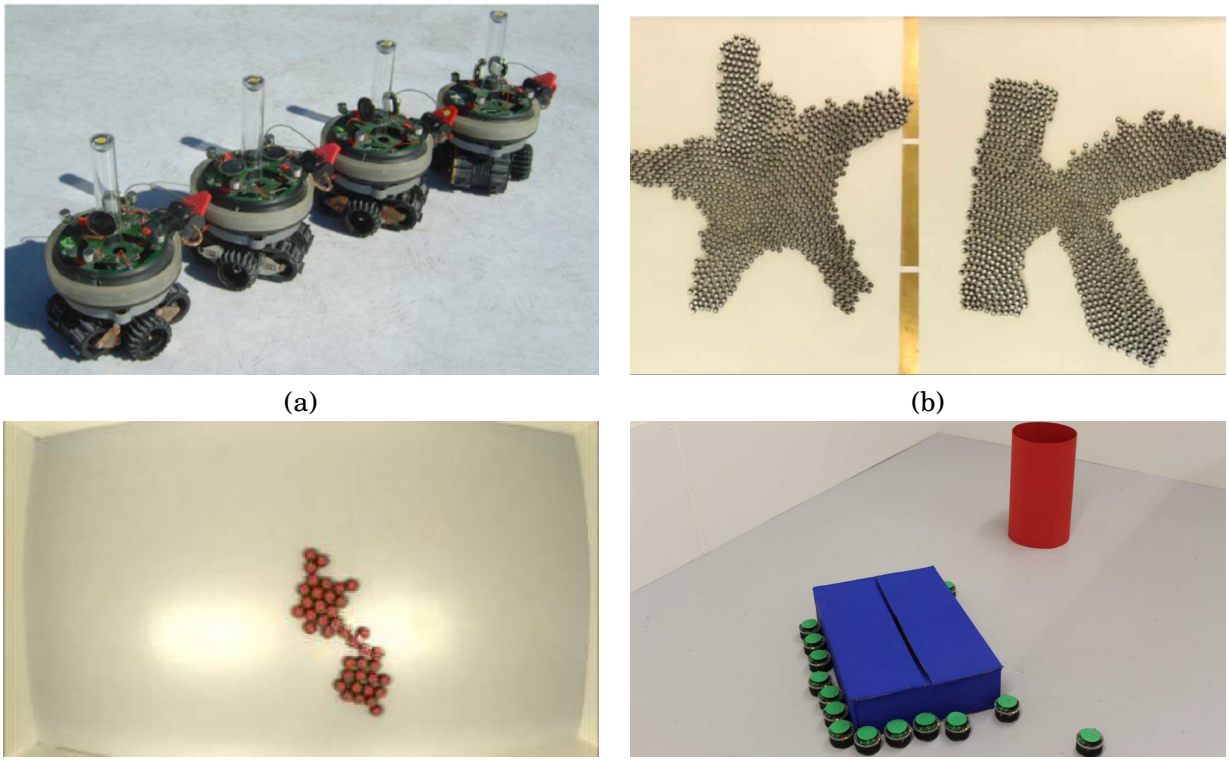

(a) (b)

(c) (d)

Figure 3.1: Examples of collective behaviors of social animals. (a) A chain; (b) a patter; (c) an example of aggregation; (d) example of object transport. Sources: (a) CC BY - Kasi Metcalfe (b) CC BY - Alan Duncan (c) CC BY - Melvin Gauci (d) CC BY - Melvin Gauci

swarm robotics literature. These collective behaviors are basic swarm behaviors that could be combined to tackle complex real-world applications such as foraging or construction.

Pattern formation

The pattern formation task involves assigning the robots to target positions that define the final desired pattern, as well as controlling the robots to build the pattern. Robots usually need to keep a specific distance with local process and interactions in order to create a desired pattern. Pattern formation was inspired by animal fur as a molecularly realistic model for chromatic patterns (Meinhardt 1982) and by the effects of crystalline anisotropy studied by (Langer 1980). Coppola et al. (2019) proposed a method to generate a local behavior that allows the robots to self-organize into a desired global pattern despite their individual limitations. The purpose of pattern making has been a topic of significant interest in many applications, including aerial robots (Achtelik et al. 2012, Saska et al. 2016), underwater robots robots (Joordens & Jamshidi 2010), and satellites (Engelen et al. 2011, Verhoeven et al. 2011). The behavior should also ensure that collision paths are avoided for safety reasons, and that the swarm remains consistent and does not split into multiple groups.

Chain formation

Chaining behavior is where robots position themselves to connect two points. Chain patterns can be used for passing a corridor in a coordinated way or as a guide for navigation, and chain formation behaviors are found in foraging ants. The behaviors of Argentine ants (Linepithema humile) were studied and modeled by (Deneubourg et al. 1990) who constructed foraging trails between two points that are marked continually and explored collectively. Nouyan et al. (2008) developed a chain formation behavior in a sensor-based simulation in which robots used two exchangeable roles: explorer and chain member. In explorer state, robots search other chain members; when they find the end of the chain, the robots change to (and remain in) chain member state. Robot chains can be achieved in many ways, such as PFSMs, virtual physics-based design, and artificial evolution. Nouyan et al. (2008) developed a study based on PFSMs, Maxim et al. (2009) used virtual physics-based design, and Sperati et al. (2011*b*) used artificial evolution to provide a chain formation behavior. Robot formations are spawned by friendly chains and can handle smooth turns, but not sharp turns.

Self-assembling and Morphogenesis

Self-assembly is physically interconnected and is used to navigate rough terrain or to increase the pulling power of the robots. Self-assembly is observed in ants which are physically connected to each other to perform different tasks, such as forming bridges, rafts, and walls (Anderson et al. 2002). Morphogenesis is the process by which a swarm of robots self-assemble for a specific task and follow a specific pattern. An example of recent work on morphogenesis in robot swarms is the study by (Slavkov et al. 2018), who provided a demonstration of self-organizing behaviors to create emergent morphologies in large robot swarms. The results show that collective organization can be accomplished by relying solely on local interactions with neighbors, without the need for self-localization.

The challenge is how to self-assemble into a desired target structure and how to control the resulting structure to tackle certain tasks. Groß & Dorigo (2008) reviewed the literature on self-assembly and morphogenesis. In another study, they performed collaborative transport by physically connecting each robot to other robots and objects of different shapes and sizes (Gross & Dorigo 2009). Ampatzis et al. (2009) presented a homogeneous control system for how to decide who will grip and who will be gripped using artificial evaluation that can make a time-based decision.

Patterns can arise from a variety of mechanisms, including self-assembly and morphogenesis, but they can also be imposed externally, such as through the influence of a physical or chemical gradient. Patterns can arise from a variety of mechanisms, including self-assembly and morphogenesis, but they can also be imposed externally, such as through the influence of a physical or chemical gradient.

Collective exploration

Collective exploration is a navigation behavior that collectively explores the environment, finds resources, and navigates to other robots through area coverage. This behavior is inspired by social insects such as ants. Ants find the shortest route between two locations, and bees communicate destination in an environment (Camazine et al. 2001). Ducatelle et al. (2011) presented a navigation algorithm using a wireless network connection. In their first study, the swarm guided a single robot to a target. In a subsequent study, the swarm navigated collectively between two targets. In both cases the robots were able to find the shortest path in cluttered environments.

Stirling & Floreano (2010) deployed flying robots in unknown environments for a search mission. Their strategy was based on the robots' ability to explore the environment quickly and at low energy cost. The most common way to handle field coverage is to use a virtual physics-based design, as in the study by Howard et al. (2002). When robots can move away from other robots and obstacles by means of mobile sensors, large numbers of them can be deployed for maximum coverage in the environment. Collective exploration often uses PFSMs and takes inspiration from network routing protocols or native systems.

Nauta et al. (2022) investigates how group size and resource fractality affect the search strategies used by foraging groups. The authors conduct a quantitative analysis using a computational model of foraging behavior to explore how different factors influence the way groups search for resources. The authors suggest that these findings have implications for understanding the evolution of social behavior in animals, as well as for designing effective search algorithms in artificial intelligence. Nauta et al. (2020) contributes to our understanding of how animals can use cognitive strategies to improve their foraging efficiency in complex environments, and highlights the importance of considering both individual behavior and environmental factors when studying foraging behavior.

Coordinated motion

Coordinated motion refers to different types of movement of a group of individuals, for example schooling in fish and flocking in birds (Couzin et al. 2002). In swarm robotics, the first study on coordinated movement was (Reynolds 1987) computer model of flocking. Reynolds studied simple behaviors such as separation, alignment, and cohesion that use different metrics and validations. As an improvement to that model, Ferrante et al. (2012) proposed a new coordinated motion behavior using motion control that does not require robots to have a preferred direction and alignment control.

The benefits of coordinated movement are many, including more precise navigation, higher survivability, and lower energy expenditure (Parrish et al. 2002). Celikkanat & Şahin (2010) showed the largest selected flocking measurements using informed individuals for target directions and guiding non-informed individuals. Their work was extended by Ferrante et al. (2010),

who developed alternative communication strategies in which some robots clearly transmitted their headings.

Van Havermaet et al. (2022) contributes to our understanding of how animal groups coordinate their behavior in dynamic environments, and highlights the importance of considering both spatial and temporal dynamics when studying collective behavior. The adaptive metric model proposed in this study provides a valuable tool for analyzing and predicting the behavior of animal groups in changing environments.

Cooperative transport

Cooperative object transport behavior is the collective movement of an object from its current location to the target location by a sufficient number of robots when an object is too heavy for a single robot to carry. In the natural system, ants carry prey cooperatively; Kube & Bonabeau (2000) analyzed how they cooperatively retrieve large prey and carry it back to the nest. Berman et al. (2011) developed a mathematical model from the behavior of ants for carrying out collective item transport. Alkilabi et al. (2018) presented a group of robots that first moved a cuboid object in an arbitrary direction from its starting position and then pushed it toward a specific target location. The same authors had previously Alkilabi et al. (2017*a*) demonstrated that transport strategies are scalable to group size and robust enough to deal with boxes of various masses and sizes.

Ferrante, Brambilla, Birattari & Dorigo (2013) developed collective transport behavior in which robots physically attached to an object, avoided obstacles, and moved toward a common destination. Gross & Dorigo (2009) studied collective transport using artificial evaluation to set the parameters of a neural network. Each self-assembled robot was physically connected to other robots and the object and was pushed to the target location. Donald et al. (1997) produced one of the first studies of decentralized controller collective transport. They proposed force sensing, position sensing, and direction sensing behaviors. Chen et al. (2013) developed a group of e-puck robots that moved a blue box object to a red target cylinder (see in Figure 3.1d).

Collective decision making and task allocation

Task allocation is a process by which robots are allocated to different tasks in a distributed and autonomous way. In task allocation scenarios, there are usually at least two or more tasks to be performed by the agents. This phenomenon is observed in animals such as ants and bees (Theraulaz et al. 1998). Amé et al. (2006) demonstrated the experimental and theoretical study of shelter selection by cockroach groups and modeled these experiments on swarm robotics, such as PFSMs. Campo (2011) used multiple methods of collective decision making. Prasetyo et al. (2021) studied the effectiveness of the context of the best-of-n problem strategy using two classical decision mechanisms, the voter model and the majority rule, showing that the majority rule is necessary for this strategy to work; the strategy was also planned on a physical robot experiment.

Masi et al. (2021) examined the best-of-n model, which takes into account the deferentially characterized agents: zealot agents, informed agents, and uninformed agents. In their study, the interaction between fan abundance for one option and the quality ratio between the two options was investigated, along with the interaction between the informed agent rate and the quality rate.

In one of the first studies of task allocation, Krieger & Billeter (2000) implemented a simple and decentralized task allocation mission to maintain the energy stocked in the nest by collecting food items. A mathematical model for the study of a similar task allocation behavior was developed by Liu et al. (2007). Pini et al. (2009) examined the use of task partitioning as a way to reduce noise in a spatially constrained aggregation task.

Group size regulation

Group size regulation is the collective behavior of robots choosing a group of the desired size. Lerman & Galstyan (2002) showed that an excessive number of robots can reduce the performance of the swarm and that it is possible to specify a group size that maximizes the performance of the swarm for different behaviors. Pinciroli et al. (2013) studied aggregation behavior that can make group size regulation the desired size with ground robots and flying robots. Flying robots are used to perform aggregation of ground robots through probabilistic join-or-leave according to the size of the group. Brambilla et al. (2009) demonstrated a distributed algorithm for individual robots in a group to estimate the size of the group. In related work (Firat, Ferrante, Zakir, Prasetyo & Tuci 2020), we examined group size regulation with different sub-proportions of informed individuals at two aggregation sites.

Aggregation

In this thesis, we develop research that concerns the design of control mechanisms underpinning self-organized aggregation in a swarm of robots. We investigate aggregation behavior in more detail in Section 3.2. In subsequent sections, we discuss control design methods and models that are also used in aggregation behaviors.

3.2 Self-organized aggregation

Aggregation behaviors aim to group all robots of a swarm at the same region in the environment. Aggregation is a very useful behavior that allows a swarm of robots to interact with one another, as well as a necessary prerequisite for other collective behaviors, such as pattern formation and flocking, that require robots to be in the same place.

Self-organization (decentralized) control comes from the swarm robotics organization architecture. There are two organizational architectures for controlling swarm robots: centralized and decentralized. In a centralized architecture, one central agent controls the entire system. This

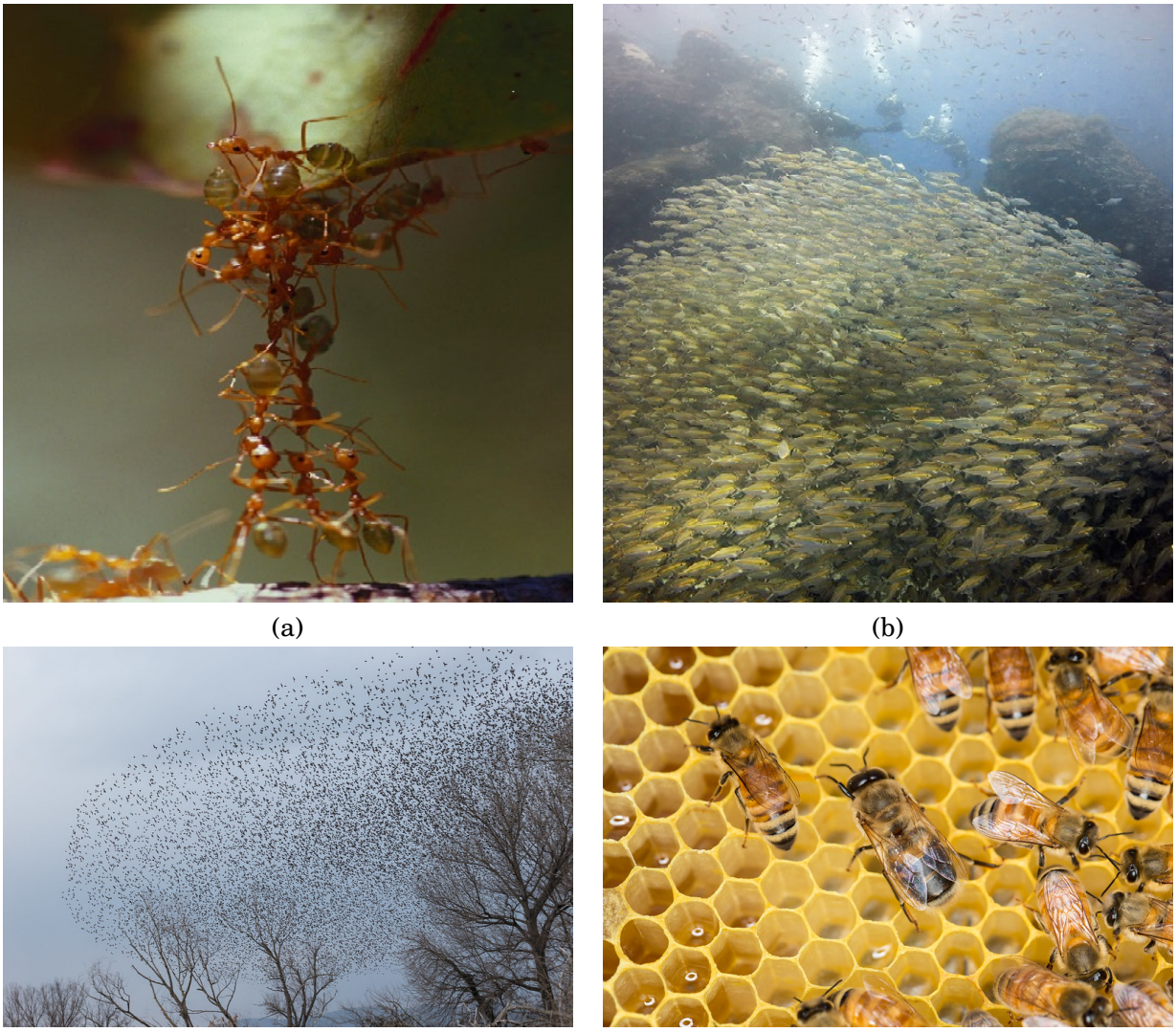

(a) (b)

(c) (d)

Figure 3.2: Examples of collective behaviors of social animals. (a) Ants physically connect one to the other to reach a leaf; (d) a school of fish; (c) a starlings flock; (d) a bee hive. Sources: (a) CC BY 2.0 - Kasi Metcalfe (b) CC BY 2.0 - Alan Duncan (c) CC BY 2.0 - Massimo Discepoli (d) CC BY 2.0 - Sy

agent can provide an overview of all other agents and the environment. The central representative, which can be a leader of a group of robots or a host computer, is responsible for decision making and distribution of tasks. Other robots collect information and send it to the central agent.

In contrast, self-organized (decentralized) aggregation is an inherently ubiquitous decision making process (Camazine 2003) in which agents gather around the same space without relying on global information, global communication, or any kind of centralized information or decision. Besides being a widely studied behavior of swarm robotics, decentralized organization is one of its

fundamental building blocks, since solving many problems in swarm robotics requires the swarm to come together. These problems include self-assembly and obstacle avoidance (O'Grady et al. 2009), coordinated movement (Ferrante, Brambilla, Birattari & Dorigo 2013), and cooperative object transport (Tuci et al. 2018).

In the rest of this section, we review the literature on aggregation, first as studied in natural systems (Section 3.2.1), and then as studied in swarm robotics (Section 3.2.2).

3.2.1 Aggregation in natural systems

In recent years, many mathematical models have been introduced in an attempt to describe collective behavior in groups of animals. Such biological aggregations are ubiquitous in nature, for example flocks of birds (Feder 2007), swarms of insects (mosquitoes, bees, or locusts) (Uvarov 1966), schools of fish (Parrish & Edelstein-Keshet 1999), flocks of sheep , and even crowds of people. Research on animal group behavior models has been driven by its applications as well as pure scientific interest. For example, the fishing industry could benefit from more information about fish behavior (Barbaro et al. 2009). Understanding swarms and raids in nature can also help improve robot communication (Balch & Arkin 1998) and coordination between autonomous vehicles (Cook et al. 1996). Applications reach even seemingly unrelated disciplines such as the social sciences and economics (Carrillo et al. 2010). Aggregation processes are extremely common in biological systems (Camazine 2003), resulting in clusters of agents in common areas in the environment. The main sources of inspiration for swarm intelligence are social animals. Swarms of ants, colonies of bees, flocks of birds, and schools of fish are examples of how simple individuals can become successful when they gather in groups. Some examples of collective behaviors of social animals in figure 3.2.

Stroeymeyt et al. (2011) studied nest site selection by the rock Temnothorax albipenni. In their experiment, they observed that some individuals visited a suitable nest site and memorized its location, and this knowledge accelerated swarm decisions about the familiar nest. This result shows that knowledgeable individuals can be used as leaders in decision making. Couzin et al. (2005) used a simple model to show how a small proportion of informed individuals in the larger group convey knowledge and guide the entire group. This model provides effective leadership and decision making mechanisms in biological systems.

Self-organized aggregation (i.e., an aggregation process not driven by exogenous forces) has been studied in a variety of biological systems (Deneubourg et al. 2002, Jeanson et al. 2005*a*). Jeanson et al. (2005*a*) performed experiments with Blattella germanica cockroach larvae in a homogeneous environment to investigate the influence of interactions between individuals on aggregations. Different densities were tested. A first phase led to radial dispersion of larvae in relation to wall-following behaviors; the consequence of this process was a homogeneous distribution of larvae around the periphery of the arena. A second phase corresponded to angular reorganization of larvae leading to the formation of aggregates. The phenomenon was analyzed

at both the individual and collective levels. Individual cockroaches modulated their behavior depending on the presence of other larvae in the vicinity: the probabilities of stopping and resting times were both higher when the numbers of larvae were greater. Szopek et al. (2013) used heterogeneous thermal environments in the arena to investigate the aggregation behavior of young honey bees based on a self-organized process in the brood nest. The bees caught another bee and waited in the arena at a higher local temperature. This finding confirms the common background of the observed thermotactic behavior, because in experiments with groups of bees, most bees aggregate where the temperature is optimal, and the percentage of bees aggregated at the optimum site is significantly higher than the percentage of single bees.

Many social species can make collective decisions. Consideration should be given to the fact that the group has different preferences and to how the interaction with group size will affect the outcome. A study discussed by (Eeckhout et al. 2021) focused on three different groups of social cockroaches (Periplaneta americana) collected in odorous and odorless shelters. The groups consisted of knowledgeable individuals who prefer odorous shelter, non-preferential individuals, and mixed individuals. It was shown that a small number of informed individuals who preferred one shelter to another were able to influence the population to reach a consensus on a single area. This result indicates that knowledgeable individuals guide the group in the social system.

In our own work, we have developed an agent-based model implementing individual behavioral rules, all derived from experiments, to explain the aggregation dynamics at the collective level. This study supports evidence that aggregation relies on mechanisms of amplification, supported by interactions between individuals that follow simple rules based on local information and without knowledge of the global structure.

3.2.2 Aggregation in swarms of robots

Self-organizing aggregation has been studied in various biological systems (Deneubourg et al. 2002, Jeanson et al. 2005*a*) and implemented on distributed robotic systems (Garnier et al. 2008*a*, 2005, Gauci, Chen, Li, Dodd & Groß 2014). Indeed, aggregation is often a necessity for many collective systems, as it is a prerequisite for other cooperative behaviors (Dorigo et al. 2004, Tuci et al. 2018). Generally speaking, in aggregation tasks, individuals have to aggregate on a common location in the environment (Garnier et al. 2005, 2008*a*, Bayindir & Şahin 2009, Correll & Martinoli 2011, Gauci, Chen, Li, Dodd & Groß 2014). Swarm robotics studies have shown that robot control methods in which the individual probability of joining and leaving an aggregation site depends on the number of robots perceived by an individual at the site lead to the emergence of a single aggregate at one site among those available in the environments (Garnier et al. 2009*c*, Campo et al. 2010*a*). Most of the swarm robotics studies that propose an algorithm to achieve aggregation in an artificial swarm have used one of the following design methods to control robot motion: control of robot behavior based on a probabilistic approach, artificial evolution, and application of virtual forces (artificial physics).

The PFSM is the most common design approach in aggregation behaviors. A finite state machine is characterized by two basic states: walk and wait. The robots walk randomly around the arena, and when they find other robots (Cambier et al. 2018*c*) or the marked aggregation site (Soysal & Sahin 2005), they stochastically decide to join or leave. Alternatively, Hamann et al. (2008) developed a macroscopic model that collects robots under a light source. In this scenario, the robot moved in a straight line, avoiding the wall and robot obstacles it encountered, and stopped when it came to the emitted IR signals. The intensity of the light affected the total number of robots gathered under the light source. In dim light, fewer robots gathered at the light source. With brighter light intensity, more robots were aggregated. Arvin et al. (2011) analyzed the behavior of the young honey bee collection scenario in the robot swarm. They applied variation of parameter values and suggested modified dynamic speed and comparative waiting times. By the end of the study, they had demonstrated the collective behavior of the swarm system by applying different algorithms. Garnier et al. (2005) applied their biological model of clustering to a group of Alice mini-robots. They were able to measure robot and cockroach behavior in terms of behavioral probabilities. They then reproduced both the individual displacement and the stopping behavior of the biological system with the artificial one. In a model inspired by German cockroach research, Correll & Martinoli (2007) developed clustering in a single cluster with possibilities to join or leave in function of cluster size. They showed that modeling could be used to optimize agents designed to create desired patterns in natural society at a collective level. Mermoud et al. (2009) explored multi-level microscopic and macroscopic modeling. They started from a spatial microscopic model, which is a programmable environment for multi-agent simulations. In the second type of microscopic model, the encounter probabilities were calculated using a geometric approach, and the fracture probabilities were shared with the other models. Finally, a macroscopic model based on discretization of the state space was proposed. In a recent study, Cambier et al. (2021) examined the impact of cultural propagation in the self-organized aggregation scenario. They used a simple finite state machine with two states. The robots communicated with each other and changed probability parameters using the so-called naming game (see Cambier et al. 2017), which investigates how linguistic or social norms spread throughout a population. They examined how the cultural propagation of traditions can provide an effective way of determining the codes of conduct invoked. Using dynamic environment behaviors rather than classical environment approaches is more efficient.

In terms of artificial evolution, (Trianni et al. 2003) investigated two behavioral strategies that emerge from evolution: static clustering behavior and dynamic clustering behavior. Clusters move around the arena and lead to a scalable behavior. Soysal et al. (2007) compared the PFSM approach with the artificial evolution approach. The aims of the study by Francesca et al. (2012) were to validate an evolutionary robotic system regarding joint decision making by cockroaches when choosing a resting shelter and to determine whether the system dynamics qualitatively and quantitatively correspond to those predicted by the biological model. Their work enabled the

formulation of hypotheses about the evolutionary pressures of evolutionary robotics that resulted in collective decision making in cockroaches. (Gauci, Chen, Dodd & Groß 2014) used controller evaluations. Robots have a long sensing range, and the sensor used only allows a robot to know if there is another robot in direct line of sight. Simulation results with both a memory controller and a memoryless controller proved that sufficient detection range is provided and that this sensor is sufficient to achieve error-free aggregation. In their study, the memory controller performed better in simulation, and other studies have consistently shown that it can aggregate at least 1000 robots into a single cluster. Gomes et al. (2013) examined the application of innovation research to the evolution of neural controllers for swarm robotic systems. They worked on two tasks. The first task was an aggregation task commonly used in the field of evolutionary swarm robotics. The other task was a resource sharing task in which the swarm coordinates to ensure that each member has periodic and exclusive access to a charging station.

In a study by Priolo (2013), the artificial physics-based swarm aggregation algorithm was tested with real robots. In this algorithm, distance and relative orientation of neighboring robots are obtained using radio frequency and infrared technologies. Fetecau & Meskas (2013) showed that the model produced realistic qualitative results that could be correlated with specific examples of predator–prey behavior in nature. They showed prey/escape relationships governed by nonlocal kinetic equations on which they focused. They also demonstrated the interaction and complexity between prey individuals, as prey can separate into clumps or stay together. Although artificial physics has been used successfully to formally characterize the aggregation dynamics of autonomous agent swarms, its application with real robots imposes some requirements on robot detection capabilities that may not be cost-effective (Mogilner & Edelstein-Keshet 1999).

An important point to note is the gap between experiments run in the simulation environment and real-world experiments. Because of this gap and the differences between simulation and the real world, there is often a drop in performance when control software is ported to physical robots. Ligot & Birattari (2020) studied the effect of the reality gap between a simulator experiment and a physical robot experiment in the automated design of robot swarms. They first developed simulator control software and used it in reality gap performance. They then showed how experiments on a physical robotic platform affected the gap in reality. Depending on the purpose of the aggregation, the aggregation site may be an area that is clearly detectable by all agents in the environment and must be selected from among several similar shelters, or it can be an area that is nonspecific and indistinguishable from any other area. In this section, we will review both no-shelter and shelter-required approaches to creating clusters.

In summary, the gap between experiments and simulations in swarm robotics arises from the fact that the behavior of robots in the real world can be very different from what is observed in simulations. Therefore, it is important to validate the results of simulations with experiments and vice versa, to ensure that the behaviors and algorithms observed in simulations are robust and applicable to the real world. Additionally, researchers may use a combination of experiments

and simulations to explore different aspects of swarm robotics, leveraging the strengths of each approach.

Aggregation without shelters

Aggregation without shelters has been studied by Jeanson et al. (2005*b*) who performed experiments with Blattella germanica cockroaches. They designed separate experiments with groups of two to four larvae in a featureless arena, and calculated the resting times of individuals by following the path taken by the larvae. They artificially reconstructed the model on the basis of this work. This model was transferred to robots in further studies, which showed that the robots depended on external parameters such as density and communication range (Garnier et al. 2008*a*). Correll & Martinoli (2007, 2011) studied the quantitative estimation of aggregation dynamics using the probability model. They showed how the agent communication range works, which affects the structure of the resulting cluster topology. Bayindir & Şahin (2009) developed shelter-less aggregation using a PFSM.

Trianni et al. (2003), Dorigo et al. (2004), Şahin (2004) used the evolutionary swarm robotics framework to create self-organized aggregation dynamics. Silva et al. (2015) proposed a new approach, namely a decentralized neuroevolution algorithm called odNEAT for online learning in robot groups. Each robot optimizes an internal population of genomes and exchanges genetic information between robots. Gauci, Chen, Li, Dodd & Groß (2014) studied biologically inspired approaches to evolutionary robotics with a homogeneous aggregation model (see Figure 3.1 c). They achieved scalable results with deterministic controlled robots equipped with a single-bit sensor. Katada (2018) determined the parameters of a PFSM for a set of robot controllers using evolutionary computations. Their results show that the proposed method is useful for the aggregation problem and that the best developed controllers are applicable.

In existing studies, shelter selection is considered implicitly as a simplified version of aggregation. Although the two problems (aggregation and shelter selection) have the same basic dynamics, the latter simplifies the matter by preventing search robots from creating new aggregates at locations other than predefined shelter locations. The creation of aggregates outside predefined shelter locations and the use of larger environments in aggregation allows the swarm system to reach equilibrium more slowly (Bayindir & Şahin 2009). Amé et al. (2004) reported that the time required to reach equilibrium states increases exponentially with the number of individuals, even in the problem of shelter selection. For these reasons, the formula proposed in Amé et al. (2004) is inadequate to solve the addition problem.

Aggregation with shelters

Aggregation with shelters has been studied as a best-of-n collective decision making problem in Valentini et al. (2017), Garnier et al. (2008*a*), and Campo et al. (2010*b*). In these studies, the authors considered the presence of two circular aggregation sites in the environment, the

only two areas where robots could stop, that were indistinguishable to the robots. Garnier et al. (2008*a*)considered two cases. In the first case, where the two sites were of equal size, under special circumstances the swarm could break the symmetry and aggregate on one of the two sites at random. In the second case, where the two sites were of different sizes, robots were able to collectively chose the bigger of the two aggregates. In a setting that is similar to this second case, but using a different model, Campo et al. (2010*b*) designed a swarm able to select the smallest site that could host the entire swarm, rather than the biggest site.

Bodi et al. (2012) used the BEECLUST algorithm inspired by honey bee behavior and proposed a very similar principle to cockroach aggregation in hotspots. An important difference between the two behaviors is that the probability distribution of staying in the aggregation area increases with local temperature and not with the amount of neighbors, but the decision to stay or not is only triggered when other agents or clusters are encountered. Hasselmann et al. (2018) studied automatic designs of aggregation with shelters. They focused on the situation where robots can broadcast a single message locally and can be redefined on a per-task basis through automated design.

3.2.3 Aggregation with informed individuals

Our study was inspired by the self-organized behavior of cockroaches studied in biological observation. In this section, we discuss the works that inspired us. First, we describe how authors worked with cockroaches and the models they created, summarizing how they studied the size of the aggregation area and the size of the populations, and how they used mathematical models (Jeanson et al. 2005*b*, Amé et al. 2004). Next, we explain how other authors transformed the cockroach aggregation process to apply to robots using the PFSM method (Garnier et al. 2009*a*, Campo et al. 2010*b*). Finally, we clarify how some authors have used robots and cockroaches together to create cluster dynamics (Halloy et al. 2007). Building on these studies, we add a new concept to the literature to explore heterogeneity and consider the influence of individual differences in organizing self-aggregation. We show that this valuable design is fine-tuned for individual differences to determine the best mix for achieving the desired kind of global behavior. We end by summarizing the innovation our work has led to.

Cockroaches are a good model to explore the link between an interesting interpersonal recognition ability and the organization of populations in communities and to discuss their evolutionary implications. The aim of the studies that we will shortly summarize is to use a theoretical model with experimental results and a few functional rules to investigate how groups arise. Blattella germanica cockroaches present a rudimentary type of social organization known as presocial organization. They are often found in restaurant kitchens. Since they feed at night, during the day they form aggregates in low outdoor humidity environments. They rest under kitchen appliances and sinks and behind baseboards. Blattella germanica cockroaches are 3 mm long and 2 mm wide with antennae 3 mm long. Individuals do not show attraction in the presence

of different forms or toward the sexes. For more details on the origin and reproduction of animals, see Jeanson et al. (2005*b*).

Jeanson et al. (2005*b*) studied clustering with Blattella germanica to investigate the interaction between individuals of different densities. They set up a homogeneous arena (an arena without special shelters for aggregation). The authors observed the behaviors of individuals resting in the cluster, which depend on local interaction. In this interaction, they worked on a model that showed that rest periods were correlated with a large or small number of neighbors. The aim of these modeling efforts was to understand the emergence of individuals interacting at the microscopic level. Each individual either moves or stops. They stand alone in the arena or stand near the rest group. To calculate the probability of stopping and moving, Jeanson et al. (2005*b*) developed an equation assuming the perception of the number of larvae gathered around individuals per unit time. They analyzed the individual-level behavior of a single larva, and analyzed cluster dynamics and spatial distribution of individuals at the collective level. They hypothesized that cockroaches have local interaction only and do not have any long-range global information. They developed a numerical model based on these experimental behavioral roles and showed that as the number of cockroaches in the gathering group in the arena increased, individuals tended to rest more.

Amé et al. (2004) also investigated Blattella germanica, but with two aggregation sites on the arena. Binary selection tests were initially conducted with groups of 20 cockroaches. The tests were conducted in petri dishes with filter papers that served as attractive resting areas large enough to accommodate the entire group. The experiments used a single strain or two strains. All strains were kept under strictly the same growing conditions to minimize environmental impacts, and each test was performed under the same experimental conditions. At the end of the tests, the individuals on each paper (aggregation site) were counted. It was observed that at least 80% of the larvae were resting on the papers. In 75% of the experiments, 80% of the larvae were observed to be aggregated in one of the sites. In these results, a mixed aggregation was seen in two strains, similar to one strain. The authors then developed a mathematical model that accounts for the aggregation behavior observed in cockroaches by linking the individual resting time to the perception of conspecific resting on the aggregation site. Generally speaking, the model provides a rationale for individuals of different strains aggregating on a single resting site in spite of segregation dynamics induced by chemical signals that would tend to generate same-strain individual aggregates. In subsequent work, Amé et al. (2006) extended the model, predicting that, in an environment with up to four aggregation sites, cockroaches form a single aggregate only when each aggregation site can host more than the totality of the individuals. The model also predicts how the cockroaches distribute in different environments according to the number of aggregation sites and the diameter of each site as it bears upon the site's capacity to host individuals (see in Figure 3.3a).

Based on these aggregation behaviors in cockroaches, mathematical models have been pro-

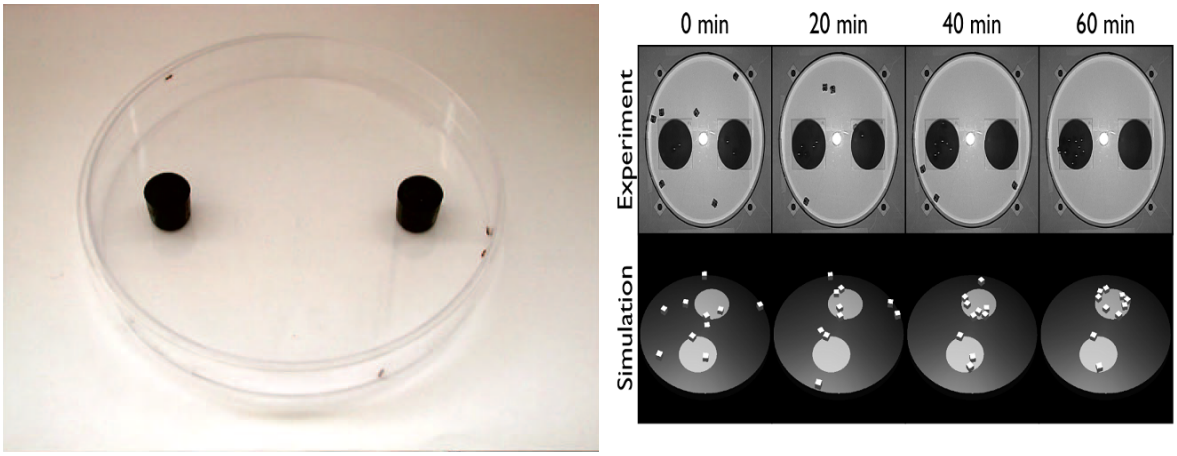

(a) (b)

Figure 3.3: (a) Selection tests were conducted with groups of cockroaches in Petri dishes (14 cm in diameter) with small plastic lids for shelter. Source: Amé et al. (2006) (b) Temporal evolution of the collective decision process in a robotics experiment (top row) and a simulation study (bottom row). Source: Garnier et al. (2005)

posed to predict the swarm's performance in obtaining self-organized aggregation. These models allow the calculation of macroscopic quantities that describe the collective behavior of a swarm from parameters that govern its individual behavior. Halloy et al. (2007) developed a mathematical model that takes into account findings from cockroach experiments. In the model, when individuals come across one of the arena gathering sites, they stop inside the site. The authors used for mathematical equations to show that the resting time on the site of an individual is affected by the presence of individuals around them. With this model, they created the basic behavioral module of the swarm and allowed them to respond stochastically to social stimuli according to the equations. In the model, robots and cockroaches exhibit similar behavior. Mathematical models are used quite frequently in the study of collective behavior in artificial swarms to avoid the time and computational costs incurred by robotic and other agent-based models in investigating the effects of a wide variety of experimental conditions. The mathematical model of self-organizing aggregation, one of the common approaches to modeling to study collective behavior, is ODE. Differential equations provide a tool for analyzing the mechanisms underlying colony-level patterns and have frequently been applied to aggregation by insect communities. These models are built from simple mathematical formalism to explain how populations change over time.

The principle of attraction between individuals, which nicely accounts for the aggregation dynamics observed in cockroaches, has been imported into robotics to design effective and relatively simple control mechanisms for achieving aggregation behavior. In particular, roboticists have shown that robot controllers in which the individual probabilities of joining and of leaving an aggregation site depend on the number of robots perceived by an individual at the site,

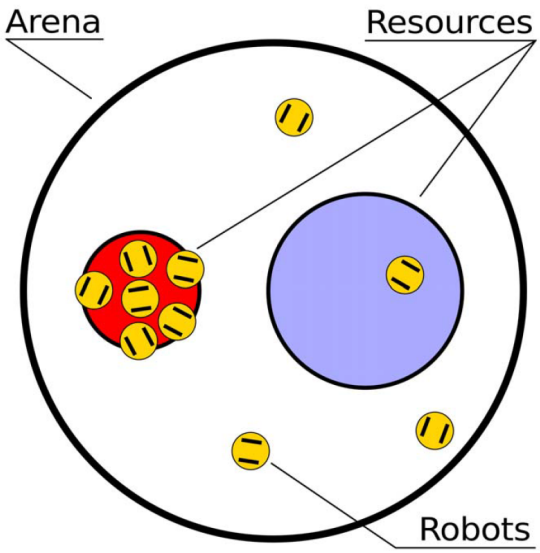

(a)

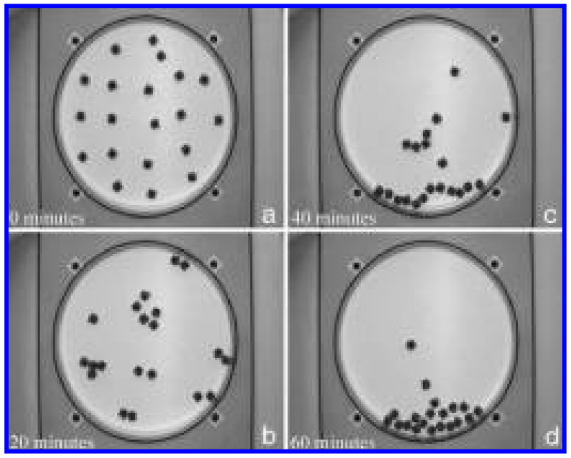

(b)

Figure 3.4: (a) In an arena, two resources are represented by two different size coloured. Source: Campo et al. (2010*a*) (b) Snapshots were made at the beginning of the experiment, after 20 minutes, after 40 minutes, and at the end of the experiment. Source: Amé et al. (2006)

leading to the formation of a single aggregate in environments with multiple aggregation sites. Garnier et al. (2008*b*) applied cockroach collecting behaviors to the autonomous robot group in a homogeneous environment, extending the Jeanson et al. (2005*b*) cockroach collection model to robots. They showed that the behavior of animals provides great advantages and suggested how it can be used in artificial agents. As well as describing analytical tools for biological and artificial systems, they discussed the general issue of the transition from animals to robots (see in Figure 3.3 b). In a study by Garnier et al. (2008*b*), individuals in the group stopped when one to three individuals had stopped nearby; the more individuals had stopped nearby, the more likely they were to stop for a long time. With this structure, when a robot stopped near N robots, the authors calculated the stop time. They then showed the stop-time survival curve for each group size (two to four, including the observed robot). As with cockroaches, all survival curves showed a bilinear pattern (biexponential on a normal scale). Once a robot left the cluster, it was possible to predict the stopping parameters for each group size by directly fitting the equation. Both Garnier et al. (2009*a*, 2005) and Campo et al. (2010*b*)used the abovementioned probabilistic controller to look at aggregation dynamics in scenarios with two circular aggregation sites, that is, sites that the robots can perceive but cannot distinguish one from the other(see in Figure 3.4a). Garnier et al. (2009*a*) considered two cases. In the first case, where the two sites had equal size, under special circumstances the swarm could break the symmetry and aggregate on one of the sites at random. In the second case, where the two sites had different sizes, robots were able to collectively chose the bigger of the two aggregates. In the study by Campo et al. (2010*b*), the robots were required

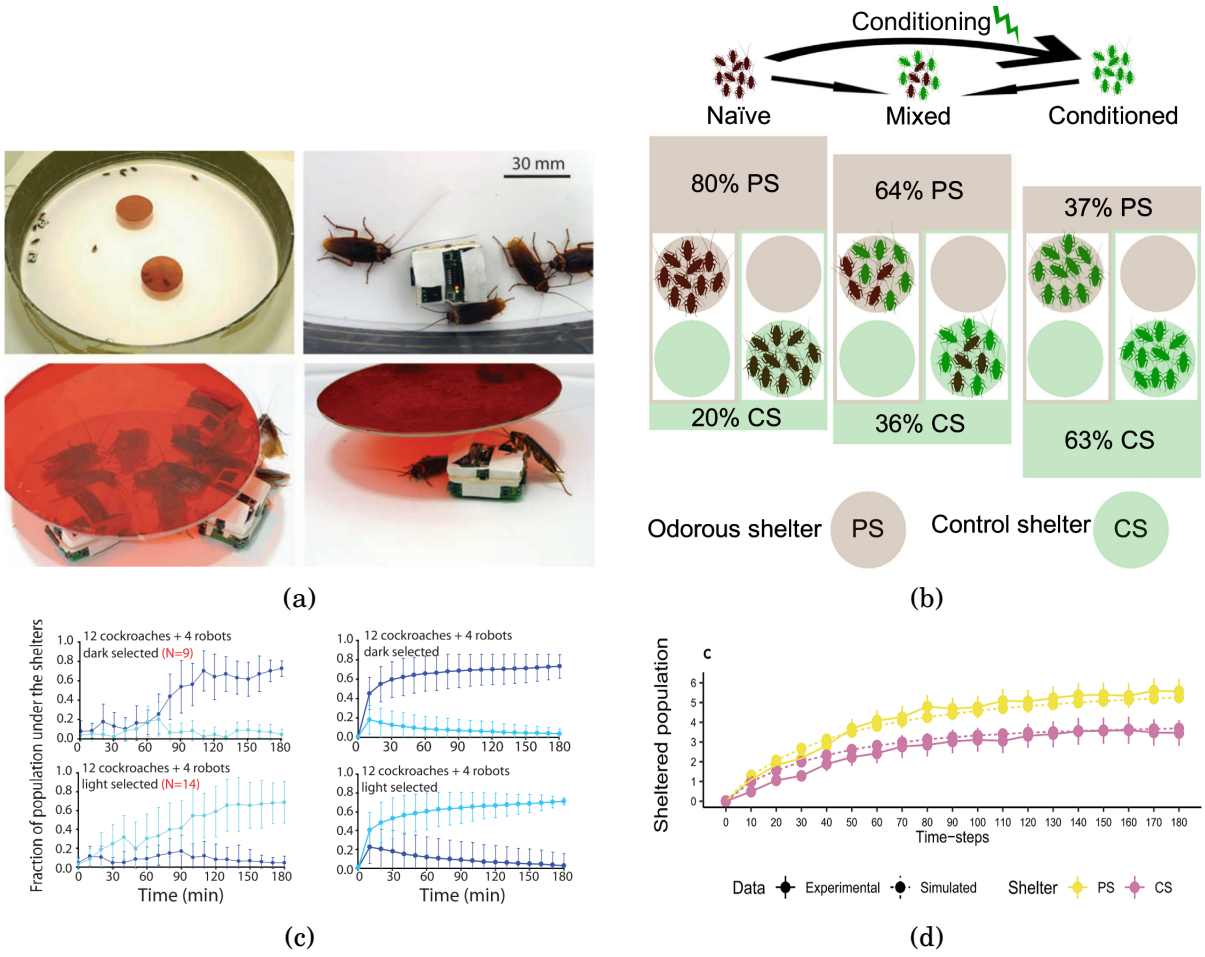

Figure 3.5: (a) Examples of cockroaches robot interaction with two shelter arena. (b) Cockroaches populations on the two different shelter in two different group. (c) the ratio of the group under the shelters as a function of time selection in both group types (dark blue, dark shelter; light blue, light shelter). The N values in red are the number of selections made from 30 trials. Source: Halloy et al. (2007) (d) Experimental and simulated dynamic of the sheltered population that under the PS (yellow) and the CS (violet) over time (minutes) for the experiments (solid lines) and stochastic simulations. Source: Calvo et al. (n.d.).

to aggregate in environments in which the carrying capacity of a site was systematically varied, while the carrying capacity of the target site remained fixed to a value that allowed it to host all the robots of the swarm. Their results shows that robots avoid aggregation sites that are too small or too big with respect to the swarm size.

In a seminal study, Couzin et al. (2005) investigated the influence of informed individuals on group decision making. They showed that a very small proportion of informed individuals is required to lead large groups. They also demonstrated how groups can make consensus decisions even if informed individuals do not know whether there are other informed individuals. In Halloy et al. (2007)'s study, robots controlled by similar principles influenced the aggregation dynamics

of cockroaches in mixed robot-animal groups (in a similar structure to informed individuals). In particular, the robots programmed to rest preferentially on the lighter (rather than on the darker) shelter, induced cockroaches to behave similarly, even if the animals would preferentially aggregate on the darker shelter in the absence of robots (see in figure 3.5 a). A recent study on cockroaches by Calvo et al. (n.d.) obtained similar results using informed individuals. In their models with cockroaches, one shelter was prepared without odor, and the other was prepared with a peanut butter odor. Individuals were used in three different ways: in a conditional group deterred by electric shocks to avoid the scented shelter, in a naive group, and in a mixed group. Nearly all the trials for the three conditions resulted in at least 90% of the total population being in the same shelter. The hypotheses put forward here are that, regardless of individual knowledge and behavior, consensus is always reached, and that group preference and group dynamics are regulated by group composition. The same authors also developed a mathematical model based on experiments that suggest that conditioning does not affect interactions, but only individual preferences. In the completed trials, 80% of the naive group were collected in the odorous shelter and 20% in the control shelter; in the mixed group, % in the odorous shelter and 36% in the control shelter; and in the conditioned group, 37% in the odorous shelter and 63% in the control shelter (see in figure 3.5b). In mixed groups, a minority of naive individuals initiated the resettlement process, and their intrinsic preference for the odorous shelter increased the frequency with which this shelter was chosen collectively. Similar results were obtained in a study by Halloy et al. (2007) that gave mixed cockroach–robot groups the option to settle in a dark or a light shelter(see in Figure 3.5c and 3.5d).

We implemented the idea that a group of autonomous vehicles can affect cluster dynamics using robotic systems, which was originally discussed by Halloy et al. (2007) in the context of robot–cockroach interaction and has more recently been studied in a mixed group of cockroaches by Calvo et al. (n.d.). We extended the analysis of the aggregation process in a dual shelter field scenario, as in previous studies (Garnier et al. 2009*a*, Campo et al. 2010*b*), to the case where the swarm is characterized by the presence of informed individuals (Firat et al. (2018), Firat, Ferrante, Gillet & Tuci (2020); see Chapter 4). We used these studies to explore heterogeneity, which is a new concept in self-organized aggregation work using informed individuals. The sites have distinctive features that allow the agents to discriminate between them. Informed individuals are programmed to selectively avoid resting on one of the two sites. Non-informed individuals rest with equal probability on each site. These studies show that with a small proportion of informed individuals it is possible to selectively drive the aggregation dynamics on a designer preferred aggregation site. In other words, this research takes the neighbor of a robot i to be another robot j belonging to the same swarm, which is located close to robot i. The distance between robot i and robot j has to be such that robot i perceives robot j through its range-and-bearing sensors (see Chapter 4for a detailed description of the robot's sensory apparatus). Since robot aggregates are not persistent (that is, robots join and leave an aggregate

over time), within an aggregate the neighboring robots of an arbitrary robot i can change over time.A variety of proximity and long-range distance sensors can be used to perceive neighboring robots. We chose to use range-and-bearing sensors because they are available on the robotic platform that we simulated in our experiments (see Chapter 4). A robot aggregate emerges whenever two or more physical or simulated robots rest close to each other. Due to the distributed nature of the swarm, self-organized aggregation dynamics in physical and simulated swarms are generally driven by the individual propensity of the robots to stop close to other robots. This behavioral response mimics actions that have been observed in insects such as cockroaches, as described by Amé et al. (2004). Here, we complete our work on aggregation dynamics by using a mathematical model. Our proposed model is based on ODE and aims to examine the two aggregation-site scenario. In particular, we extend the ODEs that were originally introduced and discussed by Amé et al. (2004) and reused in other studies on self-organizing clustering (Amé et al. 2006, Campo et al. 2010*b*). The extension we propose contains a term that models the existence of informed robots. In the self-organized aggregation with multiple shelters reported in Chapter 4, we work with informed robots to assemble the entire swarm in a single-shelter area from two-, three-, and four-shelter options. The model in Chapter 5 uses a system of ODEs to examine how informed individuals can be used in a foraging context to distribute agents of a swarm between two different collection sites according to two established rules. Chapter 6 reports our study of the aggregation of robots in two-shelter areas with a supervised group size regulation. Our aim was to collect the entire swarm, guided by the sub-proportion of informed individuals in both aggregation sites, reflecting the relative proportion of informed robots.

CHAPTER 4

ON SELF-ORGANISED AGGREGATION DYNAMICS IN SWARMS OF ROBOTS WITH INFORMED ROBOTS

4.1 Introduction

In this chapter, the working hypothesis we aim to test is the following: given a swarm of robots where agents are programmed to stop and to leave aggregation sites with probabilities based on the number of perceived neighbours at each aggregation site, can informed robots induce, with their behaviour, such a swarm to aggregate on a single specific aggregation site when the environment offers multiple types of aggregation sites? If yes, which is the minimum proportion of informed robots in the swarm required to generate the single aggregate on the informed robots' chosen aggregation site? Informed robots are members of the swarm that have been informed a priori about the aggregation site to stop on, in an environment that offers multiple sites for aggregation. Apart from the preference on the site on which to aggregate, the behaviour of informed robots is controlled by exactly the same mechanisms of non-informed robots. The roles of informed robots is to influence the aggregation dynamics, in a very indirect way, since none of the robots has any means to discriminate informed from non-informed robots. To the best of our knowledge, this is the first time this working hypothesis is being tested in robot swarms in the context of self-organised aggregation, while previous work has studied a similar hypothesis in the different context of collective motion (see Couzin et al. 2005, Ferrante et al. 2014). We perform our study with a series of simulation experiments on different scenarios, represented by a circular arena with two to four aggregation sites. In the simplest possible scenario, the arena is characterised by two aggregation sites, the desired one coloured in black, and the one to be avoided, coloured in white. Only informed robots are programmed to avoid to stop on the white site. For all the other robots of the swarm, both the black and the white

site are equally good resting locations. We show that with less than 20% of informed robots, the swarm systematically aggregate on the desired black site (see section 4.4.1, Exp. I). The results of subsequent experiments show that with a slightly larger proportion of informed robots the swarm can systematically aggregate on the desired black site even in an "asymmetrical" scenario with two white and only one black site, and also in a scenario with two white and two black sites (see section 4.4.2, Exp. II, and Exp. III). For each experiment, we provide an analysis of the aggregation dynamics that lead to the formation of a single aggregate. We also show interesting relationships between swarm size and proportion of informed agents, both on quality and speed of convergence on the desired aggregation site. Moreover, we propose an Ordinary Differential Equation model that extends the one originally illustrated in (Amé et al. 2006) in a way to include the effect of informed robots. The analysis of the model with the same parameters as in (Amé et al. 2006) indicates that a very large proportion of informed robots (i.e., about 80%) is needed to qualitatively replicate the aggregation dynamics we observed in the two-site scenario. However, by exploring the parameter space of the model in a way that goes beyond the analysis done in (Amé et al. 2006), we identified a region of the parameter space whereby the stable equilibria qualitatively match those found in experiments with simulated robots. The analysis of the model's parameters leads to a deeper understanding of the relationships between environmental features and agents' exploration strategies. We show how these relationships bear upon the emergence of a single aggregate and how they interfere by amplifying or by reducing the effects of informed robots on the group aggregation process.

The rest of the chapter is structured as follows. Section 4.2 describes the self-organised aggregation method used. In Section 4.3, we present the experimental setup and how we study the effect of informed robots. Section 4.4 presents the results of the three experiments with simulated robots. Section 4.5 shows the analysis of the ODEs' model. Finally, in section 4.6, we discuss the significance of our results for the swarm robotics community, and we point to interesting future directions of work.

4.2 The robots' controller

Each robot is controlled by a probabilistic finite state machine (PFSM, see also Figure 4.1a), similar to the one employed in (Jeanson et al. 2005*a*, Bayindir & Şahin 2009, Correll & Martinoli 2011, Cambier et al. 2018*b*). The PFSM is made of three states: Random Walk ($\mathscr{RW}$), Stay ($\mathscr{S}$), and Leave ($\mathscr{L}$). When in state $\mathscr{RW}$, the robot performs a random walk strategy introduced in (Dimidov et al. 2016) that is very effective in covering the whole environment. With this strategy, the movement of the robot is characterised by an isotropic random walk, with a fixed step length (5 seconds, at 10 cm/s), and turning angles chosen from a wrapped Cauchy probability

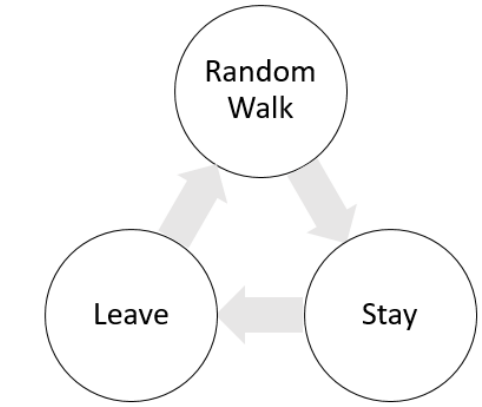

a

n	P_{stay}	P_{leave}
0	0.03	n.a.
1	0.42	1/49
2	0.5	1/424
3	0.51	1/700
4+	0.51	1/1306

b

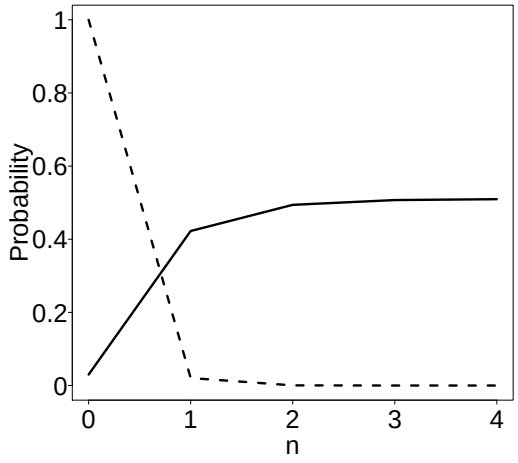

c

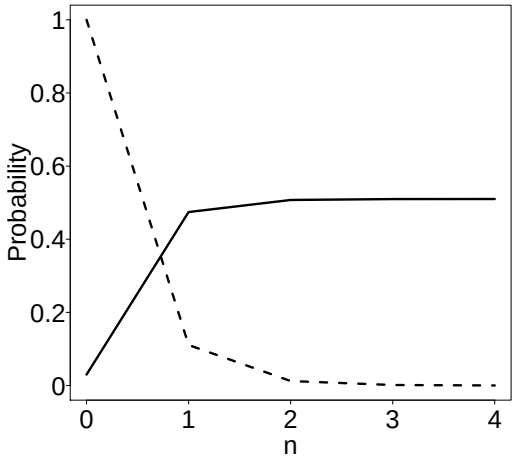

d

Figure 4.1: In a) State diagram of the robots' controller. In b) averaged probability to join and leave an aggregate as computed by (Jeanson et al. 2005*a*, Correll & Martinoli 2011) from observation of gregarious arthropods (cockroaches). The look-up table shows the probability per second of a single insect to stop and to leave and aggregate based on the number of perceived neighbours. In c) plotting of P_{stay} and P_{leave} according to eq. 4.2, and eq.4.3 with $a = 1.7$ and $b = 3.88$ as illustrated in (Cambier et al. 2018*a*). In d) plotting of P_{stay} and P_{leave} according to eq. 4.2, and eq.4.3 with $a = 2.6$ and $b = 2.2$ as illustrated in Section 4.2 for our experiments.

distribution characterised by the following PDF:

$$f(\theta,\mu,\rho) = \frac{1}{2\pi}\frac{1-\rho^2}{1+\rho^2-2\rho\cos(\theta-\mu)},\ 0<\rho<1, \tag{4.1}$$

where $\mu = 0$ is the average value of the distribution, and ρ determines the distribution skewness (see also Kato & Jones 2013). For $\rho = 0$ the distribution becomes uniform and provides no correlation between consecutive movements, while for $\rho = 1$ a Dirac distribution is obtained, corresponding to straight-line motion. In this study $\rho = 0.5$. Any robot in state $\mathscr{RW}$ is continuously performing an obstacle avoidance behaviour. To perform obstacle avoidance, first the robot stops,

and then it keeps on changing its headings of a randomly chosen angle uniformly drawn in $[0, \pi]$ until no obstacles are perceived.

A robot that, while performing random walk, reaches an aggregation site, it stops with probability (P_{stay}). This probability is computed using the following function:

$$P_{stay} = 0.03 + 0.48 * (1 - e^{-an}); \tag{4.2}$$

with n corresponding to the number of other robots currently stationing on the site that are perceived by the robot currently deciding whether to stop or not; and $a = 2.6$. This function was first introduced in (Cambier et al. 2018*a*). It interpolates the probability table considered in classical studies such as (Jeanson et al. 2005*a*, Correll & Martinoli 2011). Once the robot has decided to stop based on P_{stay}, it moves forward for a limited number of time in order to avoid stopping at the border of the site thus creating barriers preventing the entrance to other robots, and at the same time attempting to distribute uniformly with other robots on the site. It then transitions from state $\mathscr{RW}$ to state $\mathscr{S}$. Once in state $\mathscr{S}$ the robot leaves the aggregation site with probability P_{leave}. This probability is computed in the following:

$$P_{leave} = e^{-bn}; \tag{4.3}$$

with $b = 2.2$. This function was also introduced in (Cambier et al. 2018*a*). A robot that decides to leave the aggregation site based on P_{leave} transitions from state $\mathscr{S}$ to state $\mathscr{L}$. Both P_{stay} and P_{leave} are sampled every 20 time steps. When in state $\mathscr{L}$, the robot moves away from the site by moving forward while avoiding collisions with other robots until it no longer perceives the site. At this point, the robot transitions from state $\mathscr{L}$ to state $\mathscr{RW}$. Note that P_{stay} is sampled every 20 time steps when the robot is in state $\mathscr{RW}$ (Random Walk) and is on a white or a black floor (i.e., on an aggregation site), while P_{leave} is sampled every 20 time steps when the robot is in state $\mathscr{S}$ (i.e., Stay). Note also that, as far as it concerns the interactions between robots, during random walk the robots avoid to collide with each others using their infra-red sensors. The robots interact only when they are on the same aggregation site. These interactions are relatively simple since each robot currently on an aggregation site is only interested in estimating the number of other robots (also referred to as neighbours) that are located on that aggregation site and in state $\mathscr{S}$ (Stay). Each robot can perceive up to a maximum of twelve neighbours. The perception of neighbours is accomplished with the range-and-bearing sensors, whose functionalities are illustrated in the last paragraph of section 4.3. The information related to the number of neighbours is estimated by each robots i) while on an aggregation site and in state $\mathscr{RW}$ in order to set the variable n required to derive the probability P_{stay} which governs the transition from state $\mathscr{RW}$ (Random Walk) to state $\mathscr{S}$ (Stay); and ii) while on an aggregation site and in state $\mathscr{S}$ (Stay) in order to set the variable n required to derive the probability P_{leave} which governs the transition from state $\mathscr{S}$ (Stay) to state $\mathscr{L}$ (Leave).

The probability functions for computing P_{stay} and P_{leave} are first illustrated in (Cambier et al. 2018*a*) to replace a transition probability look-up table originally described in (Correll &

Martinoli 2011) and shown in Figure 4.1b. In (Correll & Martinoli 2011), the authors observed the behaviour of cockroaches placed in a close arena. These insects move randomly through the arena, eventually stop, and aggregate into clusters of different sizes, in which every insect can sense the presence of at least one other cockroach. Clusters are not persistent, because cockroaches might resume movement and quit the cluster. Experimental observations have shown that cockroaches stop and leave an aggregate with the probabilities shown in the look-up table in Figure 4.1b. The look-up table shows the probability of a single insect to stop and to leave and aggregate based on the number of perceived neighbours. In (Cambier et al. 2018*a*), the author have generated probability functions with parametrisable steepness from the values shown in the look-up table proposed by (Correll & Martinoli 2011). The Cambier et al. (2018*a*)'s probability functions, illustrated in eq. 4.2 and eq. 4.3 with $a = 1.70$ and $b = 3.88$, generate the curves shown in Figure 4.1c. In these equations, the parameter a and b handle the strength of the aggregation and dispersion forces, respectively. The parameters a and b have to be set in order to generate a virtuous trade-off between aggregation and dispersion forces that eventually leads to the formation of a single aggregate. If cohesion is too weak (low a and b), no durable cluster forms; if cohesion is too strong (high a and b), the robots aggregate in several sparse and static clusters that never break. Both cases need to be avoided. We have adopted the Cambier et al. (2018*a*)'s probability functions in our experiments. In order to adjust these probabilities to the group dynamics observed in our setup, we further tuned, with a trial-an error process, the parameter a and b. The curves generated by eq. 4.2 and eq. 4.3 with our parameters $a = 2.6$ and $b = 2.2$ are illustrated in Figure 4.1d. Parameters tuned by trial and error procedure by rounding simulations. We defined maximum number of perceived robots base on capability of Foot-bots mobile robots. The reader can notice that, first the probability functions as illustrated in (Cambier et al. 2018*a*) match very closely the originally probability shown in the look up table illustrated in (Correll & Martinoli 2011) (see Figure 4.1c). Second, our probability functions are very similar to the one illustrated in (Cambier et al. 2018*a*) (see Figure 4.1c and 4.1d).

Derived from the behaviour of cockroaches, the probability functions as illustrated in (Cambier et al. 2018*a*) and also in our setup, they are characterised by a very steep trend, since they both reach saturation values in correspondence of 3/4 robot neighbours. In addition of tuning the parameters a and b with a trial and error process, we have also tuned, with another trial-and-error processes, other parameters of our experimental setup, such as the frequency with which P_{stay} and P_{leave} are sampled, the type of random movement of the robots that impacts on the frequency with which each robot finds an aggregation site, the maximum number of neighbours that can be perceived by each robot while on an aggregation site, and the world dimensions including the diameter of the aggregation site (see section 4.3 for details). All these parameters, when fine tuned, contribute in a mutualistic way, to avoid undesired dynamics such as those characterised by the formation of multiple aggregates, and those in which the aggregates dissolve to quickly to allow the group to aggregate on a single site. We acknowledge that finding the

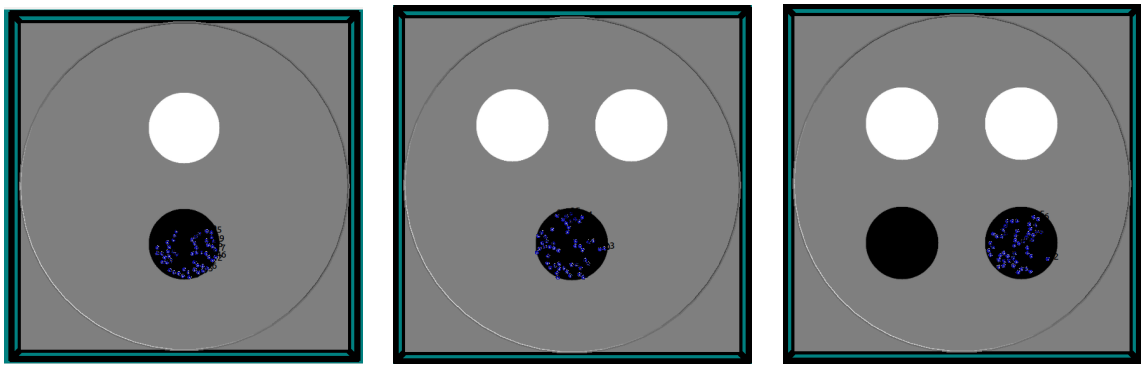

(a) (b) (c)

Figure 4.2: The robots' arena for (a) experiment I, with two aggregation sites, one black and one white; (b) experiment II, with three aggregation sites, two white and one black; (c) experiment III, with four aggregation sites, two white and two black.

correct setting for all these parameters is not an easy task. We can not exclude that a different set of parameters would not produce similar or even better results of those illustrated in section 4.4. The task of further tuning the model parameters can be performed with dedicated optimisation algorithms, and can be one subject for future work.

In our model we consider two kinds of robots: *informed* and *non-informed*. Informed robots are agents that possess extra information on what is the site or the sites on which the swarm has to aggregate. Ideally, this extra information could be either generated by additional sensors, mounted only on informed robots, which allow these robots to perceive the quality difference among the available aggregation sites, or communicated by the experimenter with the intention to influence the swarm aggregation dynamics. In our simulated scenario, we consider aggregation sites in two different colours: black and white. Informed robots are aware that the task requires to stop only on black sites. This information is implemented into the PFSM of informed robots with the instruction: do not stop on any white site. This means that informed robots ignore white sites, and only stop on black sites based on P_{stay}, as described above. Non-informed robots do not possess this extra information, therefore they can stop both on black and on white sites based on P_{stay}, as described above. Recall that any robot is not able to recognise whether any other individual is an informed or a non-informed robots.

4.3 Experimental Setup

In this set of simulations, a swarm of robots is randomly initialised in a circular area with the floor coloured in grey except for the circular aggregation sites, where the floor can be coloured in white or in black (see Figure 4.2). We have studied three different scenarios. In experiment Exp. I, there are two aggregation sites in the arena, one black and one white. In experiment Exp. II,

there are three aggregation sites in the arena, one black and two white. In experiment Exp. III, there are four aggregation sites in the arena, two black and two white. The task of the robots is to find and aggregate on a single black site. Some of the robots are informed on which type of site (i.e., black or white) to aggregate. The proportion of informed robots, henceforth denoted as ρ_I is systematically varied from $\rho_I = 0$ (i.e., no robot is informed on which type of site to aggregate) to $\rho_I = 1$ (all the robots are informed on which type of site to aggregate) with a step size of 0.1. For each experiment, we have three different conditions, in which we varied the swarm size (N). As aggregation performance are heavily influenced by swarm density (Cambier et al. 2018*a*), in this chapter we have decided to study scalability with respect to the swarm size by keeping the swarm density constant. Therefore, the diameter of the area as well as the diameters of the aggregation sites are varied in proportion to N. Table 4.1 reports a summary of all experimental conditions. Note that in all experimental conditions, the area of each aggregation site is always large enough to accommodate all the robots of the swarm.

For each Exp., each condition can be divided in 11 tests which differ in the proportion of informed robots ρ_I. For each test, we execute 200 independent runs. In each run, the robots are randomly initialised within the arena, and then they are left free to act according to actions determined by their PFSM for 100,000 time steps. One simulated second corresponds to 10 time steps. Each run differs from the others in the initialisation of the random number generator, which influences all the randomly defined features of the environment, such as the robots initial position and orientation, as well as noise added to sensors readings.

We use ARGoS multi engine simulator (see Pinciroli et al. 2012). The simulation environment models the circular arena as detailed above, and the kinematic and sensors readings of the Foot-bots mobile robots (see Bonani et al. 2010). For our experiments, we made use of only a subset of all possible sensors mounted on the Foot-bots. In particular, the sensory apparatus

Table 4.1: Table showing, for each experiment (Exp.), the characteristics of each experimental condition. In Exp. I, there are two aggregation sites in the arena (one black and one white); in Exp. II, there are three aggregation sites in the arena (one black and two white); in Exp. III, there are four aggregation sites in the arena (two black and two white).

Exp.	swarm size (N)	arena radius (m)	aggregation site radius (m)
I	20	4	0.9
	50	6.32	1.4
	100	8.94	2.0
II	20	4.17	0.9
	50	6.47	1.4
	100	9.16	2.0
III	20	4.19	0.9
	50	6.62	1.4
	100	9.38	2.0

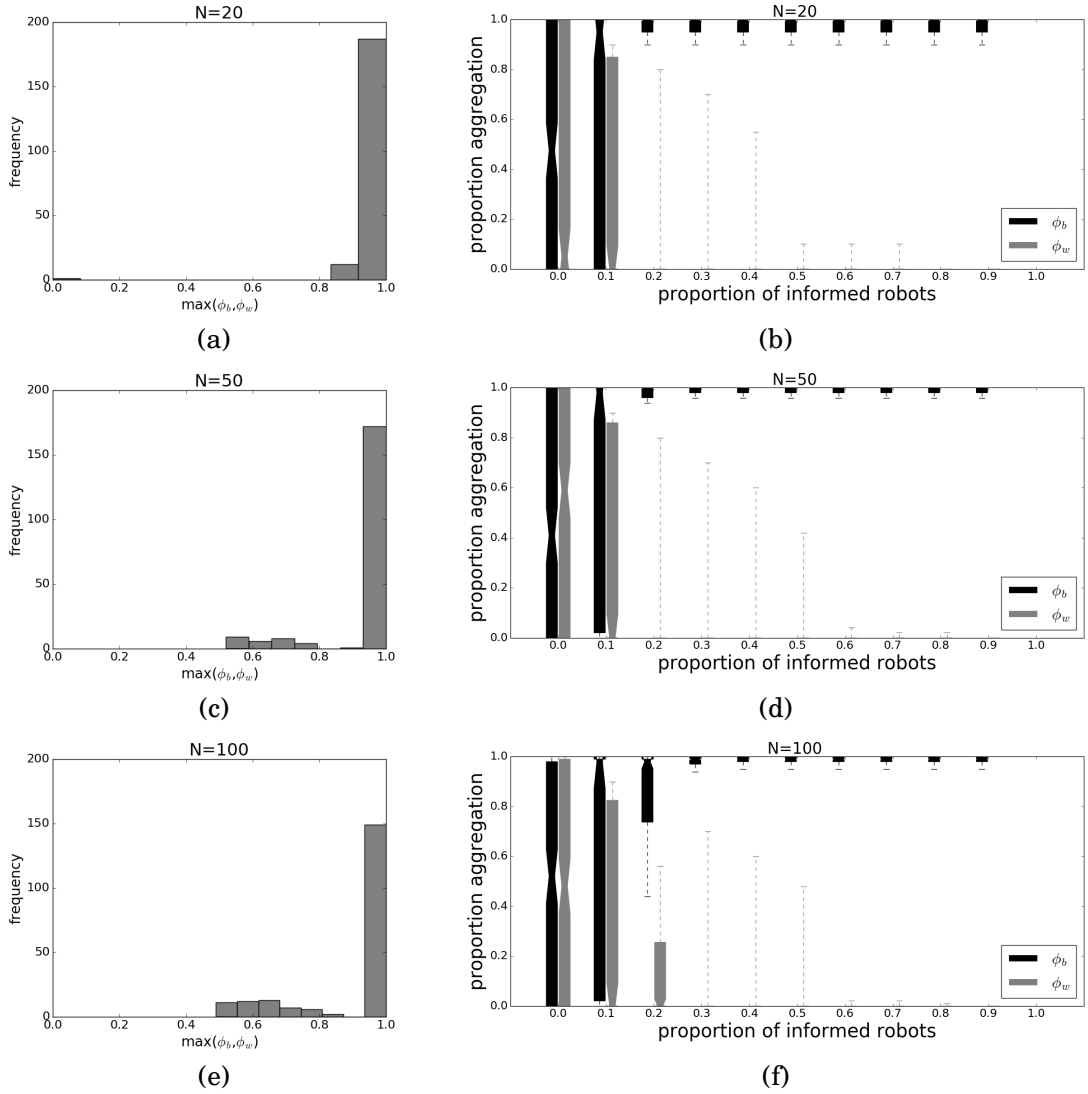

Figure 4.3: Results of the experiments in arena with two aggregation sites. The graphs in first column show frequency histograms of the proportion of robots aggregating on the largest aggregate (max(ϕ_b,ϕ_w)) for swarms without informed robots ($\rho_I = 0$) of size a) N=20; c) N=50; and e) N=100. Graphs on the second column show the percentage of aggregated robots on the white site (i.e., ϕ_w, see grey boxes) and on the black site (ϕ_b, see black boxes) for swarms of size b) N=20; d) N=50; and f) N=100. In each graph, the x-axis refers to the proportion of informed robots. Each box is made of 200 observations. Every observation in black/white boxes corresponds to ϕ_w/ϕ_b computed at the end of a single run, respectively.

of the simulated robots used in this study includes twenty-four proximity sensors positioned around the robot circular body. These proximity sensors have a range of few centimetres and are used for sensing and avoiding the arena's walls and also for sensing and avoiding collisions with other robots. Each robot is also equipped with four ground sensors positioned two on the front and two on the back of the robot underside. These sensors are used to detect the colour

of the floor. In particular, the readings of each ground sensors is set to 0.5 if the sensor is on grey, to 1 if on white, and 0 if on black. A robot perceives an aggregation site when all the four ground sensors return a value different from 0.5. Each robot is also equipped with twelve range and bearing sensors. These sensors are also distributed at equal distance around the robot body. Each sensor can emit a one byte signal and receive a signal sent by another robot positioned at a maximum distance of one metre. Generally speaking, the range and bearing sensors allow a robot to measure the relative distance and angle of neighbouring robots, as well as to allow robots to perceive different neighbouring robots as distinguished entities, which in turns allows robots to count the number of neighbours. Despite this, in the spirit of the existing research done in the context of self-organized aggregation, we only allow our robots to use the second feature (i.e. counting the number of neighbours), whereas the relative distance and angle is not used by our simulated robots to plan their actions. As already mentioned in section 3, for these set of experiments, the range and bearing signals are used by the robots to estimate the parameter n necessary to compute P_{stay} and P_{leave}. The maximum number of neighbours a robot can detect is equal to the number of range and bearing sensors (i.e., twelve).

During an experiment, each robot signals its state (i.e., signal 0 for state $\mathscr{RW}$, signal 1 for state $\mathscr{S}$, and signal 2 for state $\mathscr{L}$). A robot that first enters into an aggregation site or a robot currently stationing into an aggregation site counts how many of its range and bearing sensors receive a signal 1. These signals are undoubtedly sent by robots, in state $\mathscr{S}$, currently positioned on the same aggregation site of the robot receiver. This is guaranteed by the fact that the aggregation sites are positioned more than one metre away from each other in any experimental scenarios, and by the fact that the range and bearing can only detect signals sent by robots positioned at less than one metre distance. The number of signal 1 received corresponds to the number of neighbours and is used to set the parameter n in equation 4.2 and 4.3 (see section 4.2).

4.4 Results

The main aim of this study is to look at how informed robots influence the aggregation dynamics in scenarios where there are two or more possible aggregation sites, that can be differentiated only by informed robots. To do this, we used as performance indicator the proportion of robots aggregated on black site as $\phi_b = \frac{N_b}{N}$ and on white site as $\phi_w = \frac{N_w}{N}$ (where N_b and N_w are the number of robots aggregated on the black and white site, respectively) at the end of each run (i.e., after 100,000 time steps). For those scenarios with more than one site of the same colour as in Exp. II and in Exp. III, N_w refers to the largest aggregate on white sites while N_b refers to the largest aggregate on black sites. The goal of the swarm is to maximise ϕ_b and to minimise ϕ_w. Note that $\phi_b + \phi_w \leq 1$ as it is possible that not all robots have aggregated in either type of site by the end of a run.

4.4.1 Exp. I: arena with two aggregation sites, one black and one white

In this section, we describe the results of Exp. I, which refers to the two-site aggregation scenario, with one black and one white site (see Figure 4.2a). Prior to testing the effect of informed robots, we conduct a first set of experiments to validate our model. The model we used is strongly influenced by the work of Garnier et al. (2009*c*). According to this study, in presence of perfectly symmetrical aggregation sites, this aggregation model results in a symmetry breaking, whereby robots tend to chose one of the two sites at random. They aggregate in the chosen site, provided that the site is big enough to host the entire swarm. This symmetry breaking property is an essential feature of a self-organised aggregation method as it provides the positive feedback mechanism necessary for such behaviour. In order to test whether our model has this feature, we have executed experiments without informed robots in order to replicate the results in (Garnier et al. 2009*c*). To calculate the strength of the positive feedback mechanism, we calculate the proportion of robots aggregated in the largest aggregate as $\max(\phi_b, \phi_w)$, independently on whether it is on the black or the white site. Results are shown in Figure 4.3 first column, in form of frequency distribution. The graphs shows that, independently on the swarm size, the distribution looks multi-modal, with the highest peak at 1.0. This indicates that, for all considered swarm sizes, the swarm is able to create large aggregates (i.e., larger than 90% fo the swarm size) around one of the sites.

With the introduction of informed robots, we analyse how aggregation performance depend on their proportion (i.e., ρ_I). The results are shown in Figure 4.3 second column. We notice that for all swarm size, and when no robot is informed in the swarm ($\rho_I = 0.0$), both ϕ_b and ϕ_w are centred around 0.5 with a strong variation. Without informed robots, aggregates that include more than 90% of the swarm's components occur 98 times on the white site and 100 times on the black site in 200 runs for N=20; 94 times on the white site and 79 times on the black site in 200 runs for N=50; 72 times on the white site and 77 times on the black site in 200 runs for N=100. In summary, without informed robots, swarms form relatively large (i.e, with more than 90% of the swarm's components) aggregates quite frequently (99% of the runs for N=20, 86% of the runs with N=50, and 75% of the runs with N=100). These aggregates can be either on the black or on the white site. This may be explained by the fact that robots chose one aggregate at random without informed robots.

The introduction of as little as 10% of informed robots clearly breaks the almost equal-frequency bimodal aggregation dynamics between the black and the white site and generates new dynamics that tend to bring the majority of the robots on the black site. Furthermore, all three graphs in Figure 4.3 second column, show a similar trend in which the higher the number of informed robots, the higher the proportion of robots aggregated on the black site. This trend is non-linear and reaches saturation at around $\rho_I = 0.2$ for $N = 20$ and $N = 50$, and for $\rho_I = 0.3$ for $N = 100$. With as little as 20% to 30% of informed robots, the totality of the runs finishes with more than 90% of the robots aggregated on the black site (see black boxes for $\rho_I = 0.2$ in

Figure 4.3b and 4.3d, and for $\rho_I = 0.3$ in Figure 4.3f). For the smallest and the medium swarm size (N=20 and N=50, see Figure 4.3b and 4.3d) 20% of informed robots is enough to bring forth very robust and consistent aggregation dynamics that take the entire swarm on the black site. For the largest swarm size, similar robust and consistent dynamics can be observed when the proportion of informed robots is at least 30% (N=100, see Figure 4.3f). In summary, the above results indicate that with a proportion of informed robots varying from 0.2 to 0.3 of the entire swarm, it is possible to generate robust and consistent aggregation dynamics that take the totally of the swarm on a single site, in a task in which two possible aggregation sites are available.

The graphs in Figure 4.4 show details on the time dynamics of the aggregation process for three different values of ρ_I ($\rho_I = 0.1$ in Figure 4.4a, $\rho_I = 0.3$ in Figure 4.4b, and $\rho_I = 0.6$ in Figure 4.4c) and with the largest swarm size N=100. All figures feature a non-linear increase of the proportion of robots aggregated on the black site (i.e., ϕ_b), which eventually reaches saturation. By increasing the percentage of informed robots, we initially observe that distribution of convergence values changes dramatically from $\rho_I = 0.1$ to $\rho_I = 0.3$. In the latter case, we already observe the almost totality of the runs converging to all robots aggregated on the black site, as the dashed top curve in Figure 4.4b tend to converge to $\phi_b = 1$. When we increase ρ_I to 0.6, we observe that the variation between the different runs reduces dramatically while converging, and that all quartile of the distributions tend to converge to $\phi_b = 1$. Additionally, we can also notice that, with the increment of the proportion of informed robots from $\rho_I = 0.1$ to $\rho_I = 0.3$, the slope of the curve becomes slightly steeper during both the first and the second phase. That is, by progressively increasing ρ_I the aggregation dynamics unfold in such a way that higher proportion of robots aggregated on the black site appear earlier during the run. To conclude, we can state that both speed (in terms of convergence) and accuracy (in terms of increase of percentage of robots aggregating on the desired site) of the aggregation process increase with increasing proportion of informed robots.

4.4.2 Arena with three and four aggregation sites

In this section, we report the results of the simulations in a scenario with three sites (see Figure 4.2b) and four sites (see Figure 4.2c).

The three-site scenario features an asymmetry in terms of the characteristics of the aggregation sites. White sites take up twice as much arena's area than the single black site. Thus, each robot is roughly twice as likely to find and eventually to stop on a white than on the black site. Our aim is to investigate whether and which proportion of informed robots is eventually required to invert the asymmetry and to induce the swarm to aggregate on the black site. As for the two-site scenario, prior to testing the effect of informed robots, we look at the frequency distribution of the largest aggregate for three different swarm sizes without informed robots ($\rho_I = 0$). For this scenario, since it features a clear asymmetry in favour of the white site, we expect the swarm to systematically form large aggregate—with more than 90% of the swarm—and to preferentially

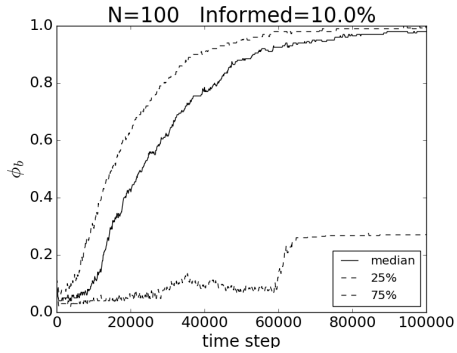

(a)

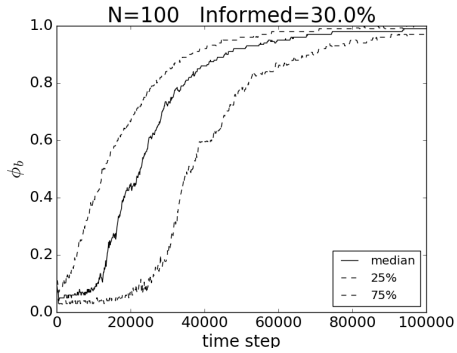

(b)

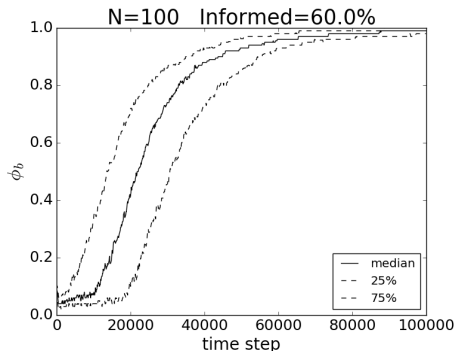

(c)

Figure 4.4: Graphs showing the median (see continuous line), the first and third quartile (see dashed lines) of the proportion of robots aggregated on the black site (ϕ_b) at every time step for 200 runs with swarm size N=100, in arena with two aggregation sites. In a) 10% of the swarm is informed; in b) 30% of the swarm is informed; in c) 60% of the swarm is informed.

aggregate in any of the two white site. Results of this test are shown in Figure 4.5 first column. The graphs indicate that, independently of the swarm size, in the absence of informed robots, the distributions look multi-modal with the highest peak at 1.0. We have also observed that aggregates that include more than 90% of the swarm's components occur 131 times on the white site and 66 times on the black site in 200 runs for N=20; 97 times on the white site and 70 times on the black site in 200 runs for N=50; 99 times on the white site and 41 times on the black

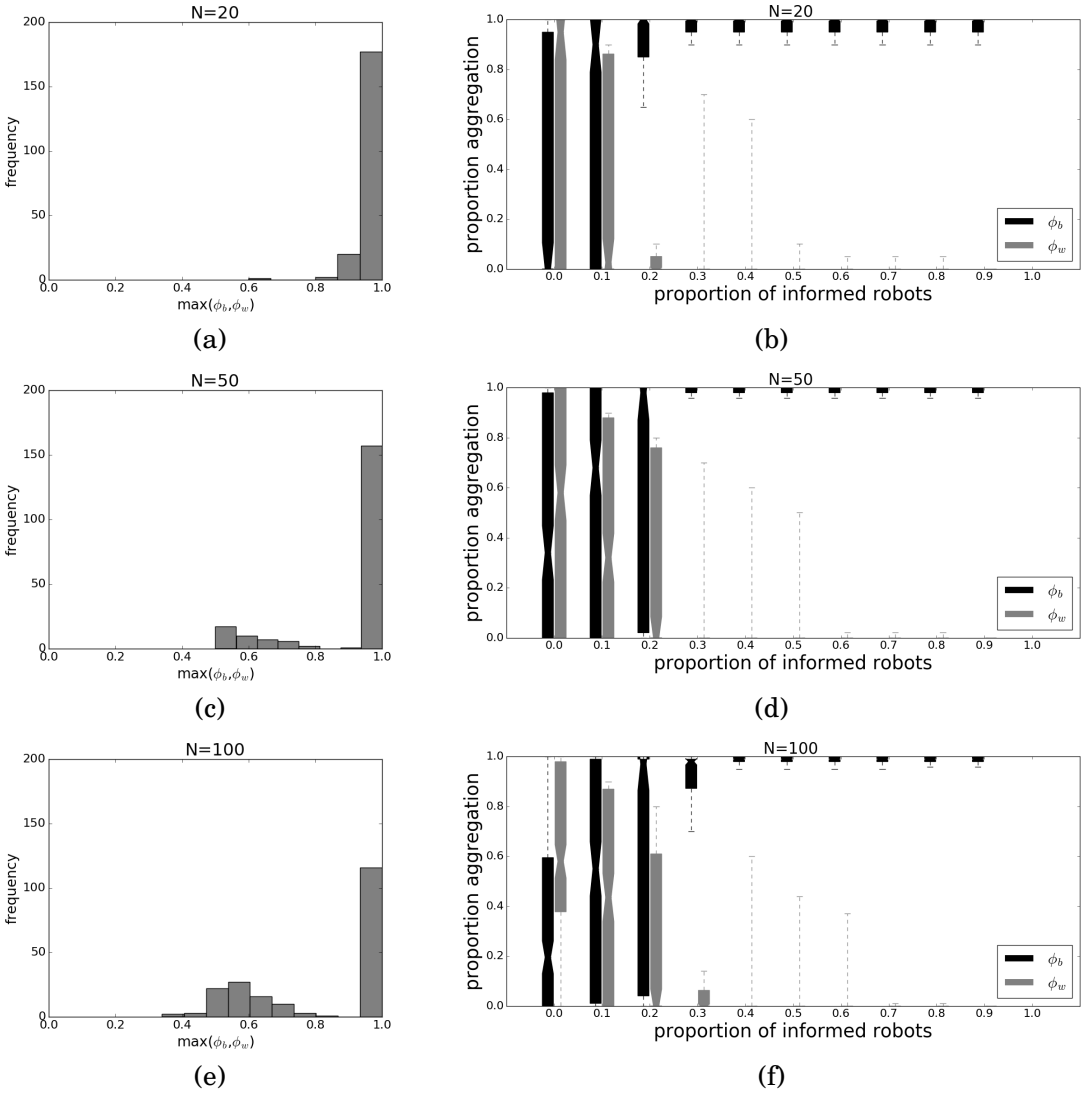

Figure 4.5: Results of the experiments in arena with three aggregation sites. The graphs in first column show frequency histograms of the proportion of robots aggregating on the largest aggregate (max(ϕ_b,ϕ_w)) for swarms without informed robots ($\rho_I = 0$) of size a) N=20; c) N=50; and e) N=100. Graphs on the second column show the percentage of aggregated robots on the white site (i.e., ϕ_w, see grey boxes) and on the black site (ϕ_b, see black boxes) for swarms of size b) N=20; d) N=50; and f) N=100. See also caption Figure 4.3 for more details.

site in 200 runs for N=100. This suggest that, without informed robots, large aggregates (i.e., aggregates with more that 90% of the swarm's components) are relatively frequent (i.e., they occur in 98% of the runs for N=20; in 84% of the runs for N=50; in 70% of the runs for N=100), and they are more likely to occur on a white than on the black site.

With the progressive introduction of informed robots ($0 \leq \rho_I \leq 1$)), the aggregation dynamics change quite radically as indicated in Figure 4.5 second column. For the small swarm size, 20%

of informed robots (i.e., $\rho_I = 0.2$) is sufficient to invert the above mentioned trend, by generating a large majority of runs that end with more than 80% of the robots aggregated on the single black site. For the medium and the large swarm size, a slightly higher proportion of informed robots (i.e., $\rho_I = 0.3$) is required to observe the desired aggregation dynamics. As for the two-site scenario, also in the three-site scenario we observe that the higher the number of informed robots, the higher the proportion of robots aggregated on the black site. In summary, the above results indicate that with a proportion of informed robots varying from 0.2 to 0.3 of the entire swarm, it is possible to invert the swarm tendency to aggregate on the more represented (in terms of arena's area taken) type of site, and to generate robust and consistent aggregation dynamics that take the large majority of the swarm on the less represented (in terms of arena's area taken) type of site.

The four-site scenario, like the two-site scenario, is symmetric with respect to the arenas's area taken by the two types of site. However, the fact that there are two black sites instead of one represents a further challenge for the emergence of a single aggregate on a black site. Informed robots, which avoid to stop on white sites, are likely to stop on both black sites. This can be a deterrent to the formation of a single aggregate. For example, in the likely event in which informed and non-informed robots distribute on both black sites, a single aggregate can emerge only if the robots, including informed robots, in one of the two target sites leave that site for eventually joining the other target site. Therefore, in this scenario more than in the two previously seen, it is the combination of the probability of staying on a site (P_{stay}) and the probability of leaving (P_{leave}) that generate the desired swarm dynamics.

As for the previous two experiments, we look at the frequency distribution of the largest aggregate for three different swarm sizes without informed robots ($\rho_I = 0$). Since the scenario is symmetric, we expect the swarm to display the symmetry breaking property discussed above by forming large aggregate—with more than 90% of the swarm—in any of the two types of site. Results of this test are shown in Figure 4.6 first column. The graphs indicate that, independently of the swarm size, in the absence of informed robots ($\rho_I = 0.0$), the distributions look multi-modal with the highest peak at 1.0. For $N = 20$ and for $N = 50$ large aggregate are relatively frequent and tend to occur in roughly the same quantity, on both types of site. For large swarms $N = 100$ (see Figure 4.6e) large aggregate are less frequent than for smaller swarms. The graphs in Figure 4.6e shows that the highest peak at 1.0 occurs less than 100 times over 200 runs, with a quite frequent second highest peak at 0.5 occurring about 50 times. This suggests that on this scenario, robots of large swarms are not as likely as robots of small and medium size swarms to form large aggregate (i.e., aggregates with more than 90% of the swarm's components) on a single site. However, we observed that when the largest aggregate is larger than 90% of the swarm components, the aggregate can be with about equal probability on one of the black or on one of the white sites.

With the progressive introduction of informed robots ($0 \leq \rho_I \leq 1$), the aggregation dynamics

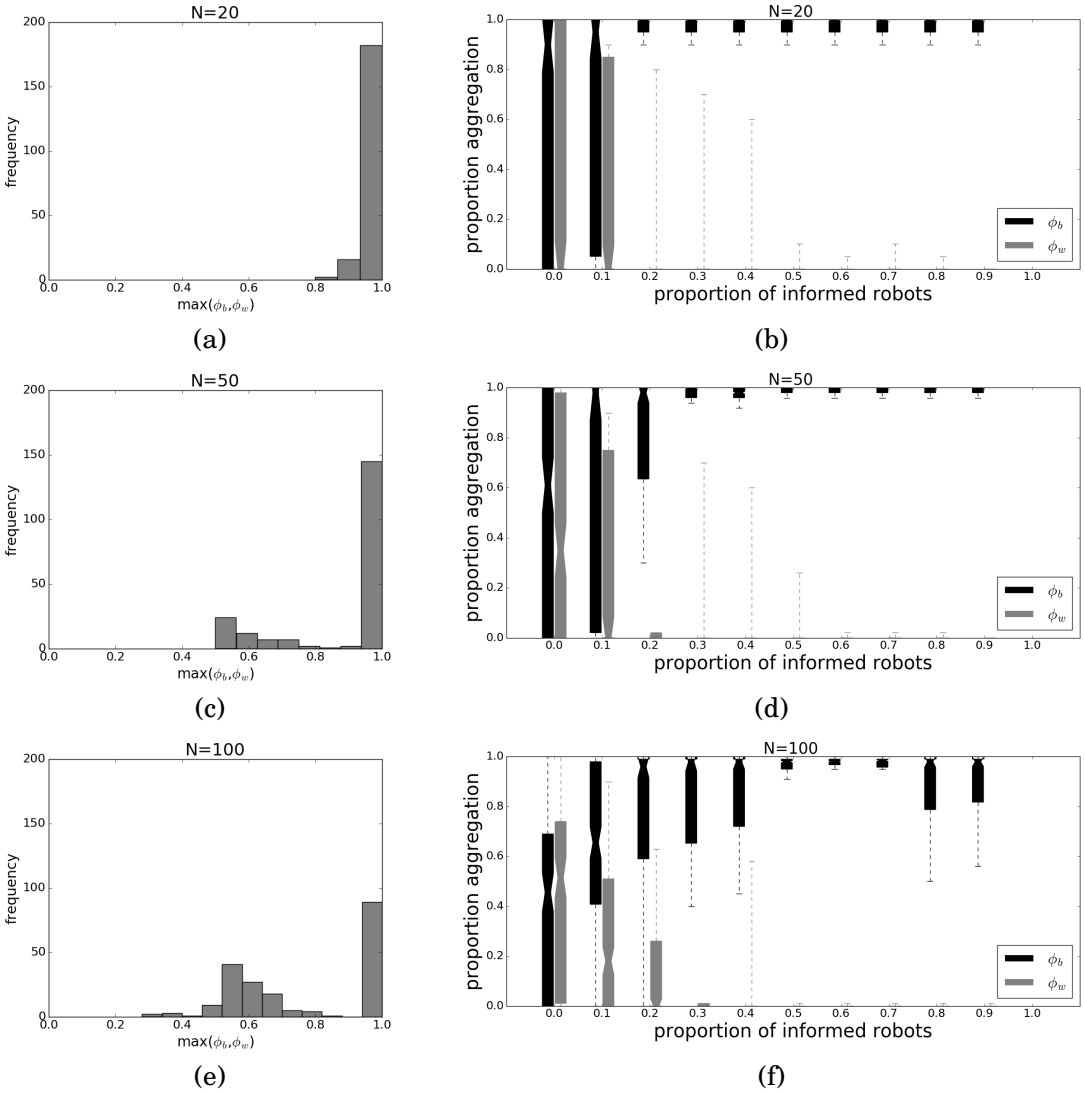

Figure 4.6: Results of the experiments in arena with four aggregation sites. The graphs in first column show frequency histograms of the proportion of robots aggregating on the largest aggregate (max(ϕ_b,ϕ_w)) for swarms without informed robots ($\rho_I = 0$) of size a) N=20; c) N=50; and e) N=100. Graphs on the second column show the percentage of aggregated robots on the white site (i.e., ϕ_w, see grey boxes) and on the black site (ϕ_b, see black boxes) for swarms of size b) N=20; d) N=50; and f) N=100. See also caption Figure 4.3 for more details.

change quite radically as indicated in Figure 4.6 second column. For the small and medium size swarm, 20% of informed robots (i.e., $\rho_I = 0.2$) is sufficient to result in the large majority of runs ending with more than 80% of the robots aggregated on a single black site (see Figure 4.6b, and 4.6d). Moreover, the higher the proportion of informed robots, the higher the proportion of robots aggregated on a single black site. For the large swarm size, results are quite different, since the progressive increment of the proportion of informed robots does not result in a progressively

higher proportion of robots aggregated on a single black site (see Figure 4.6f). Observation of the behaviour of the simulated robots reveal that with more than 70% informed robot (i.e., $\rho_I > 0.7$), swarms are very likely to form a large aggregate on a black site and a smaller aggregate on the other black site. In view of this, we claim that the aggregation dynamics generated by swarms with a high proportion of informed robots can be explained in the following. A high proportion (i.e., $\rho_I > 0.7$) of informed robots (i.e., robots that avoid to stop on white sites) in the swarm makes very likely the emergence of two aggregates, one on each black site. These aggregate can become large enough to generate cases in which each robot currently on black has enough neighbours to have an extremely low probability of leaving. Recall that the probability of leaving a site decreases with respect to the number of neighbours (see also section 4.2). This makes the two aggregates relatively stable. Therefore, anytime they emerge they are likely to last until the end of the run. This is also a consequence of the fact that the maximum number of neighbours a robot can perceived does not scale up with the swarm size, but it is bounded to 12 by the characteristics of the sensor used to collect this information. With progressively less informed robots these dynamics do not emerge even in large swarm. This is the reason why with a proportion of informed robots in $0.4 \leq \rho_I \leq 0.7$ we manage to systematically induce the swarm to aggregate on a single black site even in a scenario with two back and two white sites. This undesired effect observed in large swarms when $\rho_I > 0.7$ does not occur when the swarm size is smaller, since the neighbours of robots on black are rarely large enough to reduce the P_{leave} of each single robot currently on a black site to the point at which any aggregate becomes stable. Thus, smaller aggregates on a black site tend to disappear relatively quickly.

In summary, the results of our study indicate that, for all experimental scenarios, a properly balanced proportion of informed robots is sufficient to generate robust and consistent aggregation dynamics that take more than 90% of the swarm's components on a single aggregation site chosen by the experimenter. In all our simulations, the chosen site is the black one. In all scenarios (i.e., the two-site, the three-site, and the four-site scenario), we observed that the higher the number of informed robots, the higher the proportion of robots aggregated on a black site. In the two-site and the three-site scenario similar aggregation dynamics have been observed for what concerns the relationships between the swarm size and the proportion of informed robots in the swarm. In particular, we observed that the larger the swarm size, the higher the minimal proportion of informed robots required to systematically generate a single aggregate on a black site. Both in the two-site and and in three-site scenario, for the smallest swarm (swarm size $N = 20$), the minimum number of informed robots required to systematically generate a single aggregate on a black site is 4 (that is, 20% of the swarm size) while, for the largest swarm (swarm size $N = 100$), the minimum number of informed robots required to systematically generate a single aggregate on a black site is 30 (that is, 30% of the swarm size). Slightly different aggregation dynamics have been observed in the four-site scenario for what concerns the effect of informed robots on the largest swarm size. Indeed, we observed that, with two black and two white aggregation

sites, when the swarm is large (swarm size $N = 100$), a too high proportion of informed robots (higher than 60%) makes the emergence of a single aggregate on a black site less likely than with a smaller proportion of informed robots. We accounted for this observation by calling upon the fact that the capability of each robot to sense the local density at an aggregation site is bounded to the characteristics of its sensors. This capability does not scale up with the swarm size. Thus, with a relatively large swarm and with two potentially good aggregation sites, whenever two relatively big aggregates emerge one on each black site, none of them can be easily dissolved if the robots that are part of them have the perception to be in a "crowded" site. This phenomenon does not appear with smaller swarms (swarm size $N = 50$ and $N = 20$) because apparently there is not enough robots to form two aggregates, one on each black site, where the robots that are part of them feel in a "crowed" site. This is an effect that brings forth unexpected and possible undesired relationships between proportion of informed robots and swarm size. However, it is worth to notice that, even in the four-site scenario with swarm size $N = 100$ we observed that i) the minimum number of informed robots required to systematically generate a single aggregate on a black site is 30 (that is, 30% of the swarm size), and ii) for proportion of informed robots between 0 and 60%, the usual relationship emerges by which the higher the number of informed robots, the higher the proportion of robots aggregated on a single black site.

4.5 Analysis of aggregation dynamics with an ODEs' model

In this section, we complement our study on the aggregation dynamics using a macroscopic mathematical model. The model we propose is based on ODEs and is targeted at studying the two-site scenario (see Figure 4.2a). In particular, we extend the ODEs originally introduced and discussed in (Amé et al. 2004) and subsequently reused in other studies on self-organised aggregation (e.g., Amé et al. 2006, Campo et al. 2010*a*). The extension we propose includes a term that models the presence of the informed robots. The resulting model is the following:

$$\begin{cases} \dot{N_b} = -N_b\lambda_b + \mu\Big(1 - \dfrac{N_b}{S}\Big)\Omega; & (4.4) \\ \dot{N_w} = -N_w\lambda_w + \mu\Big(1 - \dfrac{N_w}{S}\Big)\Omega(1-\rho_I); & (4.5) \end{cases}$$

with

$$\lambda_b = \frac{\epsilon}{1+\gamma\Big(\frac{N_b}{S}\Big)^2}; \qquad \lambda_w = \frac{\epsilon}{1+\gamma\Big(\frac{N_w}{S}\Big)^2}; \tag{4.6}$$

and

$$\Omega = (N - N_b - N_w); \tag{4.7}$$

In this model, the two state variables are the number of robots on the black and white sites, that is N_b and N_w. μ represents the "discovery rate" of a site, λ_b is the rate of leaving a black site, λ_w

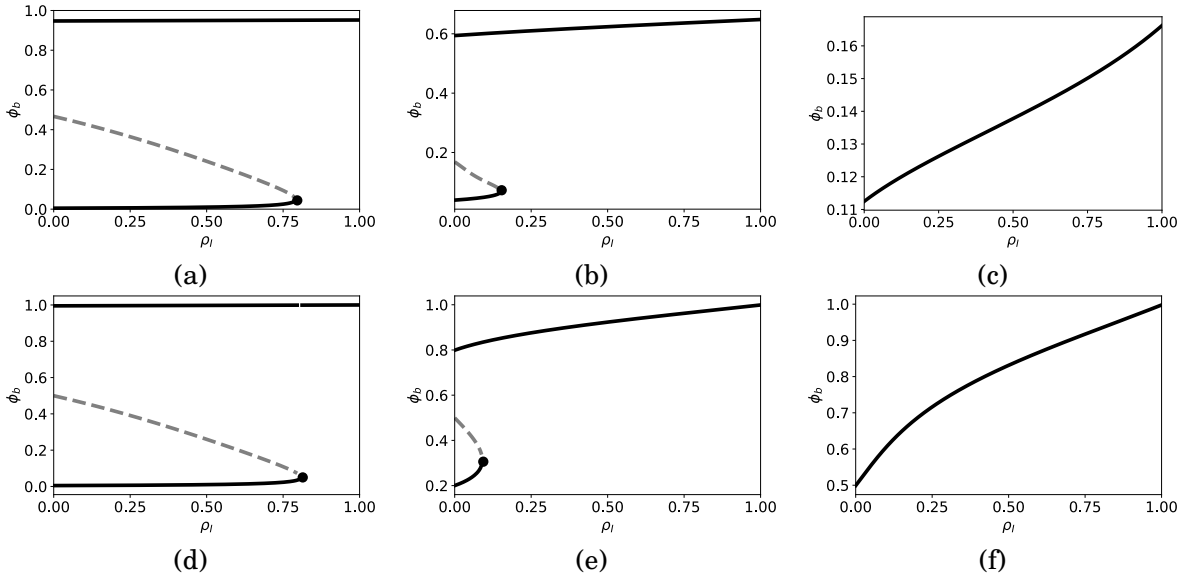

Figure 4.7: Bifurcation diagrams of the system of ODEs we propose as an extension of the model in (Amé et al. 2006). These plots show what happens to the proportion of robots aggregating to the black site ϕ_b as a function of the proportion of informed robots ρ_I. Continuous line represent stable equilibria, while dashed lines represent unstable ones (i.e. saddle points). The big filled dots represent bifurcation points, in this case saddle-node bifurcations. In all plots, $\epsilon = 0.01$. In the first row, $\mu = 0.001$, while in the second row $\mu = 1.5$. Parameter γ is set to the following values. (a) $\gamma = 1667$, (b) $\gamma = 250$, (c) $\gamma = 170$, (d) $\gamma = 1667$, (e) $\gamma = 50$, (f) $\gamma = 20$. For all graphs, $\sigma = \frac{S}{N} = 2.0$.

is the rate of leaving a white site, N is the swarm size, and S is the site carrying capacity. The leave probabilities for the black (λ_b) and the white site (λ_w) are expressed as sigmoidal response to the density of robots ($\frac{N_{b/w}}{S}$) at each site, with ϵ and γ being the parameters of the sigmoid. The probability to join a site is ($1 - \frac{N_{w/b}}{S}$), which is 1 when no other robots is on the site, decreases linearly as the number of robots on the site increases, and is 0 when the site is full. The number of robots on the black (resp. white) site decreases proportionally to the leave probability $\lambda_{b/w}$ and to the current number of robots on the black (resp. white) site. It increases proportionally to the rate μ at which a site is encountered, to the join probability ($1 - \frac{N_{w/b}}{S}$), and to the proportion of robots "free roaming" available to join a site, that is robots that are in neither of the aggregates Ω. In our version of the model, we also introduce the term $(1 - \rho_I)$ for the equation concerning the white site (w). This term rescales the number of robots that can potentially join a white site to only the non-informed robots, since informed robots never rest on the white site. The model in (Amé et al. 2006) can be recovered by setting $\rho_I = 0.0$.

In the original study (Amé et al. 2006), some model parameters were kept fixed while others were studied in details. The parameters that were kept fixed were tuned after the experiments performed with the real cockroaches, and the corresponding values were: $\mu = 0.001s^{-1}$, $\epsilon = 0.01s^{-1}$, and $\gamma = 1667$. Different values for the ratio $\sigma = \frac{S}{N}$ were tested. Only when $\sigma > 1$ ($S > N$) (e.g., when $N = 100$, and $S = 200$) the swarm manage to fully aggregate on a site. In this study, we

will only consider the case $S > N$, but we will study how the dynamics change by varying the other parameters μ, ϵ, and γ, as those are the parameters that vary when robotics experimental conditions (such as the size of the arena, the size and speed of the robots, the random walk strategy followed, etc ...) are varied.

Our main objective is to study the effects of different proportions of informed robots ($0 \leq \rho_I \leq 1$) on the aggregation dynamics, and in particular on the proportion of robots on the black site (ϕ_b). This analysis is best exemplified using a bifurcation analysis, that is, by checking what happens to the steady states of the systems when we vary our key parameter ρ_I. For the sake of generality, we report on the y-axis the proportion, rather than the number, of robots on the black site $\phi_b = \frac{N_b}{N}$.

To start with, we consider the original values of the parameters studied in (Amé et al. 2006), that is $\mu = 0.001s^{-1}$, $\epsilon = 0.01s^{-1}$, $\gamma = 1667$, and $\sigma = 2.0$. As shown in Figure 4.7a the model predicts that when ρ_I is smaller than a critical value very close to 0.8, two equilibria exist: $\phi_b \approx 1$ and $\phi_b \approx 0$. This means that the two states represented by having all robots aggregated to the black or to the white site are equally likely, according to the model. This result is exactly the same obtained in (Amé et al. 2006). However, at the critical threshold for ρ_I, a saddle-node bifurcation occurs. After this value, only one stable equilibrium is found, which corresponds to the state seeing all robots aggregated on the black site. In other words, the model predicts that, in the original experimental setup with cockroaches, about 80% of the cockroaches would need to be informed in order to have aggregation on the website.

Since our robots are not cockroaches, we were curious to see what happened when varying the parameters, in order to get as close as possible to the regime observed in the robotics simulations. We observed that by varying the parameter ϵ and σ no changes is observed with respect to the proportion of robots required to get the entire swarm aggregate on the black site. Instead, we observed interesting changes at the variation of the parameter γ. As shown in Figure 4.7b, with a much lower value of $\gamma = 250$, the bifurcation occurs much earlier in the ρ_I parameter space. However, the higher stable equilibrium is no longer close to 1, but to 0.6. This means that slightly more than half of the robots can aggregate on black site with as little as 20% of informed robots, but there is no way to have all robots aggregating on the black site. When we further decrease γ to 170, we observe completely different dynamics, whereby the bifurcation no longer exists and even smaller aggregates form, with a size that increases with increasing ρ_I, reaching a maximum of about 20% of the swarm (see Figure 4.7c).

In the above analysis, we observed that none of those parameters could replicate the results that we obtain in simulation, that sees robots aggregating in large proportions to the black site with a small proportion of informed robots. Therefore, we hypothesised that the remaining parameter, μ, had to be studied in order to find a regime in which our simulation experimental results could qualitatively be reproduced. After exploring this new parameter, we found that those dynamics can be reproduced with a much larger value for the site discovery rate μ.

We report in the bottom row of Figure 4.7 the results of the analysis performed with $\mu = 1.5$ and with $\gamma = 1667$ (Figure 4.7d), $\gamma = 50$ (Figure 4.7e), and $\gamma = 20$ (Figure 4.7f). As we can see, the results are qualitatively similar to those obtained with low discovery rate $\mu = 0.001s^{-1}$, but the stable state in the higher branch is now very close to 1. When $\gamma = 1667$, the critical ratio of informed robots is above 80%. When $\gamma = 50$, we obtain near ideal results, similar to those obtained in simulation, whereby the critical ratio of informed robots is below 20%. With $\gamma = 20$ once again no bifurcation occurs, however with 100% informed robots the system is able to aggregate all robots on the black site.

Although the fine tuning of the model parameters after the simulation is out of scope for this chapter, we have clearly seen here for the first time that the extended model of (Amé et al. 2006) is indeed very rich in terms of dynamics. Experimental parameters μ and γ play a crucial effect. However, many of these are out of the designer controls, with the exception of γ, a component of the leave probability. This suggests that the leave probability is of critical importance when designing self-organized aggregation, even in presence of informed robots.

4.6 Conclusions

In this chapter, we have contributed to the wider agenda of studying the role of informed individuals in the context of collective decision making in swarms of robots. We have focused on self-organised aggregation in scenarios that feature two types of aggregation sites: a site coloured in black and a site coloured in white. The circular arena's floor where the robots operate is coloured in grey. We studied three different scenarios: two symmetrical scenarios, in which either two or four aggregation sites are available in the environment, and an asymmetrical scenario in which three aggregation sites are available. In the symmetric scenario, the two types of aggregation site (the black and the white) are equally represented. In the asymmetric scenario, one type of aggregation site (the white) is twice as much represented than the other type of site. In all scenarios, the robots are required to form a single aggregate, on a black site. We considered a swarm of robots divided in two sets: informed robots, that possess extra information on which site the swarm has to aggregate. Therefore, they selectively avoid to stop on any white site. Non-informed robots do not possess this extra information. Therefore, they are equally likely to stop on a white and on a black site according to the mechanisms of the finite state machine that controls their behaviour. The objective of this study is to look at whether and eventually which proportion of informed robots is required to direct the aggregation process toward a pre-defined type of site (i.e., the black) among those available in the environment.

We conducted experiments using the ARGoS simulator in which we varied the proportion of informed robots from 0% to 100%. Our results show that, in absence of informed robots, in all the three different scenarios, and for different swarm size, the swarms tend to form a single large aggregate (i.e., aggregates made of more than 90% of the robots). In symmetric scenarios,

these large aggregates emerge with almost equal frequency on both the black and the white site. In the asymmetrical scenario, the large aggregates are more frequently observed on the most represented type of site (i.e., the white one). The original contribution of this study is in showing that the above mentioned dynamics can be modified with as little as 20% of informed robots. In particular, in the simplest two-site scenario, we show that when at least 20% of the robots are informed, the entire swarm aggregates on the black site, for all swarm sizes we have considered. We have also shown that the speed and accuracy of convergence is also strongly affected by the proportion of informed robots. In the asymmetrical three-site scenario, largest aggregates can be easily induced to emerge entirely on the black site with 20% to 30% of informed robots depending on the swarm size. On the four-site symmetrical scenario, 20% of informed robots are sufficient to systematically generate large aggregates on one of the black site. However, for large swarms (i.e., swarm size $N = 100$) the presence of too many informed robots in the swarm is counterproductive, since it frequently leads to the formation of more than one aggregate on different black sites. We believe that the formation of multiple aggregates in this scenario is a results of the relationships between the high proportion of informed robots, the robots' perceptual apparatus used to detect and count neighbouring agents currently resting on a site, and the mechanisms that regulate the probability of a robot to leave a site. Future work, in which we will explore the relationships among these three factors, by systematically varying them, are needed to fully corroborate our claim.

Another valuable contribution of this study is the analysis of the ODEs model discussed in (Amé et al. 2006) to account for the dynamics of self-organised aggregation observed in cockroaches by calling upon the principle of attraction between individuals. In (Amé et al. 2006) and in (Campo et al. 2010*a*), this model is used to investigate how the aggregation dynamics changes by varying the size of aggregation site and consequently their carrying capacity. We extended the model by introducing the concept of informed robots. By exploring the parameters of the model, we show that under specific conditions, the model predicts the results we observed in the simplest two-site scenario (see section 4.3). That is, the model shows that with about 20% of informed robots the emergence of a large aggregate on black is a stable equilibrium of the system. The analysis of the model's parameters leads to a deeper understanding of the relationships between environmental features and agents' exploration strategies. We show how these relationships bear upon the emergence of a single aggregate and how they interfere by amplifying or by reducing the effects of informed robots on the group aggregation process.

CHAPTER 5

GUIDING AGGREGATION DYNAMICS IN A SWARM OF AGENTS VIA INFORMED INDIVIDUALS: AN ANALYTICAL STUDY

5.1 Introduction

In this chapter, we discuss the results of a mathematical model that looks at aggregation dynamics in a swarm of agents with different proportions of informed and non-informed individuals. Mathematical models are quite frequently used in the study of collective behaviour in artificial swarms to avoid the time and computational costs that robotics and others agent-based models undergo to explore the effects of a wide range of experimental conditions (Brambilla et al. 2013). Mathematical model of self-organised aggregation include geometric models (Bayindir & Şahin 2009) and Markov chains (Soysal et al. 2007). To study other collective behaviours, common approaches to modelling include ordinary differential equations (Montes de Oca et al. 2011, Valentini et al. 2016*b*), stochastic differential equations such as rate equations (Lerman & Galstyan 2002), chemical reaction networks (Valentini et al. 2016*b*), Fokker-Planck and Langevin equations (Hamann & Wörn 2008), and control theory (Hsieh et al. 2008), among others. Our model uses a system of ordinary differential equations to study how informed individuals can be used in the context of aggregation to distribute the agents of a swarm between two distinctive aggregation sites (one perceived by the individuals as black and the other as white) according to two arbitrary rules specified by the designer. There are two types of informed individuals in our model: the "informed for black" individuals which rest only on the black site, and the "informed for white" individuals which rest only on the white site. Excluding the informed individuals of any type, the rest of the swarm is made of non-informed individuals, that is agents that rest on both aggregation sites with equal probabilities. Both informed and non-informed individuals leave an aggregation site with a probability given by a non-linear function of the density of individuals at

the site.

Our objective is to find out whether and eventually for which parameter range the swarm distributes between the two sites according to the relative proportion of one type of informed individuals with respect to the other type, by keeping the total proportion of informed individuals as small as possible. We analyse the system for different total percentage of informed individuals in the swarm, from 0% to 100% informed individuals. For each percentage of informed individuals, we systematically vary the relative proportion of informed individuals of one type with respect to the proportion of individuals of the other type. In this chapter, we report the results of two representative scenarios: one in which informed individuals are equally distributed in numbers between the two sites; and one in which the informed individuals for one type of site are three times more than the informed individuals for the other type of site. The first scenario has been chosen to represent the designer aims to induce the agents to aggregate in equal proportion on both sites. The second scenario has been arbitrarily chosen among those representative of the designer intention to induce the agents to aggregate in different proportions on each site. For each of the two scenarios illustrated in this chapter, we varies the total proportion of informed individuals from 0% to 100% of the swarm population size. Moreover, we analyse the systems for different values of the site carrying capacity, that is the total number of individuals that can simultaneously rest on a site. We are interested in identifying the conditions whereby agents equally split on the two aggregation sites when both types of informed individuals are equally represented in the swarm, and the conditions whereby aggregation dynamics see agents aggregated 75% on a site and 25% on the other site, when one type of informed individuals is three time more represented than the other type. The results of this study shows that there are parameters' values for which the distribution of individuals between the two sites matches the relative proportion of one type of informed individuals with respect to the other type. In particular circumstances, the desired aggregation dynamics can be observed with a small minority of informed individuals in the swarm. In other words, the analysis of the mathematical model indicates that informed individuals are a potentially effective means to control the aggregation dynamics in swarms of autonomous agents. In section Conclusions, we discuss the significance of our results for the swarm robotics community, and we explain how we intend to use these finding in our future research works.

5.2 Methods

In this section, we describe the system of Ordinary Differential Equations (ODEs) used to investigate the effects of different proportions of two different types of informed individuals on the aggregation dynamics in a scenario with two sites, a black and a white site. We draw inspiration from another ODEs system originally discussed in (Amé et al. 2004), and subsequently extended in (Amé et al. 2006) to model the aggregation dynamics observed in cockroaches. The

distinctive feature of both the above cited models is that the individual probability of leaving a site is a non-linear function of the number of individuals currently resting at that site. Our departure point is the Amé et al. (2006)'s model, where two aggregation sites, with same characteristics, are symmetrical locations for aggregation for a group of N equal type individuals. The Amé et al. (2006)'s model is the following:

$$\dot{N}_i = -N_i \lambda_i + \mu\Big(1 - \frac{N_i}{S}\Big) N_{ext}; \tag{5.1}$$

with

$$\lambda_i = \frac{\epsilon}{1 + \gamma\Big(\frac{N_i}{S}\Big)^2}; \qquad N_{ext} = (N - \sum_{i=1}^{p} N_i); \tag{5.2}$$

where N_i is the number of individual resting on site i, λ_i is the individual probability to leave site i, the parameter $\epsilon = 0.01 s^{-1}$, the parameter $\gamma = 1667$, S is the maximum number of individuals that a site can host (i.e. the site carrying capacity), $\mu = 0.001 s^{-1}$ is the rate of entering a site, N_{ext} is the number of individuals outside the sites, and $p = 2$ is the number of sites. The analysis of this model shows that the agents form a single aggregate only when each aggregation site can host more that the totality of the swarm's individuals. The model also predicts how the agents distribute in different environments varying for the number of aggregation sites and the diameter of each site bearing upon the site capacity to host individuals (see Amé et al. 2006).

We modified the system in Eq. 5.1 to take into account two novel features that distinctively characterised our study: that is, the differences between the two sites, one of which is perceived by the individuals as black, and the other as white, and the presence of two different types of informed individuals. With the introduction of colour differences between the two sites, the total number of individuals in a group N is given by $N = N_b + N_w + N_{ext}$, with N_b and N_w being the number of individuals resting on the black and on the white site, respectively.

Defining $\sigma = S/N$, $x_b = N_b/N$ and $x_w = N_w/N$, with $N_{ext} = N - N_b - N_w$, leads us to the following system:

$$\begin{cases} \dot{x_b} = -x_b \lambda_b + \mu\Big(1 - \frac{x_b}{\sigma}\Big)(1 - x_b - x_w) \\ \dot{x_w} = -x_w \lambda_w + \mu\Big(1 - \frac{x_w}{\sigma}\Big)(1 - x_b - x_w) \end{cases} \tag{5.3}$$

with

$$\lambda_b = \frac{\epsilon}{1 + \gamma\Big(\frac{x_b}{\sigma}\Big)^2}; \qquad \lambda_w = \frac{\epsilon}{1 + \gamma\Big(\frac{x_w}{\sigma}\Big)^2}; \tag{5.4}$$

where λ_b and λ_w refer to the probability of leaving the black and the white site, respectively. As shown in Eq. 5.3, the system is independent of N and depends only on the fraction of individuals on the two sites.

The distinction between informed and non-informed individuals is introduced into the system with the notation i_w (informed for white) for informed individuals that do not rest on the black

site, i_b (informed for black) for informed individuals that do not rest on the white site, and ni (non-informed) for non-informed individuals, who can potentially rest on both sites. With this distinction in place, ρ_{i_b} and ρ_{i_w} are the proportion of informed individuals of type i_b and i_w, respectively. $x_b^{i_b}$ refers to the fraction of individuals on the black site that are of type i_b; $x_w^{i_w}$ refers to the fraction of individuals on the white site that are of type i_w; x_b^{ni} refers to the fraction of individuals on the black site that are of type ni; and x_w^{ni} refers to the fraction of individuals on the white site that are of type ni. The fraction of individual on the black site (x_b) and on the white site (x_w) is then written as:

$$\begin{cases} x_b = x_b^{ni} + x_b^{i_b} \\ x_w = x_w^{ni} + x_w^{i_w} \end{cases} \tag{5.5}$$

since, by definition, informed individuals of type i_w never rest on the black site, and informed individuals of type i_b never rest on the white site.

Generalising Eq. 5.3 to the case with informed and non-informed individuals gives

$$\begin{cases} \dot{x_b^{i_b}} = -x_b^{i_b}\lambda_b + \mu\left(1-\frac{x_b}{\sigma}\right)x_{ext}^{i_b} \\ \dot{x_b^{ni}} = -x_b^{ni}\lambda_b + \mu\left(1-\frac{x_b}{\sigma}\right)x_{ext}^{ni} \\ \dot{x_w^{i_w}} = -x_w^{i_w}\lambda_w + \mu\left(1-\frac{x_w}{\sigma}\right)x_{ext}^{i_w} \\ \dot{x_w^{ni}} = -x_w^{ni}\lambda_w + \mu\left(1-\frac{x_w}{\sigma}\right)x_{ext}^{ni}, \end{cases} \tag{5.6}$$

where $x_{ext}^{i_b}$, $x_{ext}^{i_w}$, and $x_{ext}^{i_{ni}}$ are the fraction of individuals of type i_b, i_w, and i_{ni} that are outside the two sites. These fractions can be expressed in the following way

$$\begin{cases} x_{ext} = 1 - x_b - x_w = 1 - x_b^{ni} - x_b^{i_b} - x_w^{ni} - x_w^{i_w} \\ x_{ext}^{i_b} = \rho_{i_b} - x_b^{i_b} \\ x_{ext}^{i_w} = \rho_{i_w} - x_w^{i_w} \\ x_{ext}^{ni} = x_{ext} - x_{ext}^{i_b} - x_{ext}^{i_w} \\ \qquad = (1 - \rho_{i_b} - \rho_{i_w}) - x_b^{ni} - x_w^{ni}. \end{cases} \tag{5.7}$$

Finally, substituting Eq. 5.7 into Eq. 5.6 we obtain the following system:

$$\begin{cases} \dot{x_b^{i_b}} = -x_b^{i_b}\lambda_b + \mu\left(1-\frac{x_b}{\sigma}\right)\left(\rho_{i_b} - x_b^{i_b}\right) \\ \dot{x_b^{ni}} = -x_b^{ni}\lambda_b + \mu\left(1-\frac{x_b}{\sigma}\right)\left((1-\rho_{i_b}-\rho_{i_w}) - x_b^{ni} - x_w^{ni}\right) \\ \dot{x_w^{i_w}} = -x_w^{i_w}\lambda_w + \mu\left(1-\frac{x_w}{\sigma}\right)\left(\rho_{i_w} - x_w^{i_w}\right) \\ \dot{x_w^{ni}} = -x_w^{ni}\lambda_w + \mu\left(1-\frac{x_w}{\sigma}\right)\left((1-\rho_{i_b}-\rho_{i_w}) - x_b^{ni} - x_w^{ni}\right). \end{cases} \tag{5.8}$$

In the particular case when all the individuals of the group are informed (i.e. $\rho_{i_b} + \rho_{i_w} = 1$), this set of equations reduces to

$$\begin{cases} \dot{x_b} = -x_b\lambda_b + \mu\left(1-\frac{x_b}{\sigma}\right)\left(\rho_{i_b} - x_b\right) \\ \dot{x_w} = -x_w\lambda_w + \mu\left(1-\frac{x_w}{\sigma}\right)\left(\rho_{i_w} - x_w\right). \end{cases} \tag{5.9}$$

The set of equations illustrated in Eq. 5.8, is solved numerically to find equilibrium states (i.e., when $\dot{x} = 0$). Equilibrium states are studied with respect to the key parameters σ, ρ_{ib} and, ρ_{iw}. The results are discussed in next section.

5.3 Results

In this section, we show the results of our analysis, by discussing the equilibrium states of Eq. 5.8, for different sets of values for the parameters σ, ρ_{i_b}, and ρ_{i_w}. We remind the reader that the parameter σ is the ratio between the site carrying capacity S and the swarm size N. When $\sigma = 1$ each aggregation site can host as many individuals as the swarm size; when $\sigma < 1$, each aggregation site can host fewer individuals than the swarm size; when $\sigma > 1$, each site can host more individuals than the swarm size. ρ_{i_b} and ρ_{i_w} refer to the proportion of individuals of type i_b (informed for black) and i_w (informed for white), respectively. We also remind the reader that our objective is to find out the set of parameters for which the individuals distribute between the two sites according to the relative proportion of one type of informed individuals with respect to the other type. We are also particularly interested in finding what is the critical value of $\rho_i = \rho_{i_b} + \rho_{i_w}$ (i.e. the proportion of informed individuals) above which this objective is realized, and how this changes with respect to σ. For example, when $\rho_{i_b} = 0.3$ and $\rho_{i_w} = 0.3$ we expect 50% of the individuals on the white site and 50% of the individuals on the black site, and we would like to know how much we can decrease both ρ_{i_b} and ρ_{i_w} and still maintain this allocation.

When there are no informed individuals in the swarm ($\rho_{i_b} = 0$ and $\rho_{i_w} = 0$), our model reduces to the original (Amé et al. 2006)'s model. As in (Amé et al. 2006), we also find out that for $\sigma < 1$, the swarm equally distribute between the two sites. However, when $\sigma > 1$ the individuals are able to make a collective decision and to aggregate either on the black or on the white site.

When the entire swarm is composed of informed individuals (i.e. $\rho_{i_b} + \rho_{i_w} = 1$, see also Eq. 5.9), the fraction of individuals aggregated on the black site (i.e., x_b) is shown in Figure 5.1. This graph represents the steady state for x_b when σ varies from 0 to 8, and for different values of the ratio $\frac{\rho_{i_b}}{\rho_{i_w}}$.

In the low σ range, when each site is not big enough to host all the corresponding informed individuals (the black site for individuals of type i_b, and the white site for individuals of type i_w), the individuals allocate themselves to both sites until they reach the site carrying capacity. This trend does not depend on the relative ratio between $\frac{\rho_{i_b}}{\rho_{i_w}}$, therefore for low values of sigma informed agents are not able to influence the aggregation dynamics. When σ surpasses a critical value that depends on $\frac{\rho_{i_b}}{\rho_{i_w}}$, each site becomes big enough to host all the corresponding informed individuals. Steady-state dynamic for different $\frac{\rho_{i_b}}{\rho_{i_w}}$ are qualitatively different but follow a similar trend. Up to a another critical value of σ, again dependent on $\frac{\rho_{i_b}}{\rho_{i_w}}$, most individuals simply aggregate on the site they prefer. This is the regime in which informed agents have a maximal influence on the dynamics. However, above this new critical σ, individuals are no longer able

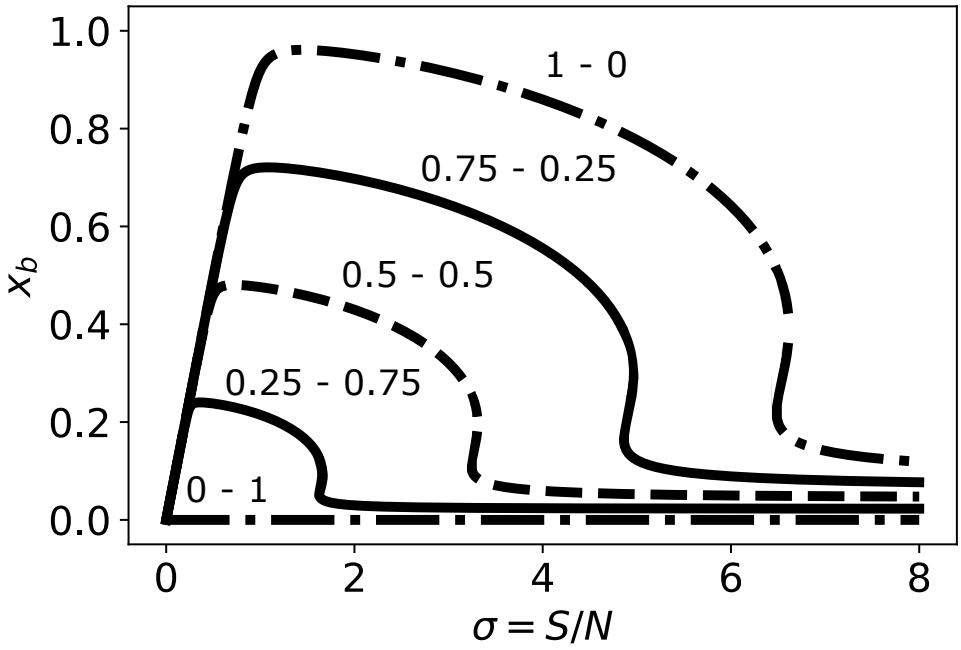

Figure 5.1: Graph showing the steady state for x_b when σ varies from 0 to 8 for different values of the ratio $\frac{\rho_{i_b}}{\rho_{i_w}}$ when the swarm is made of only informed individuals ($\rho_{i_b} + \rho_{i_w} = 1$). The numbers above each line indicate the fraction of informed individuals of types i_b and i_w. Dashed line: $\frac{\rho_{i_b}}{\rho_{i_w}} = 1$. Continuous lines: $\frac{\rho_{i_b}}{\rho_{i_w}} = 3$ or 1/3. Dashed-dotted lines: $\rho_{i_b} = 0$ or $\rho_{i_w} = 0$.

to aggregate at all. This analysis reveals that, as it happened for the original model discussed in (Amé et al. 2006), and regardless of the ratio $\frac{\rho_{i_b}}{\rho_{i_w}}$, environmental parameters such as the site carrying capacity strongly influences the aggregation dynamics and that informed agents can guide self-organisation only in a limited range of this parameter. For example, when the aggregation site becomes too large, the probability to aggregate on a site, which depends on the site current density, tends to remain too low to trigger the aggregation process. In other words, the density of individuals on each site never reaches a critical value to induce the individuals to aggregate on a site. Thus, the individuals tend to disperse rather than aggregate. For each site, the transition between the two regimes illustrated above is determined by the number of informed individuals that are attracted by that particular colour: the higher the number of informed individuals of each type, the higher the size of the site required to trigger the regime change. For each ratio $\frac{\rho_{i_b}}{\rho_{i_w}}$, there exists a maximum size σ_{max} corresponding to the point of regime change. For example, when 75% of individuals are of type i_b and 25% are of type i_w, in order to have all of them aggregated on the corresponding preferred site, σ has to be smaller than 1.6 (see Figure 5.1, continuous lines). When $1.6 < \sigma < 4.8$, the white site becomes too large to trigger aggregation for the individuals of type i_w, while the individuals of type i_b are enough to cope with the dimension of their corresponding aggregation site. When $\sigma > 4.8$, even the black site becomes too large to trigger aggregation.

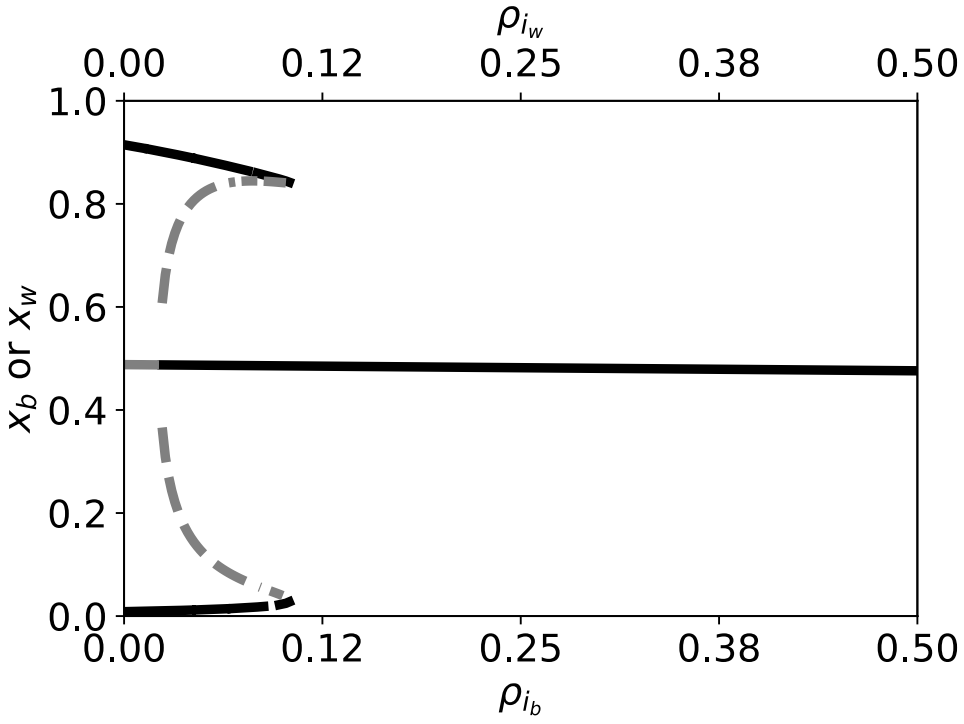

(a)

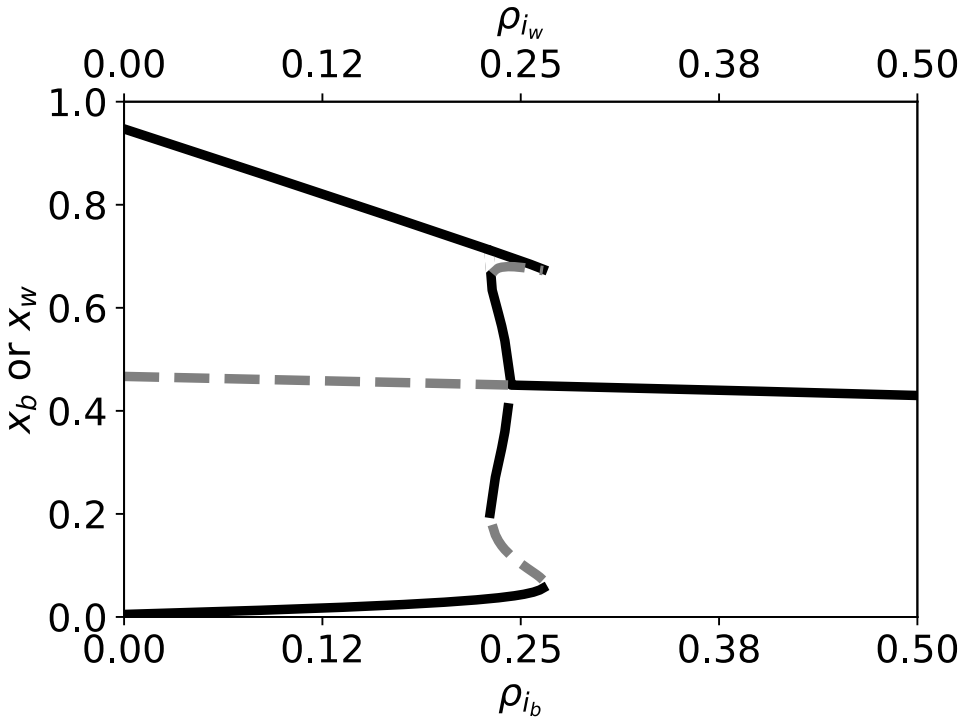

(b)

Figure 5.2: (a) Fraction of individuals on the black and on the white site, when $\frac{\rho_{i_b}}{\rho_{i_w}} = 1$ for (a) $\sigma = 1$ and (b) $\sigma = 2$. Black continuous lines: stable solutions. Dashed grey lines: unstable solutions.

The analysis carried out so far tell us that the most interesting regime is the one in which σ is in a range (dependent on $\frac{\rho_{i_b}}{\rho_{i_w}}$) that allows the individuals to aggregate in their respective preferred sites. In this range, we ask ourselves whether we can now have a hybrid swarm composed of informed and non-informed individuals, and whether informed individuals can still guide the dynamics in a similar way as when the swarm was only composed of informed individuals. We thus proceed by analysing the system for $\sigma = 1$ and $\sigma = 2$ for different proportions of informed individuals in the swarm, and for two different values of the ratio $\frac{\rho_{i_b}}{\rho_{i_w}}$. In all the figures that will follow, we will report stable equilibria with continuous black lines, and unstable equilibria with dashed grey lines.

Figure 5.2a (resp. Figure 5.2b) reports results with the ratio $\frac{\rho_{i_b}}{\rho_{i_w}} = 1$ for $\sigma = 1$ (resp. $\sigma = 2$), that is for each proportion of informed individuals in the swarm, 50% of them are of type i_b and 50% are of type i_w. The graph shows that the individuals aggregate on one site only (i.e. either the black or the white site), until a critical value for the total proportion of informed individuals ρ_i (about 24% of the swarm for $\sigma = 1$ and about 50% of the swarm for $\sigma = 2$), above which individuals are able to aggregate in equal numbers on both sites. Therefore, informed agents are able to guide self-organised aggregation only above a critical proportion of informed individuals, which increases with increasing σ, which therefore suggest that larger aggregation sites have again a counter-intuitive negative effect on the controllability of this self-organised behaviour.

In Figure 5.3, the ratio $\frac{\rho_{i_b}}{\rho_{i_w}}$ is set to 3, that is for each proportion of informed individuals in the swarm, 75% of them are of type i_b and 25% are of type i_w, and $\sigma = 1$. The graphs in Figure 5.3a and 5.3b can be globally understood as follows: below a given threshold of about 10% of informed individuals of type i_b, one of two things can happen: either informed individuals of type i_b and non-informed individuals aggregate on the black site, and informed individuals of type i_w do not aggregate on any site; or informed individuals of type i_w and non-informed individuals aggregate on the white site, and informed individuals of type i_b do not aggregate on any site. Under this condition, the behaviour of informed individuals that do not aggregate on their preferred site can be explained by observing that the dimension of the site is too large relative to their number to trigger any aggregation process. Beyond 30% of informed individuals of type i_b, 75% of the swarm aggregates on the black site and 25% of the swarm aggregate on the white site. This is the regime where informed agents are able to guide self-organised dynamics.

Mathematically, when the total proportion of informed individuals in the swarm is low, the following approximations hold:

$$\begin{cases} x_b^{i_b} \approx \rho_{i_b} \\ x_b^{ni} \approx 1 - \rho_{i_b} - \rho_{i_w} \\ x_w^{i_w} \approx 0 \\ x_w^{ni} \approx 0 \end{cases} OR \begin{cases} x_b^{i_b} \approx 0 \\ x_b^{ni} \approx 0 \\ x_w^{i_w} \approx \rho_{i_w} \\ x_w^{ni} \approx 1 - \rho_{i_b} - \rho_{i_w}. \end{cases} \tag{5.10}$$

In such a case, the swarm aggregates only on one site, with the informed individuals that prefer the other site do not join the aggregate and they do not aggregate on their preferred site. When

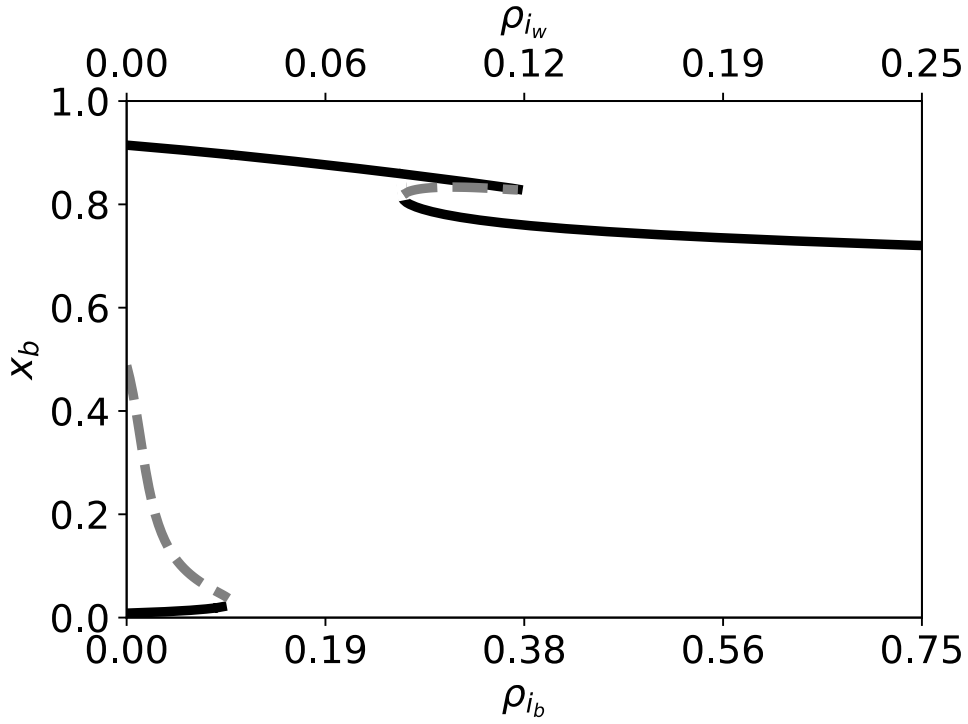

(a)

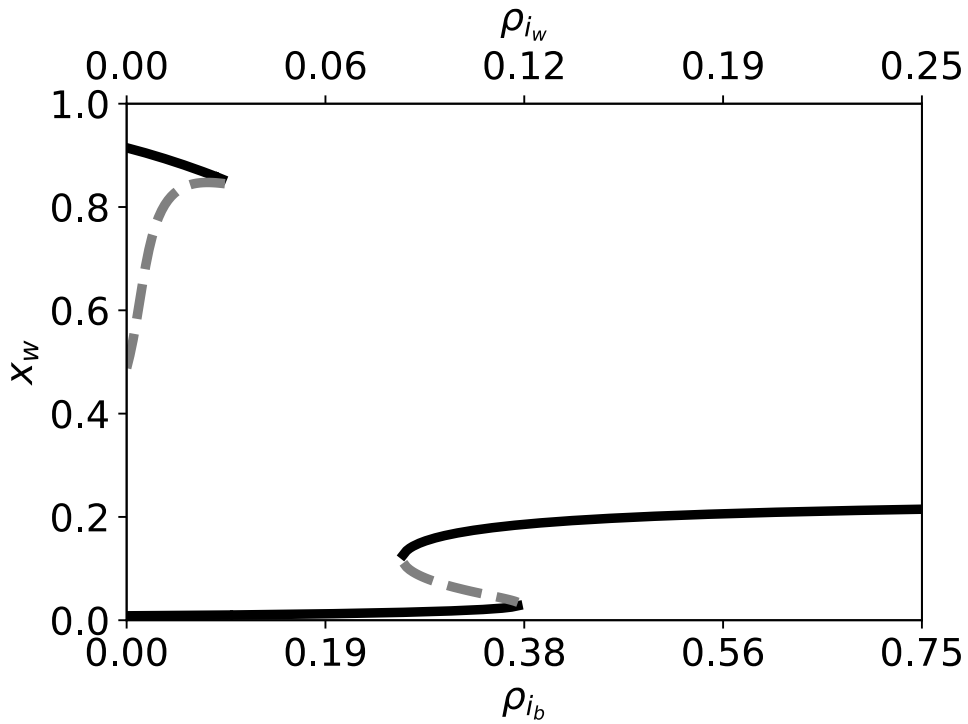

(b)

Figure 5.3: (a) Fraction of individuals, when $\frac{\rho_{i_b}}{\rho_{i_w}} = 3$ and $\sigma = 1$ for (a) the black site and (b) the white site. Black continuous lines: stable solutions. Dashed grey lines: unstable solutions.

the total proportion of informed individuals in the swarm is high, the following approximations hold:

$$\begin{cases} x_b^{i_b} \approx \rho_{i_b} \\ x_b^{ni} \approx R_b - \rho_{i_b} \\ x_w^{i_w} \approx \rho_{i_w} \\ x_w^{ni} \approx R_w - \rho_{i_w} \end{cases} \tag{5.11}$$

where R_b and R_w is the ratio of informed individuals of type i_b and i_w over the total number of informed individuals, respectively. These results are valid only when the critical value of σ_{max} is not reached for the specific values of R_b and R_w, as discussed previously.

Figure 5.4 reports results of an analysis similar to the one reported in Figure 5.3 but with $\sigma = 2$ instead than $\sigma = 1$, with the ratio $\frac{\rho_{i_b}}{\rho_{i_w}}$ still set to 3. The graphs in Figure 5.4a and 5.4b show that below a given threshold of about 20% of informed individuals of type i_b, the same behaviour is observed as in Figure 5.3a and 5.3b: informed individuals of type i_b and non-informed individuals aggregate on the black site, and informed individuals of type i_w do not aggregate on any site; or informed individuals of type i_w and non-informed individuals aggregate on the white site, and informed individuals of type i_b do not aggregate on any site. Beyond 20% of informed individuals of type i_b, 75% of the swarm aggregates on the black site but no individuals aggregate on the white site, since the dimension of the site is too large to trigger any aggregation process. In other words, with $\sigma = 2$, informed agents are never able to guide the aggregation dynamics. Indeed, when $\frac{\rho_{i_b}}{\rho_{i_w}} = 3$, in order to induce the individuals of type i_w to aggregate on their white site we need $\sigma < \sigma_{max} \approx 1.6$.

To complete the discussion, analysis has been performed for values of $\sigma < 1$. As shown in Figure 5.5, when the fraction of informed individuals is low, the swarm behaves as predicted by (Amé et al. 2006). That is, individuals distribute equally among the two sites. The distribution of individuals then changes continuously up to the desired distribution when all the individuals are informed. Note that when the site carrying capacity is not large enough to contain the corresponding informed individuals, the amount of individuals on the site is limited by this capacity and therefore never reaches the desired fraction of individuals.

5.4 Conclusions

In this chapter, we introduced a mathematical ordinary differential equations model that is inspired by the one proposed by Amé et al. (2006). We performed an analytical study of self-organised aggregation in presence of two distinctive aggregation sites, one black and one white. We consider a swarm of agents characterised by the presence of informed individuals, that is agents that are able to recognise the colour and therefore discriminate between the two sites. Our model considers sub-populations of informed individuals, distinguishing between those that prefer the white and those that prefer the black site. Each type of informed individuals never

rests on the non-preferred site. From an engineering perspective, when designing self-organised systems engaged in aggregation tasks, we would like to use informed individuals to guide the self-organised aggregation dynamics. In particular, we would like to correlate the relative proportion of one type of informed individuals with respect to the other type, with the total proportion of individuals aggregated in each site.

We analysed the equilibria of the model with respect to the site carrying capacity and to the proportion of informed individuals that prefer the white or the black site. Results show that, as in Amé et al. (2006), dynamics are strongly dependent on the environmental conditions. For intermediate values of the site carrying capacity, the informed individuals are able to guide the dynamics. And within this range, the critical mass of informed individuals needed to guide the dynamics is positively correlated with the site carrying capacity, meaning that larger sites make the collective dynamics more difficult to be guided by informed individuals. Finally, to perform a non-even allocation among the two sites, the range of the carrying capacity parameter that allows informed individuals to guide these dynamics is even more narrow compared to the case of even allocation.

This chapter has based its analysis on a seminal and important model of self-organised aggregation which was derived after experiments performed with real cockroaches (see Amé et al. 2006). However, experimental results we performed in (Firat, Ferrante, Gillet & Tuci 2020) have already given us insight that, by having more control on the microscopic self-organised model of aggregation, it is possible to have informed individuals guiding the dynamics in a wider range of environmental conditions.

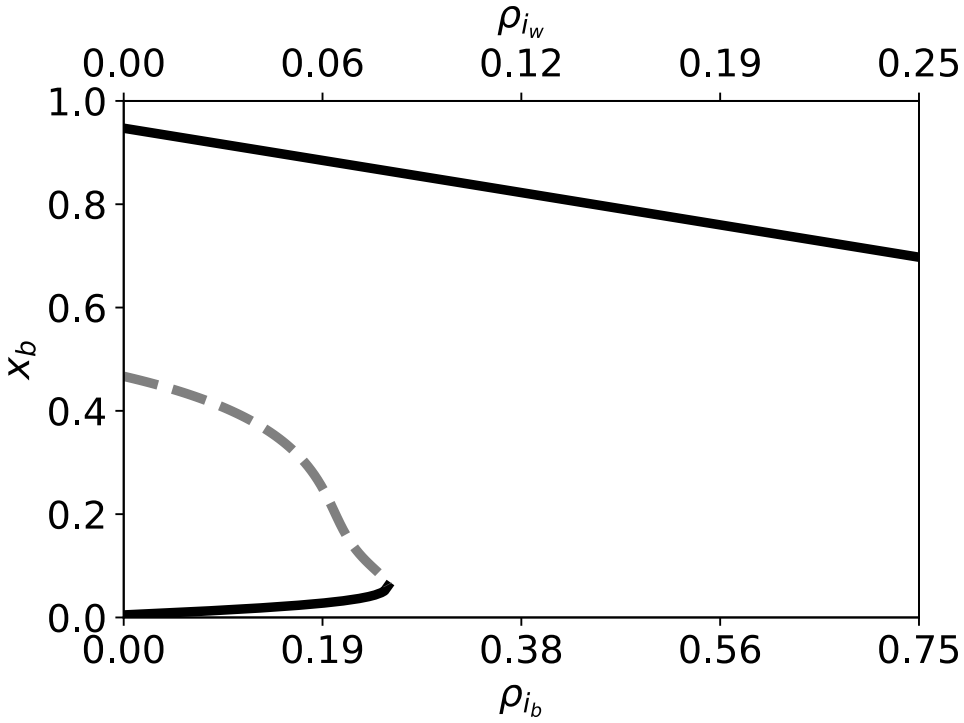

(a)

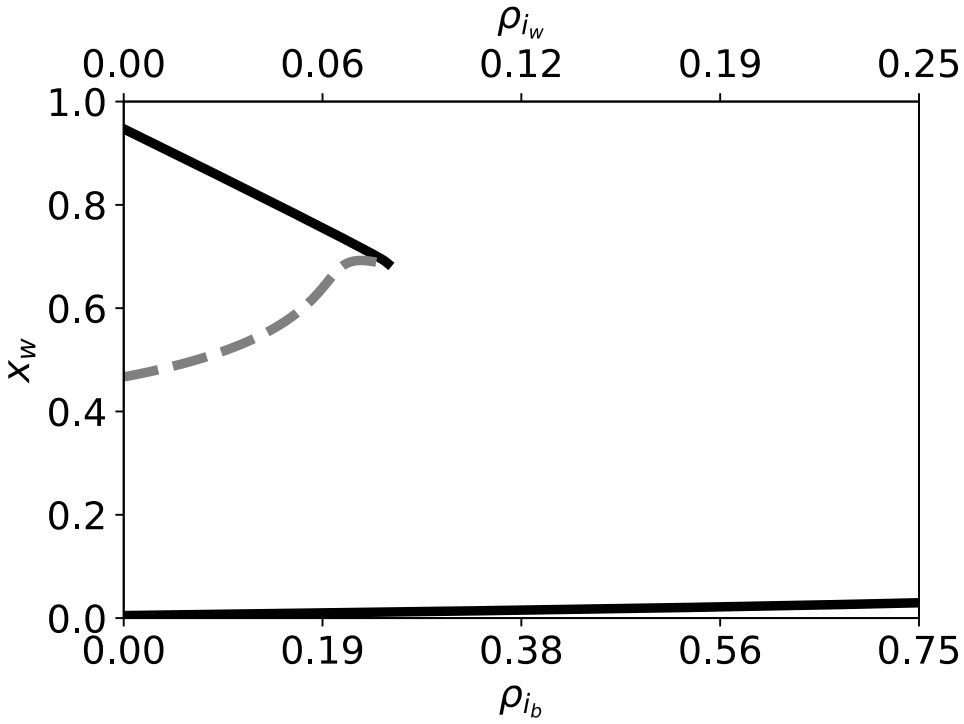

(b)

Figure 5.4: (a) Fraction of individuals, when $\frac{\rho_{i_b}}{\rho_{i_w}} = 3$ and $\sigma = 2$ for (a) the black site and (b) the white site. Black continuous lines: stable solutions. Dashed grey lines: unstable solutions.

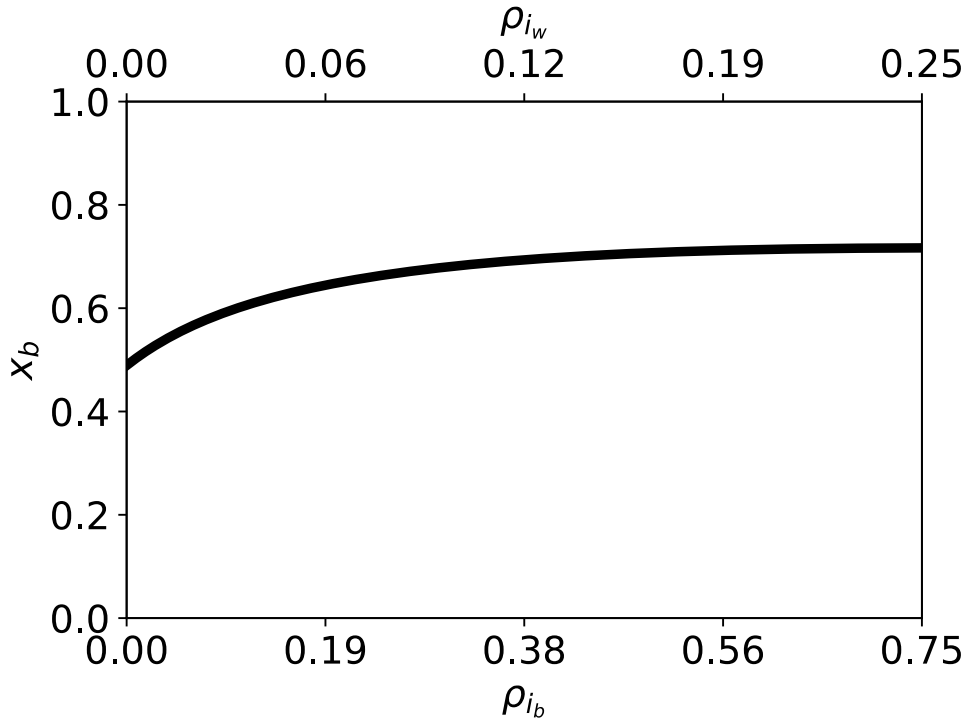

(a)

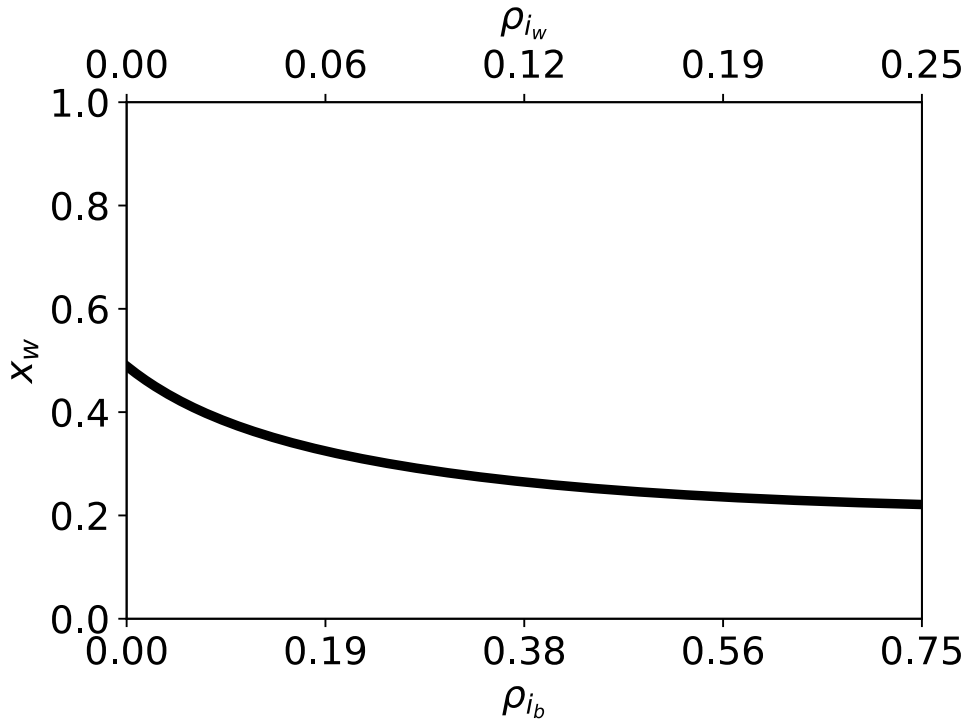

(b)

Figure 5.5: (a) Fraction of individuals, when $\frac{\rho_{i_b}}{\rho_{i_w}} = 3$ and $\sigma = 0.9$ for (a) the black site and (b) the white site. Black continuous lines: stable solutions.

CHAPTER 6

GROUP-SIZE REGULATION IN SELF-ORGANIZED AGGREGATION

6.1 Introduction

In this chapter, our objective is to go one step beyond the state of the art to investigate how the framework on informed robots can be used as a guiding principle for self-organization. We build upon recent studies on self-organized aggregation driven by informed robots (Firat et al. (2018), Firat, Ferrante, Gillet & Tuci (2020), Gillet et al. (2019), also discussed in Chapters 4 and 5 of this thesis), in which robots select only one site among n possible alternatives. Each informed robot knows which specific aggregation site to rest on and avoids other aggregation sites. Non-informed robots do not possess this information, and therefore may aggregate on any site. In addition, informed robots are assumed to be perceivable, through sensing, by other robots (e.g., they emit a signal), whereas non-informed robots cannot be sensed at all. Here, unlike in Chapters 4 and 5, robots are required to aggregate on both aggregation sites according to different proportions set by the designer. To control the proportion of robots aggregating on each of the two sites, we design a novel aggregation method. The informed robots are divided into two types, each of which prefers one of the two sites. To control the relative group sizes on the two sites, the proposed method requires only the presence of informed robots, such that the internal sub-proportions correlate with the desired global allocation for the whole swarm.

We use both simulation and physical robot experiments. In the foot-bot simulation, we study a scenario in a circular arena where the aggregation sites are represented by circles of different colors. In the kilobot simulation, we consider a scenario, again in a circular arena, where the aggregation sites are represented by kilobots positioned for different beacon sites. We then implement our method on a swarm of real kilobots, using the robots themselves as beacons to indicate the two sites because of the sensing limitation of the robot platform. We also develop

and use an platform platform of infrared emitters controlled by an Arduino microcontroller that can be sensed by the kilobots, in order to implement the boundaries of the arena and enable the kilobots to avoid the wall. The results of the simulations and of the experiments with physical robots show interesting relationships between swarm size and the sub-proportion of informed agents required for both quality and speed of convergence on the desired aggregation site. In the following sections, we detail the methods of our study, discuss the significance of our results for the swarm robotics community, and identify interesting directions for future work.

6.2 Foot-bot simulation environment

In the foot-bot simulation, a swarm of robots is placed at random in a circular area of the floor, which is colored gray except for two circular aggregation sites, one white and one black. The task of the robots is to form aggregates according to rules that prescribe what proportion of the swarm has to aggregate on the white site and what proportion on the black site. Each simulated robot is controlled by a probabilistic finite state machine (PFSM, see also Figure 6.1) similar to those employed in previous studies (Jeanson et al. 2005*a*, Bayindir & Şahin 2009, Correll & Martinoli 2011, Cambier et al. 2018*c*). The controller consists of three states: random walk ($\mathscr{RW}$), stay ($\mathscr{S}$), and leave ($\mathscr{L}$). When in state $\mathscr{RW}$, a robot's movement takes the form of an isotropic random walk, with a fixed step length (5 seconds, at 10 cm/s) and turning angles chosen from a wrapped Cauchy probability distribution (Kato & Jones 2013). Any robot in state RW continuously performs obstacle avoidance behavior: first, it stops, and then it changes its heading according to a randomly chosen angle uniformly drawn in $[-\pi,\pi]$ until no obstacles are perceived in the forward direction of motion. Negative angles refer to clockwise rotations and positive angles to anticlockwise rotations.

In the model, we consider two type of robots: informed and non-informed. Informed robots systematically rest on one site only. Some of them (the informed robots for white) avoid the black site and rest on the white site only; others (the informed robots for black) avoid the white site and rest on the black site only. Non-informed robots can rest on either site. Recall that the working hypothesis of this study is that the way in which the swarm distributes between the two aggregation sites reflects the relative proportions of informed robots for black and for white. For example, if 50% are informed for black and 50% are informed for white, the swarm should generate two aggregates of equal size, one on the black site and one on the white site. The experimental work reported here tests this hypothesis by systematically varying the proportion of informed robots within the swarm; that is, for each proportion of informed robots, we vary the relative proportion of informed robots for black and for white.

When a non-informed robot reaches an aggregation site, it systematically transitions from state $\mathscr{RW}$ to state $\mathscr{S}$. An informed robot for black undergoes the same state change only when it reaches the black site, and thus it ignores the white site. Conversely, an informed robot for white

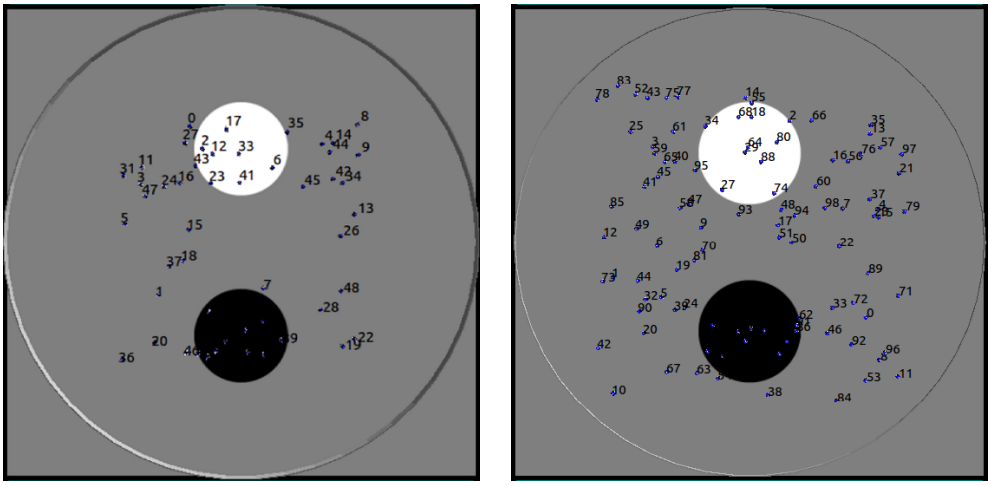

(a) (b)

Figure 6.1: (a) Arena with black and white aggregation sites for 50 swarm; (b) arena with black and white aggregation sites for 100 swarm.

systematically makes the transition when it reaches the white site, ignoring the black site. For all types of robots, the transition from random walk to resting on a site happens as follows. The robot moves forward within the site for a limited number of time steps in order to avoid stopping at the site border, which would create a barrier preventing other robots from entering the site. Then, the robot transitions from state $\mathscr{RW}$ to state $\mathscr{S}$. A robot leaves state $\mathscr{S}$ and enters state $\mathscr{L}$ with a probability P_{leave}, which is computed as follows:

$$P_{leave} = \begin{cases} e^{-a(k-|n-x|)}, & \text{if } n > 0; \text{ this applies to all types of robots;} \\ 1, & \text{if } n = 0; \text{ only for a non-informed robot;} \end{cases} \tag{6.1}$$

with $a = 2.0$ and $k = 18$. n is the current number of informed robots perceived at site, and x is the number of informed robots perceived at a site at the time of joining it. Note that, for any robot, n and x are local estimates based on the number of informed robots in the perceivable neighborhood, which is smaller than the entire site. P_{leave} is sampled every 20 time steps. A robot in state $\mathscr{L}$ leaves the aggregation site by moving forward, avoiding collisions with other robots, until it can no longer perceive the site. At this point, the robot transitions from state $\mathscr{L}$ to state $\mathscr{RW}$. While informed robots are on an aggregation site, they count themselves to estimate n and x.

To model this scenario, we use the ARGoS multi-engine simulator (Pinciroli et al. 2012). The simulation environment models the circular arena, as detailed above, as well as the kinematic and sensor readings of the foot-bot mobile robots (Bonani et al. 2010). The robot sensory apparatus consists of the proximity sensors positioned around the robot's circular body, four ground sensors (two at the front and two at the back of the robot's underside), and the range-and-bearing sensor.

The proximity sensors are used to sense and avoid the walls of the arena. The reading for each ground sensor is set to 0.5 if the sensor is on gray, 1 for white, and 0 for black. When all four ground sensors return a value other than 0.5, the robot perceives an aggregation site. The range-and-bearing sensor is used to avoid collisions with other robots and to estimate how many informed robots are resting on a site within sensor range (i.e., the parameters n and x in Eq. 6.3). With this sensor, two robots can perceive each other at a distance of up to 0.8 m.

6.3 Foot-bot simulation results

We run two sets of experiments (hereafter, setup 1 and setup 2), in which we vary the swarm size N, with $N = 50$ in setup 1 and $N = 100$ in setup 2. Because aggregation performance is heavily influenced by swarm density (Cambier et al. 2018*c*, Firat et al. 2018, Firat, Ferrante, Gillet & Tuci 2020, Gillet et al. 2019), we study scalability by keeping the swarm density constant and varying the diameter of the area, as well as the diameters of the two sites (see Table 6.1). In both setups, the diameter of each aggregation site is large enough to accommodate all the robots of the swarm. Each setup consists of 25 conditions that differ according to the total proportion of informed robots in the swarm (hereafter, ρ_I, with $\rho_I = \{0.1, 0.3, 0.5, 0.7, 0.9\}$), and in the proportion of ρ_I that are informed for black ρ_{sb}, with $\rho_{sb} = \{0.1, 0.2, 0.3, 0.4, 0.5\}$) and for white ($\rho_{sw}$, with $\rho_{sw} = 1 - \rho_{sb}$). For each condition, we execute 100 independent simulation trials in which each robot is randomly initialized within the arena. The robots move autonomously according to actions determined by their PFSM for 300,000 time steps. One simulated second corresponds to 10 simulation time steps.

We expect that, for any value of ρ_I, the swarm will distribute on each aggregation site in proportions that reflect the relative proportion of ρ_{sb} to ρ_{sw}. For example, for a given ρ_I, if $\rho_{sb} = 0.1$ and $\rho_{sw} = 0.9$, then 10% of the swarm is expected to aggregate on the black site and the remaining 90% on the white site. To evaluate the behavior of the swarm, at the end of each simulation run we record the proportion of robots aggregated on the black site ($\Phi_b = \frac{N_b}{N}$) and on the white site ($\Phi_w = \frac{N_w}{N}$), where N_b and N_w are the number of robots aggregated on the black and white sites, respectively, and N is the swarm size. We show only the results for setups 1 and 2 relative to conditions in which $\rho_I = 0.1, 0.3$ (summarized in Figure 6.2). Each graph shows the number of trials (out of 100) that terminated with a particular proportion of robots: (i) on the black site, for each value of ρ_{sb} indicated on the horizontal axes of the rightmost graph in

Table 6.1: Characteristics of each experimental condition in simulation setup swarm size arena diameter (m) aggregation site diameter (m)

setup	swarm size	arena diameter (m)	aggregation site diameter (m)
1	50	12.9	2.8
2	100	18	4.0

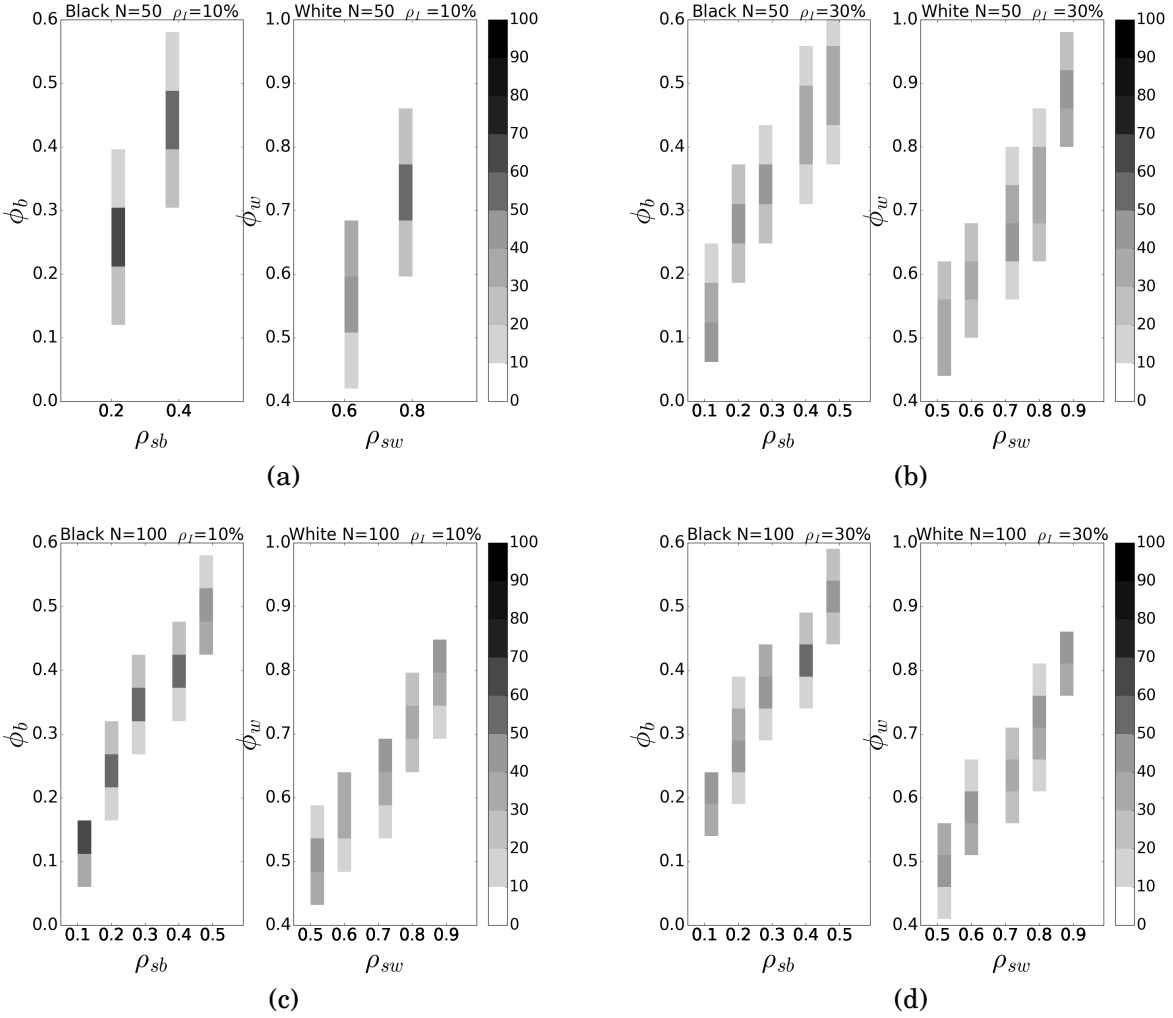

Figure 6.2: The intensity of the gray color represents the number of trials (out of 100) that terminated with a particular proportion of robots on each site (i.e., Φ_b and Φ_w). The horizontal axes show the proportion of informed robots for black (ρ_{sb}) and for white (ρ_{sw}). The swarm size N and the total proportion of informed robots (ρ_I) in the swarm are as follows: (a) $N = 50$ and $\rho_I = 0.1$; (b) $N = 50$ and $\rho_I = 0.3$; (c) $N = 100$ and $\rho_I = 0.1$; (d) $N = 100$ and $\rho_I = 0.3$. In each case, the horizontal and vertical axes of the leftmost graphs refer to ρ_{sb} and Φ_b, respectively; the horizontal and vertical axes of the rightmost graphs refer to ρ_{sw} and Φ_w, respectively.

Figure 6.2a, 6.2b, 6.2c, and 6.2d, and (ii) on the white site, for each value of ρ_{sw} indicated on the horizontal axes of the leftmost graph in Figure 6.2a, 6.2b, 6.2c, and6.2d. The swarm size N and the total proportion of informed robots (ρ_I) in the swarm are as follows: (i) $N = 50$ and $\rho_I = 0.1$ in Figure 6.2a; (ii) $N = 50$ and $\rho_I = 0.3$ in Figure 6.2b; (iii) $N = 100$ and $\rho_I = 0.1$ in Figure 6.2c; (iv) $N = 100$ and $\rho_I = 0.3$ in Figure 6.2d.

If the swarm aggregates in a way that perfectly reflects the relative proportion of informed robots for black and for white in the swarm (for both $N = 50$ and $N = 100$ and for all total

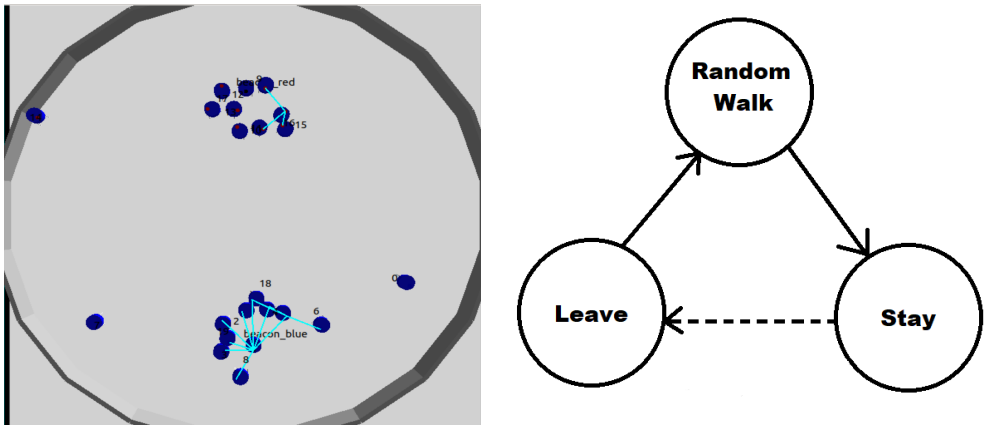

(a) (b)

Figure 6.3: (a) Arena for simulated robots with blue beacon and red beacon aggregation sites; (b) state diagram of the robots' controller. The dashed line indicates probabilistic transition, and the continuous lines indicate non-probabilistic transition.

proportions of informed robots in the swarm), the graphs in Figure 6.2 would show only a black rectangle aligned on the diagonal from the bottom left to the top right corner of each graph. Ideally, that is, all 100 trials in each condition for either setup would terminate with $\Phi_b = \rho_{sb}$ and $\Phi_w = \rho_{sw}$. Although the results of the simulations diverge slightly from this ideal case, it is clear that a high concentration of trials (the darker rectangles for each case) are aligned on the diagonal, and that the deviations from the ideal case nevertheless remain close to the expected result. This tendency is clearly observable even when the total proportion of informed robots is 0.1 of N for both setup 1 with $N = 50$ and setup 2 with $N = 100$ (see Figure 6.2a and 6.2c, respectively). Note that the results in Figure 6.2 relate to the two most challenging scenarios, in which the total proportion of informed robots in the swarm is relatively low ($\rho_I = 0.1$ and $\rho_I = 0.3$). For higher proportions of informed robots in the swarm, the results of the simulations move progressively closer to the best-case scenario, in which the simulation trials terminate with $\Phi_b = \rho_{sb}$ and $\Phi_w = \rho_{sw}$.

In summary, the PFSM described in Section 6.2 allows accurate control of the way in which the robots of a swarm distribute on two different aggregation sites, simply by regulating the relative proportion of informed robots for each site, even with a small total proportion of informed robots in the swarm ($\rho_I = 0.1$) and for different swarm sizes.

6.4 Kilobot simulation environment

For the kilobot simulation, a swarm of robots is placed at random in a circular area with a grey floor. Given that kilobots are unable to perceive obstacles or ground color, as aggregation sites we use two kilobots equidistant from the center of the arena (see Figure 6.3a). The robots' task is to form aggregates on both sites according to rules that prescribe what proportion of the swarm

has to aggregate on the blue beacon site and what proportion on the red beacon site. As in the foot-bot simulation, each simulated robot is controlled by a PFSM (see Figure 6.3b) familiar from previous work (Jeanson et al. 2005*a*, Bayindir & Şahin 2009, Correll & Martinoli 2011, Cambier et al. 2018*c*) and with three states ($\mathscr{RW}$, $\mathscr{S}$, and $\mathscr{L}$). The isotropic random walk of state $\mathscr{RW}$ has a fixed step length (moving approximately 1 cm/s and rotating approximately 45°/s) and turning angles chosen from a wrapped Cauchy probability distribution characterized by the following PDF (Kato & Jones 2013):

$$f_\omega(\theta,\mu,\rho) = \frac{1}{2\pi}\frac{1-\rho^2}{1+\rho^2-2\rho\cos(\theta-\mu)},\ 0<\rho<1, \tag{6.2}$$

where $\mu = 0$ is the average value of the distribution and ρ determines the distribution skewness. For $\rho = 0$ the distribution becomes uniform and provides no correlation between consecutive movements, whereas for $\rho = 1$ a Dirac distribution is obtained, corresponding to straight-line motion. In this study, $\rho = 0.5$. Any robot in state $\mathscr{RW}$ continuously performs the obstacle avoidance behavior of first stopping and then changing its heading according to a randomly chosen angle uniformly drawn in $[-\pi,\pi]$ until no obstacles are perceived in the forward direction of motion. As before, negative angles refer to clockwise rotations, and positive angles to anticlockwise rotations.

In this model, the informed robots for red avoid the blue beacon site and rest on the red beacon site only; the informed robots for blue avoid the red site and rest on the blue site only; the non-informed robots can rest on either site. According to our working hypothesis, the way in which the swarm distributes among the two aggregation sites will reflect the relative proportions of informed robots for blue and for red. For example, if 50% of the informed robots are for blue and 50% are for red, the swarm will generate two equal size aggregates, one on the blue beacon site and one on the red beacon site. To test this hypothesis, we systematically vary the proportion of informed robots within the swarm and, for each proportion of informed robots, the relative proportions of informed robots for each color.

A non-informed robot systematically transitions from state $\mathscr{RW}$ to state $\mathscr{S}$ on reaching any aggregation site, an informed robot for blue does so when it reaches the blue beacon site only, and an informed robot for red does so when it reaches the red beacon site only; therefore, depending on their type, informed robots ignore the red or blue beacon sites. Regardless of robot type, the transition from state $\mathscr{RW}$ to state $\mathscr{S}$ is preceded by moving forward within the site for a limited number of time steps to avoid stopping at the border and thus preventing other robots from entering. The probability of robots leaving state $\mathscr{S}$ to join state $\mathscr{L}$ is P_{leave}, computed as follows:

$$P_{leave} = \begin{cases} e^{-a(k-|n-x|)}, & \text{if } n>0;\ \text{this applies to all types of robots;} \\ 1, & \text{if } n=0;\ \text{only for a non-informed robot;} \end{cases} \tag{6.3}$$

with a $a = 3.6$ and $k = 18$. n is the current number of informed robots perceived at a site, and x is the number of informed robots perceived at a site at the time of joining it. For any robot, n and x are local estimates based on the number of informed robots in the perceivable neighborhood,

which is smaller than the entire site. P_{leave} is sampled every 100 time steps (every 10 seconds). A robot in state $\mathscr{L}$ leaves the aggregation site by moving forward, avoiding collisions with other robots until reaching a certain time limit at which it can no longer perceive the site beacon. Only then does the robot transition from state $\mathscr{L}$ to state $\mathscr{RW}$. Informed robots at an aggregation site count themselves in order to estimate n and x.

To model this scenario, we use ARGoS multi engine simulator (Pinciroli et al. 2012). The simulation environment models the circular arena as detailed above and the kinematic and sensors readings of the Kilobots mobile robots (Rubenstein et al. 2014) A Kilobot is a small (33 mm diameter, 34 mm height), and low-cost robot developed at Harvard University, explicitly designed to run swarm robotics experiments. The kilobot is equipped with infrared receiver and transmitter used for robot perceives blue or red aggregation site, It can send and receive, within a maximum distance of approximately 20 cm, infrared messages at a rate of up to 30 kb/s. Close-range communication used for measure distance to nearby neighbors to avoid collision with other robots and to estimate how many *informed* robots are resting on a site within sensor range (i.e., the parameters n and x in eq. 6.3). RGB LED light emitters used for counting number of kilobots aggregated on the aggregation site.

6.5 Kilobot simulation results

We conduct two sets of experiments with swarm sizes of N=50 and N=100, and then a comparison analysis. A swarm size of N=17 is also tested and compared with the physical kilobot results (see Section 6.6 for discussion). Each experiment runs 400,000 time steps and executes 100 independent simulation trials (1 simulated second corresponds to 10 simulation time steps). Given the influence of swarm density on aggregation performance, we keep the swarm density constant to focus on scalability. Each aggregation site is large enough to accommodate all the robots of the swarm. Table 6.2 shows the diameters of the arena for each experiment and the diameters of the aggregation regions. The selected dynamics display up to 100,000 time step rapid linear growth in the number of robots on both aggregation sites, followed by a slower growth phase during the remaining time.

In the simulation, a performance indicator is used for the proportion of informed robots

Table 6.2: Design parameters of each experimental setup in the simulation Setup Swarm Size Arena Diameter

Setup	Swarm Size	Arena Diameter(m)	Aggregation Site Diameter(m)
1	50	2	0.22
2	100	4	0.44
3	17	0.90	0.18

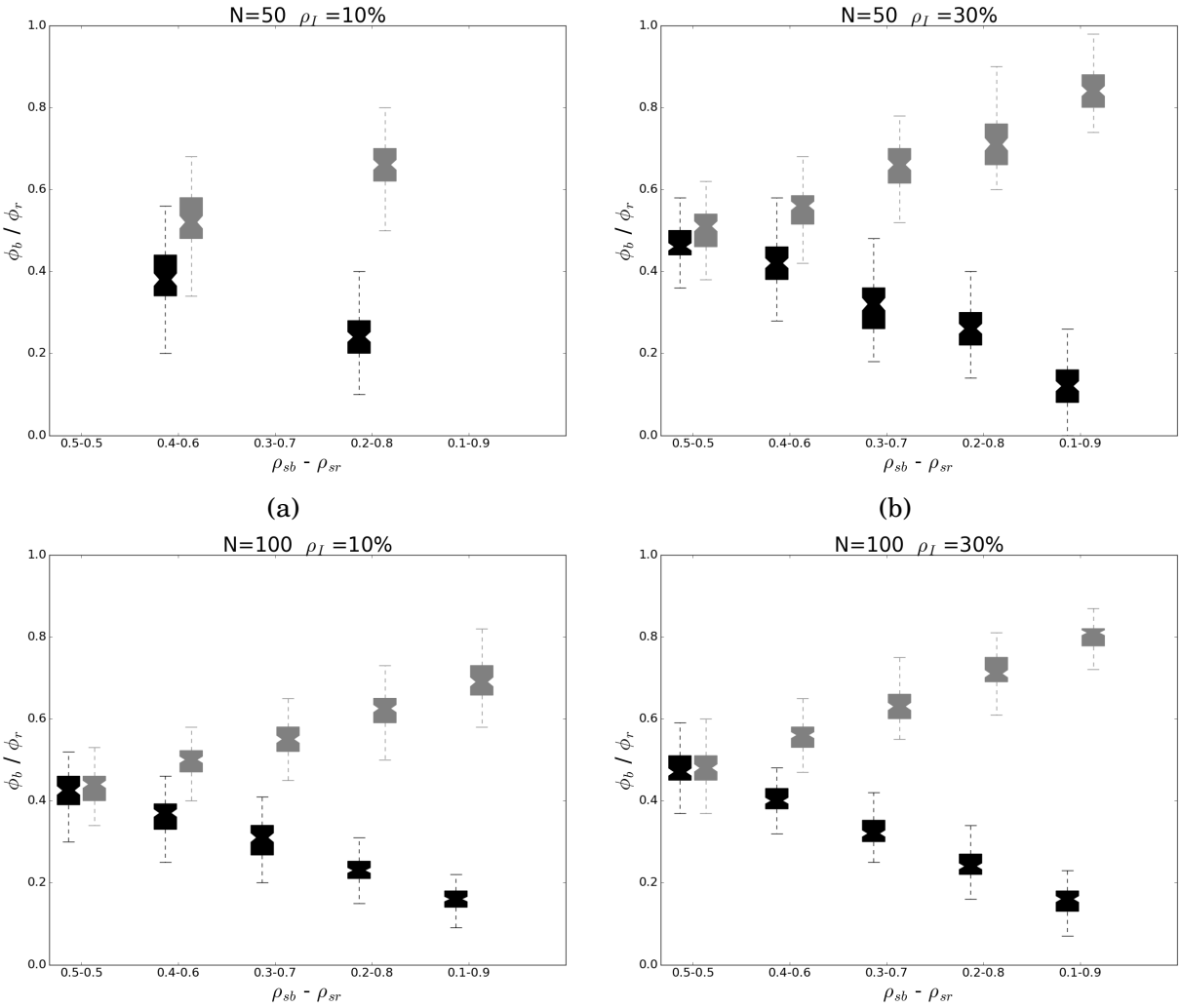

Figure 6.4: Variation of proportions of informed robots (red and blue). The intensity of the grey color represents the number of trials (out of 100) that terminated with a particular proportion of robots on each site (i.e., ϕ_b and ϕ_r). The horizontal axes show the proportion of informed robots for blue (ρ_{sb}) and for red (ϕ_r). The swarm size N and the total proportion of informed robots (ρ_I) in the swarm are as follows: (a) $N = 50$ and $\rho_I = 0.1$; (b) $N = 50$ and $\rho_I = 0.3$; (c) $N = 100$ and $\rho_I = 0.1$; (d) $N = 100$ and $\rho_I = 0.3$. In each case, the horizontal and vertical axes of the rightmost graphs refer to ρ_{sb} and ϕ_b, respectively; the horizontal and vertical axes of the leftmost graphs refer to ρ_{sr} and ϕ_w, respectively.

aggregated on the blue beacon site ($\phi_b = \frac{N_b}{N}$) and on the red beacon site ($\phi_r = \frac{N_r}{N}$). N_b and N_r are the numbers of robots aggregated on the blue and red sites, respectively, and N is the swarm size. Each setup consists of 25 conditions that differ according to the total proportion of informed robots in the swarm (hereafter, ρ_I, with $\rho_I = \{0.1, 0.3, 0.5, 0.7, 0.9\}$) and the proportions of ρ_I that are informed for blue (ρ_{sb}, with $\rho_{sb} = \{0.1, 0.2, 0.3, 0.4, 0.5\}$) and for red ($\rho_{sr}$, with $\rho_{sr} = 1 - \rho_{sb}$).

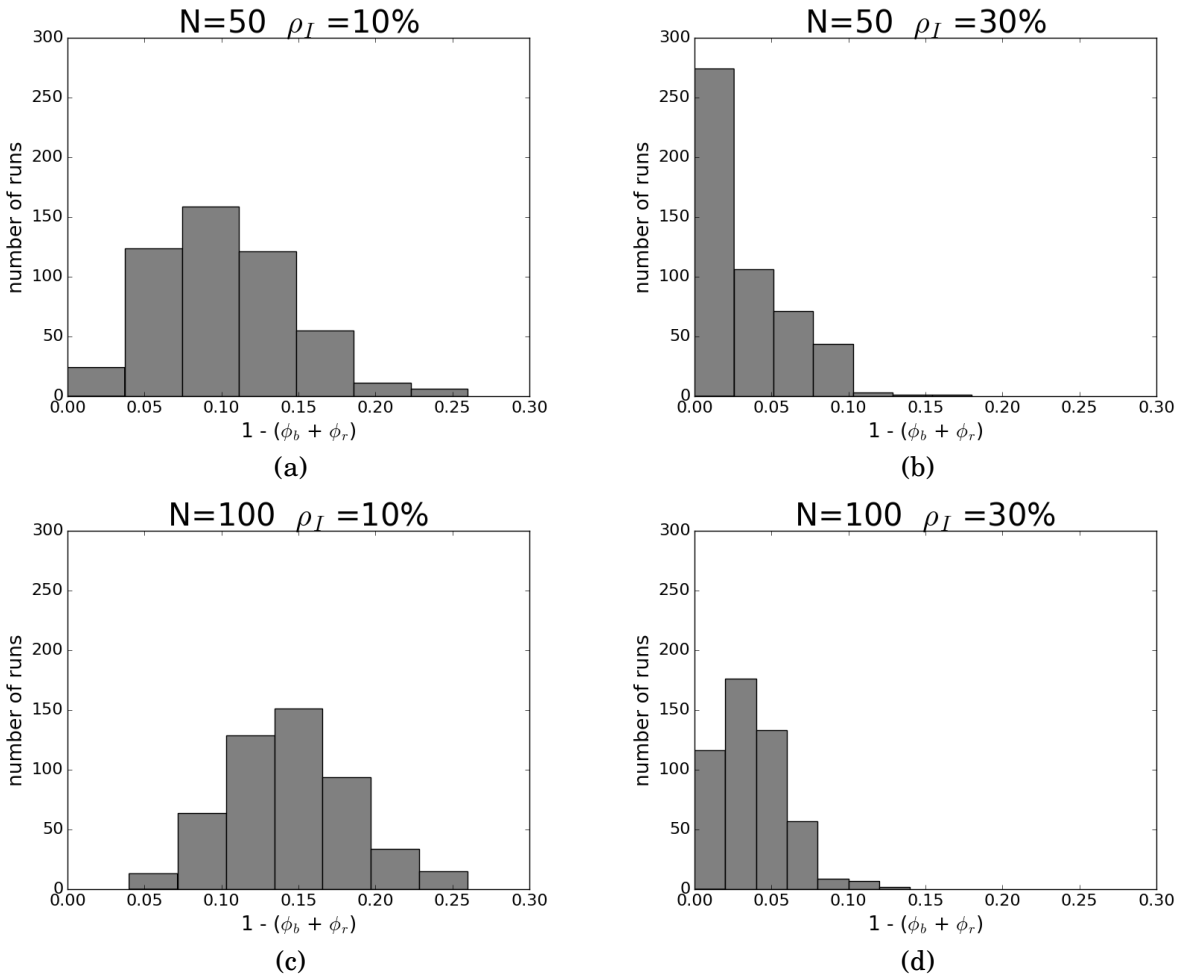

Figure 6.5: Number of runs of the proportion of robots that are not aggregated on the aggregation sites. The horizontal axis (1 - (ϕ_b + ϕ_r)) shows the proportion of robots that were not aggregated at any aggregation site at the end of the runs. The vertical axis shows the number of runs. The swarm size N and the total proportion of informed robots (ρ_I) in the swarm are as follows: (a) $N = 50$ and $\rho_I = 0.1$; (b) $N = 50$ and $\rho_I = 0.3$; (c) $N = 100$ and $\rho_I = 0.1$; (d) $N = 100$ and $\rho_I = 0.3$. Each graph shows the results of 500 trials.

For swarm size N=50, the results for $\rho_I = 0.1$ are shown in Figure 6.4a, and the results for $\rho_I = 0.3$ in Figure 6.4b. For swarm size N=100, the results for $\rho_I = 0.1$ and $\rho_I = 0.3$ are given in Figure 6.4c and Figure 6.4d, respectively. At both N=50 and N=100, the aggregations are expected to reflect perfectly the relative proportions of informed robots for blue and for red (i.e., each condition would terminate $\phi_b = \rho_{sb}$ and $\phi_r = \rho_{sr}$) in the swarm for any total proportion of informed robots. The actual results are similar to this ideal case, and the slight differences relate to the most challenging scenarios, namely the two lower proportions of informed robots ($\phi_b = \rho_{sb}$ and $\phi_r = \rho_{sr}$). In Figure 6.4b and Figure 6.4d, swarm sizes N=50 and N=100 ($\rho_I = 0.3$) are enough to produce very robust and consistent aggregation dynamics that result in swarm-relative

proportions of informed robots on each beacon site. (See the black box satisfactory conclusion for $\phi_b = \rho_{sb}$ and the grey box satisfactory conclusion for $\phi_r = \rho_{sr}$.) For higher proportions of informed robots in the swarm, the results of the simulations move progressively closer to the best-case scenario, in which the simulation trials terminate with $\phi_b = \rho_{sb}$ and $\phi_r = \rho_{sr}$.

To determine the strength of the negative feedback mechanism, we investigate the proportion of non-aggregated robots (1 - (ϕ_b - ϕ_r)) at the end of the experiments, according to whether they are on the aggregation site. Figure 6.5 gives the results in the form of a frequency distribution, the histogram showing what percentage of the swarm did not aggregate at any collection site at the end of the experiments. We executed 500 independent runs for each ρ_I condition; in other words, we explored the number of non-aggregated robots at the end of the runs. The distribution is multi-modal, with its highest peak at 0%. This indicates that, for all the swarm sizes considered, the swarm aggregated on both the blue and red sites. In Figure 6.5a and Figure 6.5c ($\rho_I = 0.1$), for a swarm size of N=50 the highest peak is around 10% with 150 trials concluded; that is, 90% of the swarm aggregated and 10% did not reach any aggregation site.For swarm size N=100, at its highest peak around 15% of the swarm did not aggregate at the end of the experiment with 150 trials. The results in Figures 6.5b and 6.5d, $\rho_I = 0.3$, show that for swarm size N=50 the highest peak was between 0% and 3% with 280 trials, that for swarm size N=100 the highest peak was between 2% and 4%, and that 170 trials did not aggregate to any of the aggregation sites at the end of the experiments. The results for $\rho_I = 0.3$ indicate a good match between the model and the simulation experiments, as well as fewer individuals without aggregation.

In summary, the PFSM described in Section 6.4 shows that the robots of a swarm distributed on two different aggregation sites can be controlled accurately simply by regulating the relative proportions of informed robots for each site, even with a small total proportion of informed robots in the swarm ($\rho_I = 0.1$), and for different swarm sizes.

6.6 Experiments and results with physical robots

To test the performances reported in Section 6.5, we run a further set of experiments with physical kilobot robots. Our physical robot scenario consists of a circular arena (diameter 90 cm). On the external side of the arena wall, infrared emitters, controlled by an Arduino micro-controller, signal to the robots the arena's edges, as illustrated in Figure e 6.6. Each kilobot can perceive these infrared signals from a distance of 10 cm , and they use them to avoid the arena walls when in a random walk state. Two kilobots, positioned approximately 40 cm from each other and at equal distances from the center of the arena, represent the aggregation sites. The LEDs of these kilobots, referred to as beacons, emit different colors: one emits blue light, the other red light, by analogy with the blue and red aggregation sites in the simulation environment. The beacons communicate their position to the other robots using the infrared transceivers, which have a range of 10 cm . The kilobots also use the infrared transceivers to estimate the parameters

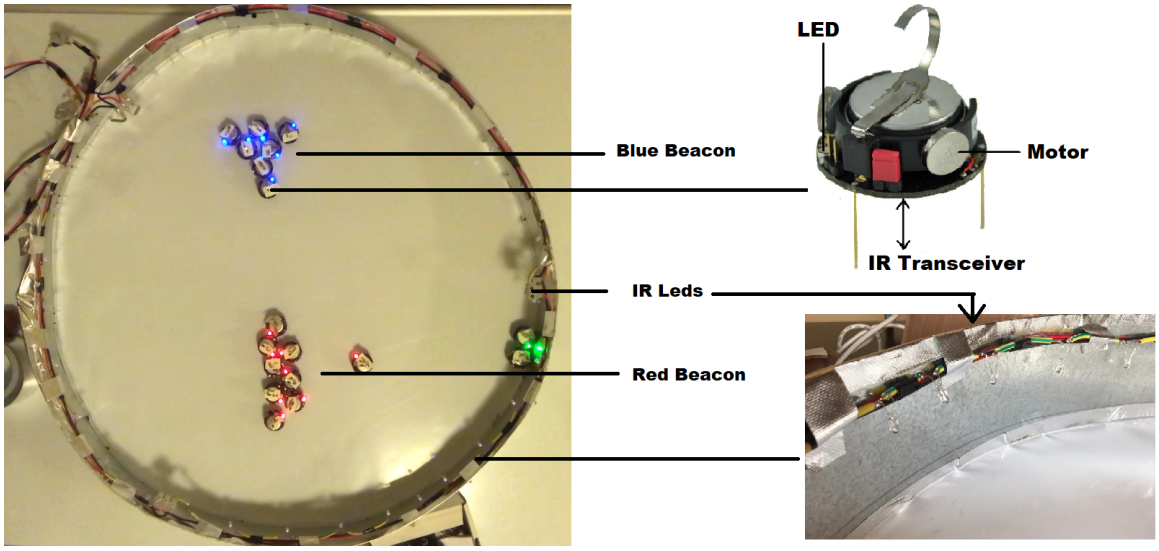

Figure 6.6: Arena for the kilobots, the aggregation sites represented by two kilobot beacons emitting red and blue light, respectively. In the image, the LED emits the light corresponding to the site on which the robot is currently resting; since the robots do not use vision, the LEDs are for visualization purposes only. On the external side of the arena wall, infrared emitters signal to the robots the arena's edges

n and x of Eq. 6.3. Each type of robot is controlled by the PFSM described in Section 6.4. The only differences between the simulated and physical robots are that for the kilobot parameter a in Eq. 6.3 is set to $a = 3.6$, and P_{leave} is sampled every 10 sec.

As the time required to execute a single trial with physical robots is significantly longer than a single trial in a simulation, the experimental design with physical robots differs slightly from the simulations. We reduce the number of conditions under which the robotic system is tested, and we choose the parameters ρ_I, ρ_{sb} and ρ_{sw} to reflect the fact that we have only 17 kilobot robots at our disposal. Accordingly, we test the following scenarios:

- for $\rho_I = 0.1$, the condition with $\rho_{sw} = \rho_{sb} = 0.5$;
- for $\rho_I = 0.3$, the condition with $\rho_{sb} = 0.2$ and $\rho_{sw} = 0.8$, and the condition with $\rho_{sb} = 0.4$ and $\rho_{sw} = 0.6$;
- for $\rho_I = 0.5$, the condition with $\rho_{sb} = \{0.1, 0.2, 0.4, 0.5\}$ and $\rho_{sw} = 1 - \rho_{sb}$;
- for $\rho_I = 0.7$, the condition with $\rho_{sb} = \{0.1, 0.2, 0.3, 0.4, 0.5\}$ and $\rho_{sw} = 1 - \rho_{sb}$;

For each of these conditions, we execute 10 trials. In each trial, the robots are initially placed within the arena in a random way. During the trial, each robot is controlled by the PFSM shown in Figure 6.3b. A trial is ended according to the following criteria: (1) as soon as at least 80%

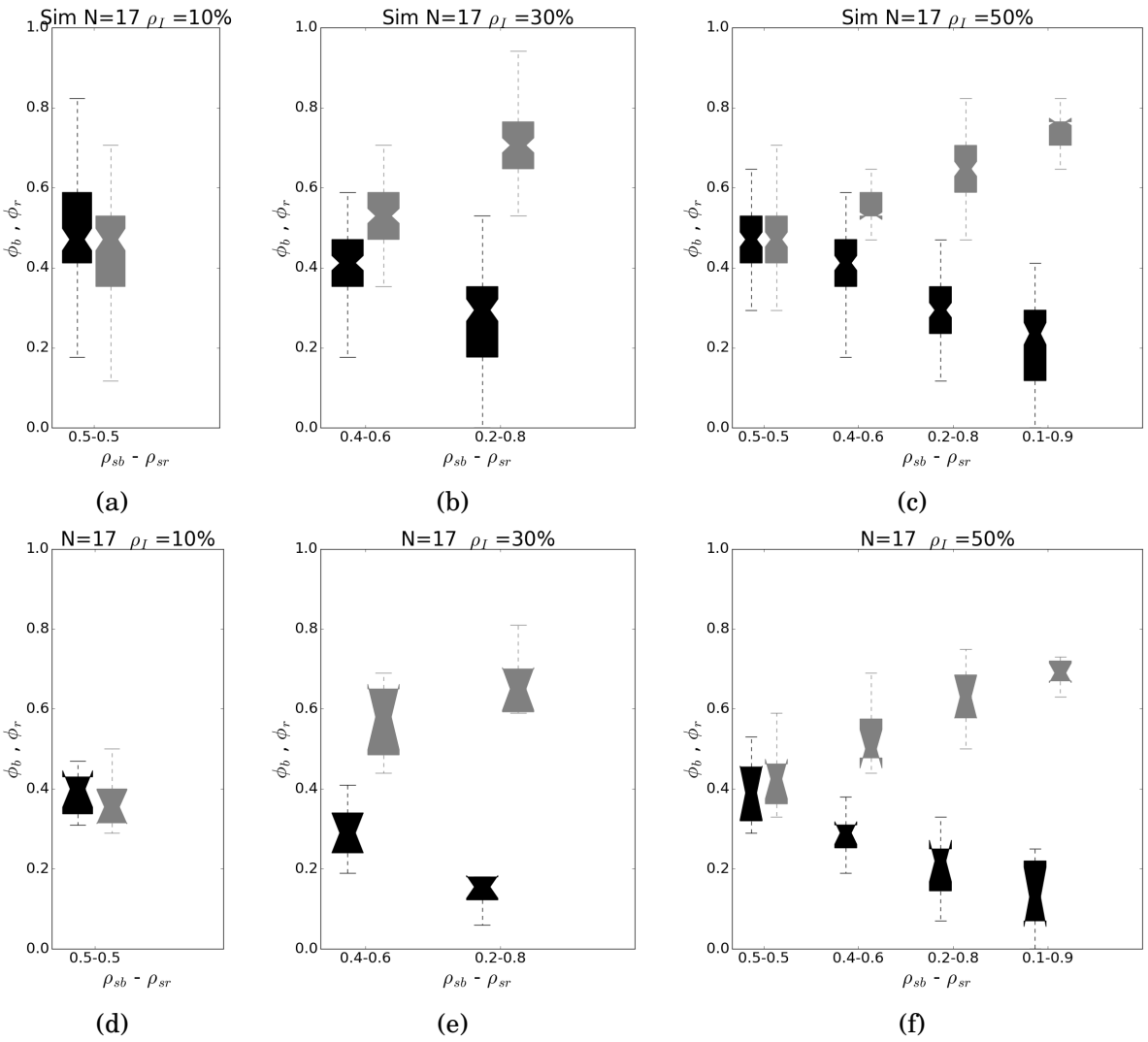

Figure 6.7: The horizontal axes show the proportion of informed robots for blue (ρ_{sb}) and for red (ρ_{sr}). The swarm size N and the total proportion of informed robots (ρ_I) in the swarm are as follows: (a) simulator $\rho_I = 0.1$; (b) simulator $\rho_I = 0.3$; (c) simulator $\rho_I = 0.5$; (d) physical robots $\rho_I = 0.1$; (e) physical robots $\rho_I = 0.3$; (f) physical robots $\rho_I = 0.5$. In each case, the horizontal and vertical axes of the rightmost graphs refer to ρ_{sb} and ϕ_b, respectively; the horizontal and vertical axes of the leftmost graphs refer to ρ_{sr} and ϕ_w, respectively.

of the kilobots are resting in any of the aggregation sites; (2) after 40 minutes if criterion (1) is never met.

The results of our tests with physical kilobot robots are shown in Figure 6.7. The graph represents the most challenging scenario, in which the proportion of informed robots is at its minimum (i.e., $\rho_I = 0.1$). In this condition, we explore only the case for $\rho_{sb} = \rho_{sw}$. In contrast to the results of the simulations, here the informed robots have only a marginal influence on the aggregation dynamics. Both Φ_b and Φ_w tend to be smaller than the expected outcomes for these

conditions, corresponding to half of the kilobots aggregating on the blue beacon site and half on the red beacon site. The differences in results between the physical and simulated robots in the same condition (i.e., $\rho_I = 0.1$, $\rho_b = \rho_w = 0.5$) could be an effect of the swarm size, which is significantly smaller for the physical robots than for the simulated robots. In all other conditions (see Figure 6.7b, 6.7c, 6.7d), the physical robots tend to generate better results. There is a strong correlation between how we vary ρ_{sb} and ρ_{sw} and the resulting Φ_b and Φ_w. Figure 6.4 shows that, in experiments with 500 independent trials for each ρ_I conditions, the results for the simulated robots are much better than for the physical robots. The physical kilobots perform at a different speed with similar calibration values; locomotion at the same speed is not guaranteed, which adds an element of uncertainty to their operation. Nevertheless, for all these conditions, the relatively small swarm size seems to have a negative effect on the possibility of informed robots controlling the aggregation dynamics. Moreover, we observe that collisions with the arena wall from specific orientations very often result in deadlocks from which the robots do not recover. These deadlocks certainly contribute to reducing the proportion of robots that manage to reach and rest on each aggregation site.

In summary, we believe that, in spite of the disruptive effects caused by the small swarm size and by collisions between the robots and the arena wall, the results in Figure 6.7 validate our approach of using relative proportions of different types of informed robots to control the aggregation dynamics of a swarm of heterogeneous robots.

6.7 Conclusions

In Sections 6.2–6.3, we showed that the aggregation dynamics of a swarm of robots can be controlled using the system heterogeneity. In the self-organized aggregation scenario in which a swarm of robots is required to operate in an arena with two aggregation sites, the system heterogeneity is represented by informed robots, that is, agents that selectively avoid one type of aggregation site (the black/white site) to rest systematically on the other type of site (the white/black site). The results of the simulations indicate that with a small proportion of informed robots a designer can effectively control the way in which an entire swarm distributes on the two aggregation sites. This is possible because the size of the aggregation at each site tends to match the relative proportions of the two different types of informed robots in the swarm.

In Sections 6.4–6.5, we replicated these results with kilobot simulator experiments, and in Section 6.6, we carried out preliminary tests with physical robots to test the effectiveness of the PFSM in controlling the aggregation dynamics of a swarm of kilobot robots (Rubenstein et al. 2014). The results of these tests, not reported in this chapter, closely match the results obtained in the simulations. Nevertheless, the behavior of physical robots was negatively affected by the frequent collisions between the robots and the arena wall, which often produced deadlock conditions, leaving the robots unable to generate the virtuous maneuvers necessary to recover

their movement. Since these tests were carried out with a maximum of 18 kilobots, we believe that the small size of the swarm of physical robots was a factor in limiting the influence of the informed robots. Further studies with physical robots are required to better characterize the nature of the relationship between swarm size and aggregation mechanisms that we have discussed in this chapter.

CHAPTER 7

CONCLUSIONS AND FUTURE WORK

In this chapter, we summarize the main contributions of this dissertation and propose future directions concerning the study of information transfer in large swarms of autonomous robots.

7.1 Contributions

In the research reported in this thesis, we used swarms of robots to explore the aggregation dynamics generated by these simple individual mechanisms. Our objective was to study the introduction of informed robots and to determine how many of these are needed to direct the aggregation process toward a predefined site among those available in the environment. Informed robots are members of a group that selectively avoid the site(s) where no aggregate should emerge, and stop only on the experimenter predefined site(s) for aggregation. We studied the aggregation process with informed robots in three different scenarios: two scenarios that are morphologically symmetric, in which the different types of aggregation site are equally represented in the environment; and an asymmetric scenario, in which the target site has an area that is half the area of the sites that should be avoided.

We first showed what happens when no robot in the swarm is informed: in symmetric environments, the swarm is able to break the symmetry and aggregates on one of the two types of site at random, not necessarily on the target site; in the asymmetric environment, the swarm tends to aggregate on the sites that are most represented in terms of area. The primary original contribution of this study is its demonstration of the effect of the introduction of a small proportion of informed robots in both environments: in symmetric environments, they selectively direct the aggregation process toward the experimenter chosen site; in the asymmetric environment, they can invert the spontaneous preference for the most represented site and induce the swarm to aggregate on the least represented type of site. We then analyzed for each scenario how the

dynamics of the aggregation process depends on the proportion of informed robots, providing analytical results from a system of ordinary differential equations (ODEs) that is an extension of a well-known model. We showed how, for certain values of the parameters, the extended model can predict the dynamics observed with simulated robots in one of the two symmetric scenarios (Chapter 4).

We went on to discuss an analytical model that uses the concept of informed individuals to allow the swarm to distribute at different aggregation sites according to proportions of individuals at each site arbitrarily chosen by the designer. Informed individuals are opinionated agents that selectively prefer an aggregation site and avoid resting at nonpreferred sites. We studied environments with two aggregation sites, and considered two different scenarios: one in which the informed individuals are distributed in equal numbers between the two sites; and one in which informed individuals for one type of site are three times more numerous than those at the other site. Our objective was to determine whether and for what range of model parameters the swarm distributes between the two sites according to the relative distribution of informed agents. Our analysis shows that the designer's ability to exploit informed individuals to control how the swarm aggregates depends on the environmental conditions. For intermediate values of the site carrying capacity, a small minority of informed individuals is able to guide the dynamics as desired by the designer. We also established that the larger the site carrying capacity, the larger the total proportion of informed individuals required to lead the swarm to the desired distribution of individuals between the two sites (Chapter 5).

In swarm robotics, self-organized aggregation is a collective process in which robots form a single aggregate at an arbitrarily chosen aggregation site among those available in the environment, or at an arbitrarily chosen location. Accordingly, instead of focusing exclusively on the formation of a single aggregate, we next discussed how to design a swarm of robots capable of generating aggregation dynamics that correspond to a variety of final distributions at the available aggregation sites. We focused on an environment with two possible aggregation sites, A and B. Our working hypothesis was that robots would distribute at sites A and B in quantities that reflect the relative proportion of robots in the swarm that selectively avoid A with respect to those that selectively avoid B, with the smallest possible proportion of robots in the swarm that selectively avoid one or the other site. We illustrated the individual mechanisms designed to implement our hypothesis, and we discussed the promising results of a set of simulations that systematically considered a variety of experimental conditions. The results obtained using simulated robots were validated using physical kilobot robots (Chapter 6).

Finally, our framework has practical relevance in the context of human–swarm interaction Kolling et al. (2016), as informed robots can correspond to robots that are controlled or teleoperated by humans. The framework can therefore be used to introduce humans into the loop in order to study how they can interact with and control swarms of robots.

Our work has since been reviewed and adopted by others. Sion et al. (2022*a*) and Sion et al.

(2022*b*) used our findings in their own experiments, and designed a new simplified finite state machine. We discuss both their studies in what follows.

In Sion et al. (2022*a*),the authors replicated our work (illustrated in Firat, Ferrante, Zakir, Prasetyo & Tuci (2020);see also Chapter 6) using a simplified approach. They removed some of the robots' communication protocols to reorganize the transition of probability states. In our study, informed robots have to be identified so that non-informed robots can stay at the aggregation site. In contrast, on the approach used by Sion et al. (2022*a*), non-informed robots do not need informed individuals to stay at the aggregation site, which increases the aggregation speed, as it may take time for the informed robots to visit the site. This makes clustering possible even if there is no informed robot at the site. Moreover, in our model, the robot at the aggregation site calculates the number of informed robots in the communication range located at the site. The approach of Sion et al. (2022*a*), however, counts all the robots, informed or otherwise, at the aggregation site within the communication range; their robots count all neighbors within sight, regardless of whether they are informed or non-informed. This small change improves the robustness and flexibility of the swarm's behavior.

Accordingly, Sion et al. (2022*a*) replaced our model equation (see 6.3) with a simpler version:

$$P_{leave} = \alpha e^{-\beta n} \tag{7.1}$$

where n is the number of robots within communication distance (both informed and non-informed), α = 0.5, and β = 2.25. In contrast to our model, P_{leave} relies on the ability of any type of robot in the swarm to broadcast and detect communication signals while standing at a site.

In summary, there are two main differences between the studies. First, in our study, informed robots only send signals and non-informed robots only receive communication signals. In the work of Sion et al. (2022*a*), informed and non-informed robots both send and receive signals. Second, in our study, non-informed robots will stop at a site only if they detect the presence of informed robots, and will likely leave a site due to the change in the number of informed robots detected. In the models used by Sion et al. (2022*a*), non-informed robots systematically stop at an aggregation site and leave with a probability determined by the current local density of robots (whether informed or not).

Sion et al. (2022*a*) compared the results obtained using our approach with the results obtained using their approach. Performance was relatively good in both cases. In the median number of robots range for N = 50 and $\rho_I > 0.3$ and $\rho_{sb} > 0.8$, their approach produced better results than ours, as it did for N = 100 and $\rho_I < 0.3$ and $\rho_{sb} < 0.7$, and for $\rho_I > 0.3$ and $\rho_{sb} > 0.8$. In the interquartile ranges of the number of robots for N = 100, N = 50 and $\rho_I < 0.3$, the results showed slightly greater variability. For all other conditions, the results on our approach were better. Swarms controlled according to the approach of Sion et al. (2022*a*) produced aggregation dynamics that performed similarly to ours, and in some experimental conditions our results were observed to be closer than theirs to target robot distributions.

Sion et al. (2022*a*) also removed the informed robots and tested with non-informed robots only. On our approach, non-informed robots need informed robots, and so non-informed robots never rest together at any of the aggregation sites. On Sion et al. (2022*a*)'s approach, because non-informed robots do not need informed robots, the robots will collect at any of the single aggregation sites. This approach increases swarm robustness and behavioral flexibility. In a comparable study (Firat, Ferrante, Gillet & Tuci 2020), we achieved similar results (illustrated in Figure 4.3) when no robot in the swarm was informed. In summary, without informed robots, more than 90% of the swarm components form aggregations at a single aggregation site. These aggregates can be on site in black or white, which can be explained by the fact that, without the informed robots, the robots select a cluster at random. Informed robots clearly break the bimodal aggregation dynamics with almost equal frequency between the black and white sites, generating new dynamics that tend to bring most of the robots to the black site.

In a subsequent study, Sion et al. (2022*b*) used a similar scenario with two collection sites. They reproduced previous work in the ARGoS simulator with kilobot robots and the kilogrid platform, which is the intelligent ground for communicating with kilobots. As before, they used circular aggregation sites, but this time they included squared aggregation sites, and they added obstacle avoidance to the walls of the kilogrid smart floor. A kilobot does not have proximity sensors for obstacle avoidance; that is, the kilogrid is resolved by the smart floor to design perimeter walls and used for the location of the robots. The kilogrid smart floor has one pick side in black and the other in white, the obstacle area in red, and the neutral area in blue (Figure 7.1). Assigning colored information to each kilogrid cell, Sion et al. (2022*b*) designed the arena as shown in the figure, such that each cell continuously broadcasts its color to the robots in the location. In our study, we proceeded differently (see in 6.4). Since there was no kilogrid smart ground ARGoS platform, we used kilobot beacons for aggregation sites. However, we did not include any obstacle avoidance solution in the simulator experiment, and sometimes the robots remained stuck on the walls for a long time and turned back randomly. In the physical kilobot experiment (see in 6.6), we found an alternative solution on the outside of the arena wall, with infrared emitters pointing the robots to the edges of the arena. The low reality gap between the simulator and the physical environment affected the results obtained using the physical robots.

Sion et al. (2022*b*) used the following calculation:

$$P_{leave} = \begin{cases} \alpha e^{-\beta n}, & \text{for non-informed robots;} \\ 0, & \text{for informed robots;} \end{cases} \tag{7.2}$$

where $\alpha = 0.5$ and $\beta = 2.25$. The higher the number of robots in the local neighborhood, the higher the probability of staying at the site. Informed robots do not leave after they find an aggregation site.

Sion et al. (2022*b*) then conducted an experiment developed with 50 kilobots and using only $\rho_I = 0.3$, $\rho_{sb} = \{0.5, 0.7, 01\}$), and $\rho_{sw} = 1 - \rho_{sb}$. They used two sampling times, 2 s and 8 s. The longer the sampling time, the higher the probability of leaving the site in a given time

4 A. Sion et al.

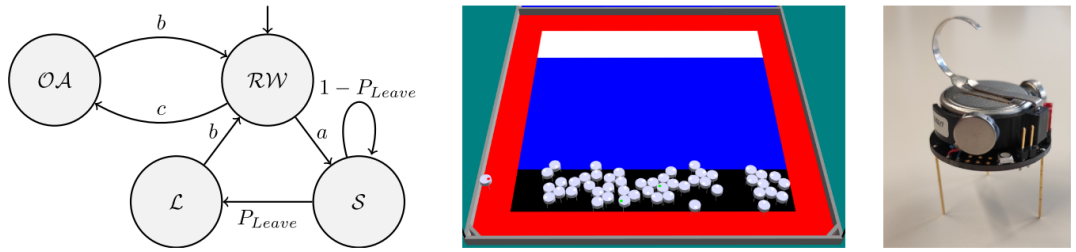

Fig. 1: (a) The probabilistic finite-state machine controller composed of four states: Random Walk ($\mathcal{RW}$), Stay ($\mathcal{S}$), Leave ($\mathcal{L}$) and Obstacle Avoidance ($\mathcal{OA}$). Letters in lowercase represent events triggering the transition between states: a is finding a suitable site for aggregating, b is getting out of a site or the obstacle area, and c is entering the obstacle area. P_{Leave} is the probability to leave the site as described in Eq. (2). (b) The simulated Kilogrid with a swarm of 50 Kilobots, an aggregation site in white, an aggregation site in black, the obstacle area in red and a neutral area in blue. (c) The Kilobot robot.

Figure 7.1: Screenshot from the Sion et al. (2022*b*) paper.

frame and the greater the opportunity to discover robots at the site. The shorter the sampling time, the more dynamic the request to leave the site. The 8 s sampling time gave better results than the 2 s sampling time, improving the total number of stays in the field and making the swarm more static. In their experiment, Sion et al. (2022*b*) found that approximately 90% of the swarm aggregated at the aggregation sites. They observed that the robots of a swarm distributed between two different aggregation sites simply by regulating the relative proportion of informed robots for each site.

Comparison of the results of Sion et al. (2022*b*) with our simulator results (see in 6.4) favors our approach (which uses a sampling time of 10 s and the equation given in 6.3). Our graph (see in 6.5) shows that for ρ_I = 0.3, about 3% of the swarm was not collected at any of the aggregation sites. In contrast, Sion et al. (2022*b*) found that for ρ_I = 0.3, the proportion of the robots that did not collect at any aggregation site was around 5% to 10%. Therefore, our test conditions resulted in a better aggregation. The reasons for the performance difference require further investigation. One possible explanation is that the larger aggregation area and the square design used by Sion et al. (2022*b*) caused poor communication between the robots standing in the aggregation area. Another possibility is that their shorter sampling time was more dynamic.

7.2 Future work

Future research could expand the work presented in this thesis in several directions. We propose here a number of extensions for each chapter.

The study in Chapter 4 has the potential to be extended in three main ways. First, in the context of aggregation, our next step will be to consider more complex scenarios. We plan to test the discrimination capabilities of our swarms with informed robots in environments with several different options (e.g. colors), corresponding to a best-of-n problem with $n > 2$ (Valentini et al. 2017). For this purpose, it is necessary to devise scenarios where informed robots may have conflicting information about which is the best site and different conflict resolution strategies. Second, we plan to introduce informed individuals into other collective behaviors. Our framework has practical relevance in the context of human–swarm interaction (see Kolling et al. 2016), as informed robots can correspond to robots that are controlled or teleoperated by humans. By introducing humans into the loop, we will be able to study how they can interact and control swarms of robots. Third, we intend to develop ODE models that closely model the robots' constraints and finite state machine controllers (as illustrated in 4.2) instead of relying on extensions of the original ODE model developed on the basis of the behavior of cockroaches (as in (Amé et al. 2006)). The resulting models will facilitate investigation of the effects of informed robots on the aggregation dynamics by varying i) the parameters that regulate the probability of joining/leaving a site, ii) the types of exploration strategies (e.g., the type of random walk) used to search for the aggregation site, and iii) the swarm density in the arena.

To build on the work in Chapter 5, we would like to develop a macroscopic ODE model that more closely captures the microscopic design method discussed in Firat, Ferrante, Gillet & Tuci (2020), rather than the behavior of natural cockroaches. In previous studies (Amé et al. 2006, Firat, Ferrante, Gillet & Tuci 2020), the individual probability of leaving a site is a non-linear function of the density of individuals at the site. However, we believe that the specific non-linear dependency can be tuned in a way that makes the dynamics less dependent on environmental conditions when informed individuals are introduced.

Drawing on our findings in Chapter 6, we believe that system heterogeneity, relatively neglected in swarm robotics to date, can play an important role in the development of mechanisms to control the self-organized collective responses of swarms of robots. Our research agenda for the future is therefore focused on a series of experiments based on the hypothesis that system heterogeneity has a measurable impact on the outcomes of certain self-organized processes. We aim to identify these processes and to illustrate how they can be effectively controlled by manipulating the system heterogeneity.

APPENDIX A

A.1 The robot and the simulation platform

This appendix completes the description of the simulation model and robotic platform used to run the experiments shown in chapter 4, chapter 5, and chapter 6 by providing further technical details. Foot-bot and ARGoS information and figures were found from Brambilla et al. (2014) and used in this appendix A.1.1 and A.1.3.

A.1.1 The foot-bot robot

The foot-bot robot is a modular robot composed of many sensors and actuators, collectively referred to as modules. Each module is controlled by a dedicated dsPIC micro-controller. The foot-bot is equipped with a main processor board, a Freescale i.MX31 ARM 11 low-energy 533 MHz processor running linux. The main board features 128 MB of DDR RAM and 64 MB of flash. The dsPICs on the modules communicate with the central processor asynchronously using a common bus and the ASEBA software platform Magnenat et al. (2010). The foot-bot is 29 cm tall and has a radius of 8.5 cm. Its weight is 1.8 Kg. It uses a lithium polymer battery with very long duration and that can be hot-swapped during an experiment thanks to the presence of a super capacitor. The complete list of robot's sensor and actuators is the following:

- Two differential drive treels, a combination of tracks and wheels, are used for locomotion in normal and rough terrains.

- A turret actuator allows a plastic ring with 12 RGB LEDs and a gripper to rotate almost 360 degrees around the Z axis of the robot. The ring is used both to emit light with different

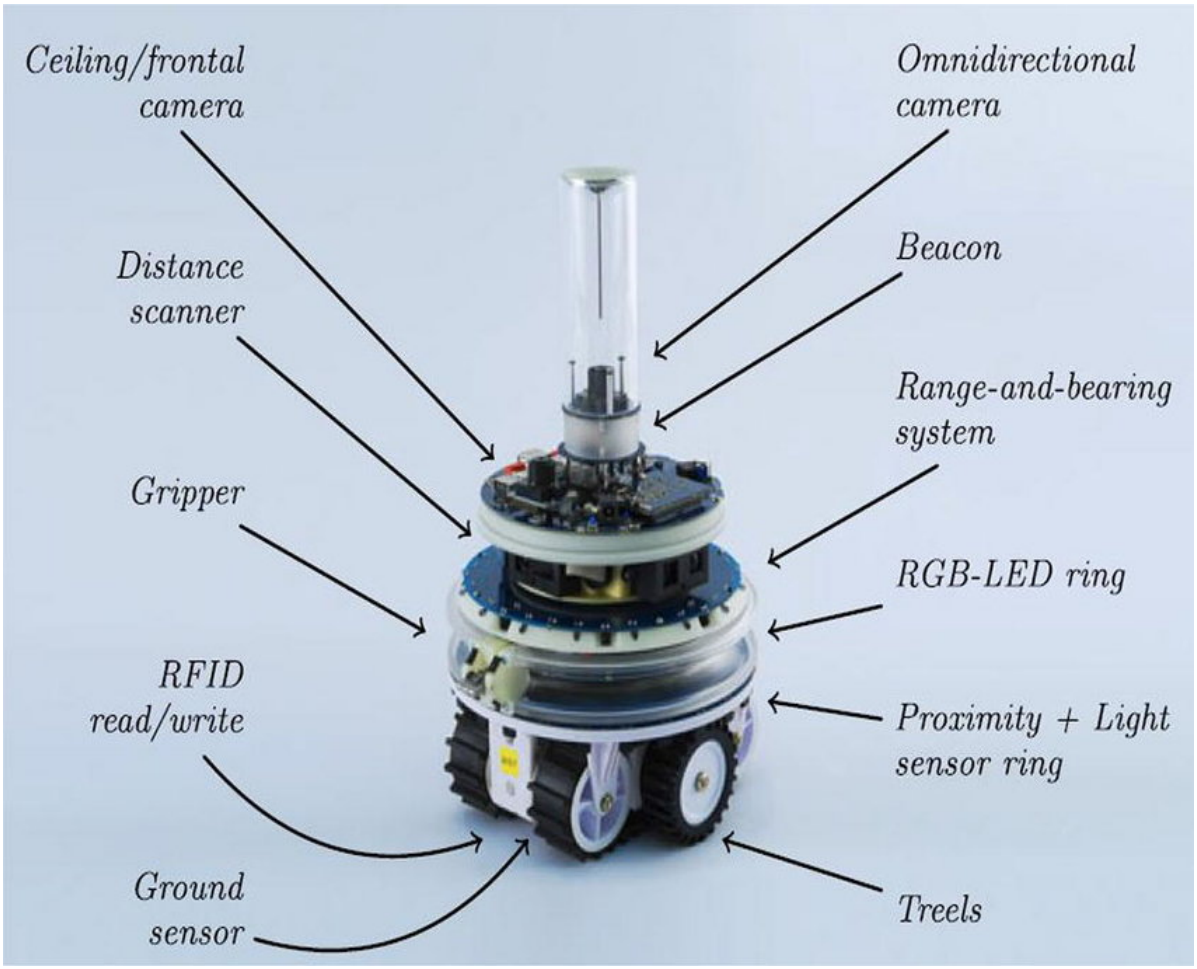

Figure A.1: The foot-bot robot. Screenshot from Brambilla et al. (2014).

colors and as a docking mechanism for another foot-bot. In fact, the gripper is especially designed to fit this specific plastic ring and to hold into it while open.

- 24 infrared sensors, that are evenly distributed around the foot-bot's body, have two functionalities. First, as a proximity sensor, they can detect obstacles in close range (5 cm). Second, as a light sensor, they can measure the intensity and the direction of the ambient light, even when placed far away from the robot. In our experiments, we use these sensors only as a light sensor.

- 4+8 additional infrared sensors, also referred to as ground sensors, are located underneath the robot, between the two tracks and on the outside part, respectively. They are used to detect the color of the ground in the gray scale.

- Two Pixelplus 2.0 MegaPixels CMOS cameras provide basic visual information. The first camera is located in the above part of the robot, in the center. It point upwards towards a

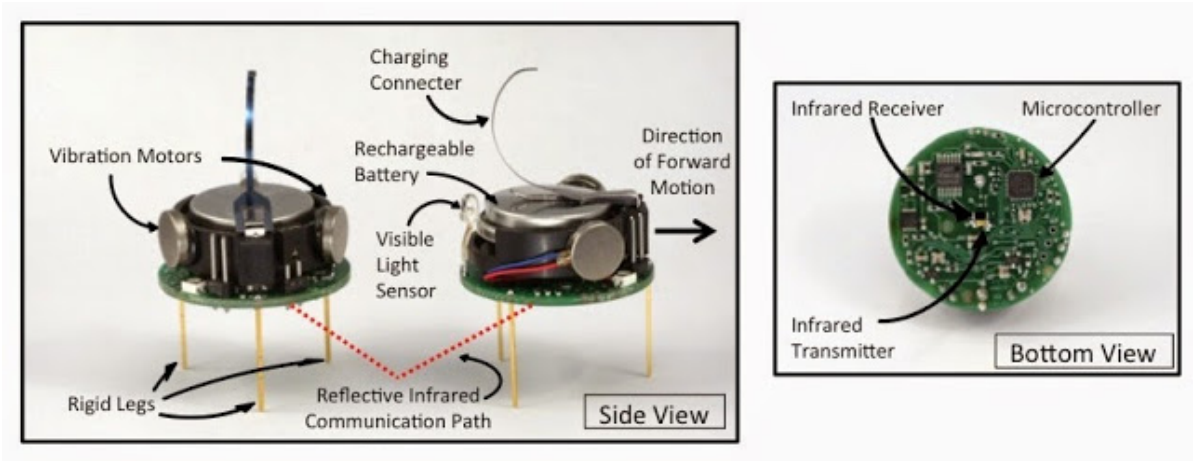

Figure A.2: The kilobot robot. Screenshot from `https://www.cgl.ucsf.edu/chimera/data/kilobots-jan2015/cancerbots.html`

mirror located at the top of a glass tube. This provides the foot-bot with omni-directional vision capabilities. The second camera is also located on the top but in a non-central position, and can be installed to either look upwards towards the ceiling or forward along the X-Y plane.

- A rotating scanner, composed of two short and two long distance scanners, is used to measure distances. It can detect distance to obstacles very precisely, at the expenses of a poor 360 degrees resolution due to the limited rotation speed.

- A range and bearing sensing and communication board. It is composed of 20 infrared transmitters, of 12 receivers, and of a radio communication device. The infrared transmitters and receivers have two functionalities. First, they are used to detect the range and the bearing of neighboring foot-bots. Second, they are used for local communication. This module is only used for communication in this dissertation.

- A three-axes accelerometer and a three-axes gyroscope installed on the left treel.

A.1.2 The Kilobot robot

In the chapter 6, the programs for kilobots are written in the C programming language. To transfer the code to a group of self-organized Kilobots, an overhead infrared controller is used, which is connected to the computer by a USB port. After sending the code to the robot, they download the program. Then, the program begins, and the same autonomous act initiates with no other communication from the computer.

The figure A.2 shows a side view of two Kilobots, a reflection of the infrared signal, and a bottom view of a Kilobot. Kilobot has an Atmega328 processor controller with 32KB of memory

running at 8MHz. To program Kilobots (Rubenstein et al. 2012) we use an overhead infrared transmitter instead of a plug-in cable, which allows batch programming of all Kilobots at once. Kilobots use a pair of vibration motors for gliding motion, a reflective infrared LED, and distance sensing to communicate with other robots in their neighborhood. Communication is transmitted by the infrared LED with pulsed messages at a range of 10cm (Rubenstein et al. 2012), allowing the robot to receive information equally from all directions. All neighbors within range from any direction can receive emitted light reflected from the surface.

Sensing measured distances between neighbors as position feedback helps make robot motion relatively accurate. This feature is useful in improving collective behavior practice. However, the lack of bearing system poses some difficulties in the swarm coordination application, such as robot-robot collision, slow wayfinding process. Also, on the outside of the arena wall, we used infrared emitters controlled by an Arduino microcontroller, signaling the robots to avoid obstacles and not get stuck at the edges of the arena.

Kilobots are limited by the simplicity of their sensors. This limits the types of experiments that can be done, as robots cannot receive feedback about their physical environment outside of the light sensor. To overcome this problem, solutions such as the ARK system Reina et al. (2017), which allows the use of virtual sensors through an overhead controller and a camera tracking system, have been proposed. Alternatively, Valentini et al. (2018) designed kilogrid smart floor for physical kilobot experiment. Kilogrid can be used to virtualize sensors and actuators and systematize data collection during an experiment. They showed that it can be used in many different experiments, such as exploration and obstacle avoidance, site selection based on multiple slopes, plant watering, and pheromone-based foraging.

A.1.3 The ARGoS simulator

The experiments described in chapter chapter 4, chapter 5, and chapter 6 have been carried out also using a physics-based simulator called ARGoS, which stands for Autonomous Robots Go Swarming Pinciroli et al. (2012). Argos is an open source simulator[1] specifically designed for research in swarm robotics. ARGoS is one of the best performance simulator for large-scale robot swarms (Pitonakova et al. 2018).

The overall architecture of ARGoS is shown in Figure A.3. ARGoS has been developed with two key concepts in mind: flexibility and efficiency. Flexibility refers to the possibility to tune the experiments according to the needs. Efficiency refers to the possibility to perform experiments with large numbers of robots by keeping satisfactory run-time performance. Flexibility has been achieved through a modular design of the simulator: all components, such as robots, sensors, actuators, physics engines, visualization engines, are plugins that can be freely selected and included/excluded.

[1]ARGoS simulator, http://iridia.ulb.ac.be/argos, February 2013.

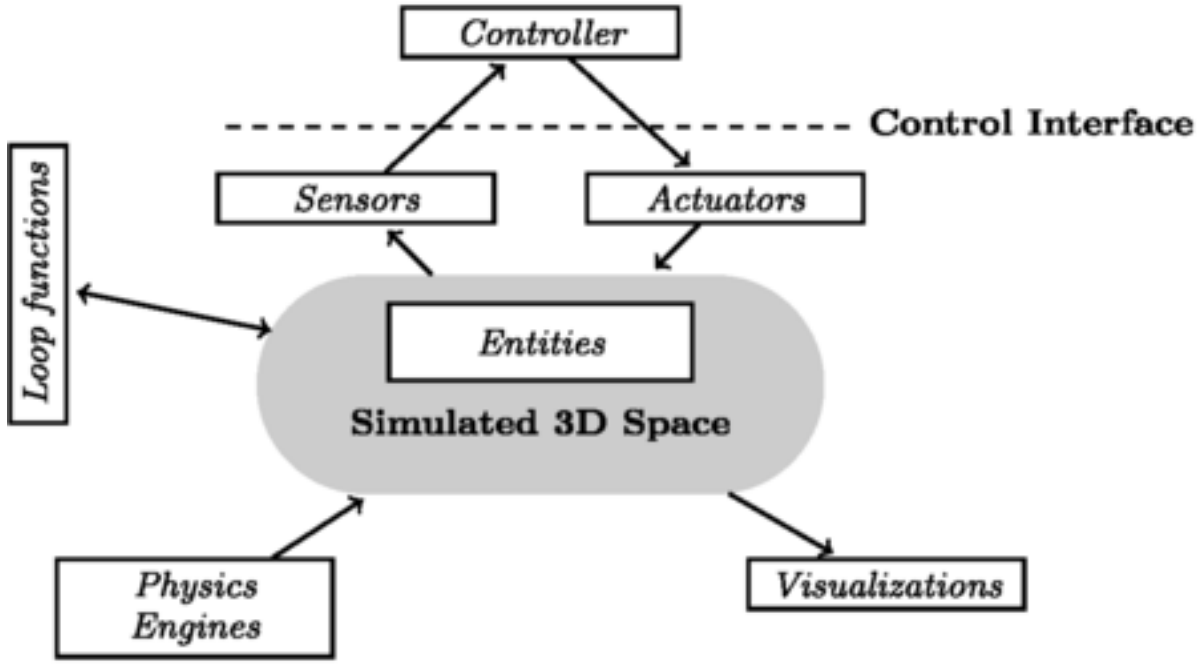

Figure A.3: Architecture of the ARGoS simulator. Screenshot from Brambilla et al. (2014).

In addition, efficiency in ARGoS has been pursued through parallelization, that is, multiple sensors or multiple physics engine can run in parallel on multiple cores. Parallelization of the physics engine has been achieved via partitioning of the simulated space into non-overlapping sub-spaces and assignment of each sub-space to a separate physics engine.

One of the key features of ARGoS, it is that the control software written for testing on ARGoS can be seamlessly instantiated on real robots without the need for any kind of modification or translation. This is achieved via a control interface (Figure A.3), which is an abstraction layer between the controller and the sensors/actuators. The user can then decide whether to compile the control software for the simulation or for the real robot.

In Study Aust et al. (2022), they developed a smart environment simulation for Kilobot robots and integrated it as an add-on ARGoS-Kilogrid. In this way, they have developed the ARGoS-Kilogrid plugin that works in Simulation, which can also be used in real Kilobots and allows the same code to be used in Kilogrid.

BIBLIOGRAPHY

Achtelik, M., Achtelik, M., Brunet, Y., Chli, M., Chatzichristofis, S., Decotignie, J.-D., Doth, K.-M., Fraundorfer, F., Kneip, L., Gurdan, D. et al. (2012), Sfly: Swarm of micro flying robots, *in* '2012 IEEE/RSJ International Conference on Intelligent Robots and Systems', IEEE, pp. 2649–2650.

Alkilabi, M. H. M., Narayan, A., Lu, C. & Tuci, E. (2018), Evolving group transport strategies for e-puck robots: moving objects towards a target area, *in* 'Distributed Autonomous Robotic Systems', Springer, pp. 503–516.

Alkilabi, M. H. M., Narayan, A. & Tuci, E. (2017*a*), 'Cooperative object transport with a swarm of e-puck robots: robustness and scalability of evolved collective strategies', *Swarm intelligence* **11**(3), 185–209.

Alkilabi, M., Narayan, A. & Tuci, E. (2017*b*), 'Cooperative object transport with a swarm of e-puck robots: robustness and scalability of evolved collective strategies', *Swarm Intelligence* **11**(3–4), 185–209.

Amé, J., Halloy, J., Rivault, C., Detrain, C. & Deneubourg, J. (2006), 'Collegial decision making based on social amplification leads to optimal group formation', *PNAS* .

Amé, J., Rivault, C. & Deneubourg, J. (2004), 'Cockroach aggregation based on strain odour recognition', *Animal Behaviour* .

Ampatzis, C., Tuci, E., Trianni, V., Christensen, A. L. & Dorigo, M. (2009), 'Evolving self-assembly in autonomous homogeneous robots: Experiments with two physical robots', *Artificial Life* **15**(4), 465–484.

Anderson, C., Theraulaz, G. & Deneubourg, J.-L. (2002), 'Self-assemblages in insect societies', *Insectes sociaux* **49**(2), 99–110.

Arvin, F., Samsudin, K., Ramli, A. R. & Bekravi, M. (2011), 'Imitation of honeybee aggregation with collective behavior of swarm robots', *International Journal of Computational Intelligence Systems* **4**(4), 739–748.

Aust, T., Talamali, M., Dorigo, M., Hamann, H. & Reina, A. (2022), 'The hidden benefits of limited communication and slow sensing in collective monitoring of dynamic environments'.

Bachrach, J., Beal, J. & McLurkin, J. (2010), 'Composable continuous-space programs for robotic swarms', *Neural Computing and Applications* **19**(6), 825–847.

Balch, T. & Arkin, R. C. (1998), 'Behavior-based formation control for multirobot teams', *IEEE transactions on robotics and automation* **14**(6), 926–939.

Barbaro, A. B., Taylor, K., Trethewey, P. F., Youseff, L. & Birnir, B. (2009), 'Discrete and continuous models of the dynamics of pelagic fish: application to the capelin', *Mathematics and Computers in Simulation* **79**(12), 3397–3414.

Bayindir, L. & Şahin, E. (2007), 'A review of studies in swarm robotics', *Turkish Journal of Electrical Engineering & Computer Sciences* **15**(2), 115–147.

Bayindir, L. & Şahin, E. (2009), Modeling self-organized aggregation in swarm robotic systems, *in* 'IEEE Swarm Intelligence Symposium, SIS'09', IEEE, pp. 88–95.

Beal, J. (2004), Programming an amorphous computational medium, *in* 'International Workshop on Unconventional Programming Paradigms', Springer, pp. 121–136.

Berman, S., Halász, A., Hsieh, M. A. & Kumar, V. (2009), 'Optimized stochastic policies for task allocation in swarms of robots', *IEEE transactions on robotics* **25**(4), 927–937.

Berman, S., Lindsey, Q., Sakar, M. S., Kumar, V. & Pratt, S. C. (2011), 'Experimental study and modeling of group retrieval in ants as an approach to collective transport in swarm robotic systems', *Proceedings of the IEEE* **99**(9), 1470–1481.

Bodi, M., Thenius, R., Szopek, M., Schmickl, T. & Crailsheim, K. (2012), 'Interaction of robot swarms using the honeybee-inspired control algorithm beeclust', *Mathematical and Computer Modelling of Dynamical Systems* **18**(1), 87–100.

Bonabeau, E., Dorigo, M., Marco, D. d. R. D. F., Theraulaz, G. et al. (1999), *Swarm intelligence: from natural to artificial systems*, Oxford university press.

Bonabeau, E., Dorigo, M. & Theraulaz, G. (1999), 'From natural to artificial swarm intelligence'.

Bonabeau, E., Sobkowski, A., Theraulaz, G., Deneubourg, J.-L. et al. (1997), Adaptive task allocation inspired by a model of division of labor in social insects., *in* 'BCEC', pp. 36–45.

Bonani, M., Longchamp, V., Magnenat, S., Rétornaz, P., Burnier, D., Roulet, G., Vaussard, F., Bleuler, H. & Mondada, F. (2010), The marxbot, a miniature mobile robot opening new perspectives for the collective-robotic research, *in* 'IEEE/RSJ Int. Conf. on Intelligent Robots and Systems (IROS)', pp. 4187–4193.

Brambilla, M., Dorigo, M. & Birattari, M. (2014), Formal methods for the design and analysis of robot swarms, PhD thesis, Ph. D. thesis, Universite Libre de Bruxelles, Berlin, Heidelberg.

Brambilla, M., Ferrante, E., Birattari, M. & Dorigo, M. (2013), 'Swarm robotics: a review from the swarm engineering perspective', *Swarm Intelligence* **7**(1), 1–41.

Brambilla, M., Pinciroli, C., Birattari, M. & Dorigo, M. (2009), A reliable distributed algorithm for group size estimation with minimal communication requirements, *in* '2009 International Conference on Advanced Robotics', IEEE, pp. 1–6.

Calvo, M., Martın, M., Eeckhout, J. & Stamatios, C. (n.d.), 'Consensus driven by a minority in heterogenous groups of the cockroach periplaneta americana'.

Camazine, S. (2003), *Self-organization in biological systems*, Princeton University Press.

Camazine, S., Deneubourg, J.-L., Franks, N. R., Sneyd, J., Theraula, G. & Bonabeau, E. (2001), *Self-organization in biological systems*, Princeton university press.

Cambier, N., Albani, D., Frémont, V., Trianni, V. & Ferrante, E. (2021), 'Cultural evolution of probabilistic aggregation in synthetic swarms', *Applied Soft Computing* **113**, 108010.

Cambier, N., Frémont, V. & Ferrante, E. (2017), Group-size regulation in self-organised aggregation through the naming game, *in* 'International Symposium on Swarm Behavior and Bio-Inspired Robotics (SWARM 2017)', Kyoto, Japan.

Cambier, N., Fremont, V., Trianni, V. & Ferrante, E. (2018*a*), Embodied evolution of self-organised aggregation by cultural propagation, *in* M. Dorigo, M. Birattari, C. Blum, A. Christensen, A. Reina & V. Trianni, eds, 'Proc. of the 11^{th} Int. Conf. on Swarm Intelligence', LNCS, Springer, p. In Press.

Cambier, N., Frémont, V., Trianni, V. & Ferrante, E. (2018*b*), Embodied evolution of self-organised aggregation by cultural propagation, *in* 'ANTS 2018', Rome, Italy.

Cambier, N., Fremont, V., Trianni, V. & Ferrante, E. (2018*c*), Embodied evolution of self-organised aggregation by cultural propagation, *in* M. D. et al., ed., 'Proc. of the 11^{th} Int. Conf. on Swarm Intelligence', LNCS, Springer, p. In Press.

Campo, A. (2011), On the design of self-organized decision making in robot swarms, PhD thesis, Université Libre de Bruxelles.

Campo, A., Garnier, S., Dédriche, O., Zekkri, M. & Dorigo, M. (2010*a*), 'Self-organized discrimination of resources', *PLoS ONE* **6**(5), e19888.

Campo, A., Garnier, S., Dédriche, O., Zekkri, M. & Dorigo, M. (2010*b*), 'Self-organized discrimination of resources', *PLoS ONE* **6**(5), e19888.

Carrillo, J. A., Fornasier, M., Toscani, G. & Vecil, F. (2010), Particle, kinetic, and hydrodynamic models of swarming, *in* 'Mathematical modeling of collective behavior in socio-economic and life sciences', Springer, pp. 297–336.

Celikkanat, H. & Şahin, E. (2010), 'Steering self-organized robot flocks through externally guided individuals', *Neural Computing and Applications* **19**(6), 849–865.

Chen, J., Gauci, M. & Groß, R. (2013), A strategy for transporting tall objects with a swarm of miniature mobile robots, *in* '2013 IEEE International Conference on Robotics and Automation', IEEE, pp. 863–869.

Cook, D. J., Gmytrasiewicz, P. & Holder, L. B. (1996), 'Decision-theoretic cooperative sensor planning', *IEEE Transactions on Pattern Analysis and Machine Intelligence* **18**(10), 1013–1023.

Coppola, M., Guo, J., Gill, E. & de Croon, G. C. (2019), 'Provable self-organizing pattern formation by a swarm of robots with limited knowledge', *Swarm Intelligence* **13**(1), 59–94.

Correll, N. & Martinoli, A. (2007), Modeling self-organized aggregation in a swarm of miniature robots, *in* 'IEEE 2007 International Conference on Robotics and Automation Workshop on Collective Behaviors inspired by Biological and Biochemical Systems', number CONF.

Correll, N. & Martinoli, A. (2011), 'Modeling and designing self-organized aggregation in a swarm of miniature robots', *The International Journal of Robotics Research* **30**(5), 615 – 626.

Couzin, I. D., Krause, J., James, R., Ruxton, G. D. & Franks, N. R. (2002), 'Collective memory and spatial sorting in animal groups', *Journal of theoretical biology* **218**(1), 1–11.

Couzin, I., Krause, J., Franks, N. & Levin, S. (2005), 'Effective leadership and decision making in animal groups on the move', *Nature* **433**, 513–516.

Deneubourg, J.-L., Aron, S., Goss, S. & Pasteels, J. M. (1990), 'The self-organizing exploratory pattern of the argentine ant', *Journal of insect behavior* **3**(2), 159–168.

Deneubourg, J., Lioni, A. & Detrain, C. (2002), 'Dynamics of aggregation and emergence of cooperation', *The Biological Bulletin* **202**(3), 262–267.

Dimidov, C., Oriolo, G. & Trianni, V. (2016), Random walks in swarm robotics: an experiment with kilobots, *in* 'International Conference on Swarm Intelligence', Springer, pp. 185–196.

Donald, B. R., Jennings, J. & Rus, D. (1997), 'Information invariants for distributed manipulation', *The International Journal of Robotics Research* **16**(5), 673–702.

Dorigo, M., Birattari, M. et al. (2007), 'Swarm intelligence.', *Scholarpedia* **2**(9), 1462.

Dorigo, M., Floreano, D., Gambardella, L. M., Mondada, F., Nolfi, S., Baaboura, T., Birattari, M., Bonani, M., Brambilla, M., Brutschy, A. et al. (2013), 'Swarmanoid: a novel concept for the study of heterogeneous robotic swarms', *IEEE Robotics & Automation Magazine* **20**(4), 60–71.

Dorigo, M., Theraulaz, G. & Trianni, V. (2021), 'Swarm robotics: Past, present, and future', *Proceedings of the IEEE* **109**(7), 1152–1165.

Dorigo, M., Trianni, V., Şahin, E., Groß, R., Labella, T., Baldassarre, G., Nolfi, S., Deneubourg, J., Mondada, F., Floreano, D. et al. (2004), 'Evolving self-organizing behaviors for a swarm-bot', *Autonomous Robots* **17**(2), 223–245.

Ducatelle, F., Di Caro, G. A., Pinciroli, C., Mondada, F. & Gambardella, L. (2011), Communication assisted navigation in robotic swarms: self-organization and cooperation, *in* '2011 IEEE/RSJ International Conference on Intelligent Robots and Systems', IEEE, pp. 4981–4988.

Eeckhout, M., Deneubourg, J., Nicolis, S. et al. (2021), 'Consensus driven by a minority in heterogenous groups of the cockroach periplaneta americana', *Iscience* **24**(7).

Engelen, S., Gill, E. K. & Verhoeven, C. J. (2011), Systems engineering challenges for satellite swarms, *in* '2011 Aerospace Conference', IEEE, pp. 1–8.

Feder, T. (2007), 'Statistical physics is for the birds', *Physics today* **60**(10), 28.

Ferrante, E., Brambilla, M., Birattari, M. & Dorigo, M. (2013), Socially-mediated negotiation for obstacle avoidance in collective transport, *in* 'Distributed autonomous robotic systems', Springer, pp. 571–583.

Ferrante, E., Duéñez-Guzmán, E., Turgut, A. E. & Wenseleers, T. (2013), Geswarm: Grammatical evolution for the automatic synthesis of collective behaviors in swarm robotics, *in* 'Proceedings of the 15th annual conference on Genetic and evolutionary computation', pp. 17–24.

Ferrante, E., Turgut, A. E., Huepe, C., Stranieri, A., Pinciroli, C. & Dorigo, M. (2012), 'Self-organized flocking with a mobile robot swarm: a novel motion control method', *Adaptive Behavior* **20**(6), 460–477.

Ferrante, E., Turgut, A. E., Mathews, N., Birattari, M. & Dorigo, M. (2010), Flocking in stationary and non-stationary environments: A novel communication strategy for heading alignment, *in* 'International conference on parallel problem solving from nature', Springer, pp. 331–340.

Ferrante, E., Turgut, A., Stranieri, A., Pinciroli, C., Birattari, M. & Dorigo, M. (2014), 'A self-adaptive communication strategy for flocking in stationary and non-stationary environments', *Natural Computing* **13**(2), 225–245.

Fetecau, R. C. & Meskas, J. (2013), 'A nonlocal kinetic model for predator–prey interactions', *Swarm Intelligence* **7**(4), 279–305.

Firat, Z., Ferrante, E., Cambier, N. & Tuci, E. (2018), Self-organised aggregation in swarms of robots with informed robots, *in* 'International Conference on Theory and Practice of Natural Computing', Springer, pp. 49–60.

Firat, Z., Ferrante, E., Gillet, Y. & Tuci, E. (2020), 'On self-organised aggregation dynamics in swarms of robots with informed robots', *Neural Computing and Applications* pp. 1–17.
URL: *https://doi.org/10.1007/s00521-020-04791-0*

Firat, Z., Ferrante, E., Zakir, R., Prasetyo, J. & Tuci, E. (2020), Group-size regulation in self-organized aggregation in robot swarms, *in* 'International Conference on Swarm Intelligence', Springer, pp. 315–323.

Francesca, G., Brambilla, M., Brutschy, A., Trianni, V. & Birattari, M. (2014), 'Automode: A novel approach to the automatic design of control software for robot swarms', *Swarm Intelligence* **8**(2), 89–112.

Francesca, G., Brambilla, M., Trianni, V., Dorigo, M. & Birattari, M. (2012), Analysing an evolved robotic behaviour using a biological model of collegial decision making, *in* 'International Conference on Simulation of Adaptive Behavior', Springer, pp. 381–390.

Garnier, S., Gautrais, J., Asadpour, M., Jost, C. & Theraulaz, G. (2009*a*), 'Self-organized aggregation triggers collective decision making in a group of cockroach-like robots', *Adaptive Behavior* **17**(2), 109–133.

Garnier, S., Gautrais, J., Asadpour, M., Jost, C. & Theraulaz, G. (2009*b*), 'Self-organized aggregation triggers collective decision making in a group of cockroach-like robots', *Adaptive Behavior* **17**(2), 109–133.

Garnier, S., Gautrais, J., Asadpour, M., Jost, C. & Theraulaz, G. (2009*c*), 'Self-organized aggregation triggers collective decision making in a group of cockroach-like robots', *Adaptive Behavior* **17**(2), 109–133.

Garnier, S., Jost, C., Gautrais, J., Asadpour, M., Caprari, G., Jeanson, R., Grimal, A. & Theraulaz, G. (2008*a*), 'The embodiment of cockroach aggregation behavior in a group of micro-robots', *Artificial life* **14**(4), 387–408.

Garnier, S., Jost, C., Gautrais, J., Asadpour, M., Caprari, G., Jeanson, R., Grimal, A. & Theraulaz, G. (2008*b*), 'The embodiment of cockroach aggregation behavior in a group of micro-robots', *Artificial life* **14**(4), 387–408.

Garnier, S., Jost, C., Jeanson, R., Gautrais, J., Asadpour, M., Caprari, G. & Theraulaz, G. (2005), Aggregation behaviour as a source of collective decision in a group of cockroach-like-robots, *in* 'European Conference on Artificial Life', Springer, pp. 169–178.

Gauci, M., Chen, J., Dodd, T. J. & Groß, R. (2014), Evolving aggregation behaviors in multi-robot systems with binary sensors, *in* 'Distributed autonomous robotic systems', Springer, pp. 355–367.

Gauci, M., Chen, J., Li, W., Dodd, T. & Groß, R. (2014), 'Self-organized aggregation without computation', *The International Journal of Robotics Research* **33**(8), 1145–1161.

Gazi, V. & Passino, K. M. (2005), 'Stability of a one-dimensional discrete-time asynchronous swarm', *IEEE Transactions on Systems, Man, and Cybernetics, Part B (Cybernetics)* **35**(4), 834–841.

Gillet, Y., Ferrante, E., Firat, Z. & Tuci, E. (2019), Guiding aggregation dynamics in a swarm of agents via informed individuals: an analytical study, *in* 'The 2018 Conference on Artificial Life: A Hybrid of the European Conference on Artificial Life (ECAL) and the International Conference on the Synthesis and Simulation of Living Systems (ALIFE)', MIT Press, pp. 590–597.

Goldberg, D. E. & Holland, J. H. (1988), 'Genetic algorithms and machine learning'.

Gomes, J., Urbano, P. & Christensen, A. L. (2013), 'Evolution of swarm robotics systems with novelty search', *Swarm Intelligence* **7**(2), 115–144.

Goss, S., Aron, S., Deneubourg, J.-L. & Pasteels, J. M. (1989), 'Self-organized shortcuts in the argentine ant', *Naturwissenschaften* **76**(12), 579–581.

Groß, R. & Dorigo, M. (2008), 'Self-assembly at the macroscopic scale', *Proceedings of the IEEE* **96**(9), 1490–1508.

Gross, R. & Dorigo, M. (2009), 'Towards group transport by swarms of robots', *International Journal of Bio-Inspired Computation* **1**(1-2), 1–13.

Halloy, J., Sempo, G., Caprari, G., Rivault, C., Asadpour, M., Tâche, F., Saïd, I., Durier, V., Canonge, S., Amé, J. M. et al. (2007), 'Social integration of robots into groups of cockroaches to control self-organized choices', *Science* **318**(5853), 1155–1158.

Hamann, H. (2018), *Swarm robotics: A formal approach*, Vol. 221, Springer.

Hamann, H. & Wörn, H. (2008), 'A framework of space–time continuous models for algorithm design in swarm robotics', *Swarm Intelligence* **2**(2), 209–239.

Hamann, H., Worn, H., Crailsheim, K. & Schmickl, T. (2008), Spatial macroscopic models of a bio-inspired robotic swarm algorithm, *in* '2008 IEEE/RSJ International Conference on Intelligent Robots and Systems', IEEE, pp. 1415–1420.

Hasselmann, K., Robert, F. & Birattari, M. (2018), Automatic design of communication-based behaviors for robot swarms, *in* 'International Conference on Swarm Intelligence', Springer, pp. 16–29.

Hauert, S., Winkler, L., Zufferey, J. & Floreano, D. (2008), 'Ant-based swarming with positionless micro air vehicles for communication relay', *Swarm Intelligence* **20**(2–4), 167–188.

Holland, J. H. et al. (1992), *Adaptation in natural and artificial systems: an introductory analysis with applications to biology, control, and artificial intelligence*, MIT press.

Howard, A., Matarić, M. J. & Sukhatme, G. S. (2002), Mobile sensor network deployment using potential fields: A distributed, scalable solution to the area coverage problem, *in* 'Distributed Autonomous Robotic Systems 5', Springer, pp. 299–308.

Hsieh, M. A., Halász, Á., Berman, S. & Kumar, V. (2008), 'Biologically inspired redistribution of a swarm of robots among multiple sites', *Swarm Intelligence* **2**(2), 121–141.

Hüttenrauch, M., Šošić, A. & Neumann, G. (2017), 'Guided deep reinforcement learning for swarm systems', *arXiv preprint arXiv:1709.06011* .

Jeanson, R., Rivault, C., Deneubourg, J., Blanco, S., Fournier, R., Jost, C. & Theraulaz, G. (2005*a*), 'Self-organized aggregation in cockroaches', *Animal Behaviour* **69**(1), 169–180.

Jeanson, R., Rivault, C., Deneubourg, J.-L., Blanco, S., Fournier, R., Jost, C. & Theraulaz, G. (2005*b*), 'Self-organized aggregation in cockroaches', *Animal behaviour* **69**(1), 169–180.

Jeanson, R. & Weidenmüller, A. (2014), 'Interindividual variability in social insects–proximate causes and ultimate consequences', *Biological Reviews* **89**(3), 671–687.

Joordens, M. A. & Jamshidi, M. (2010), 'Consensus control for a system of underwater swarm robots', *IEEE Systems Journal* **4**(1), 65–73.

Kalantar, S. & Zimmer, U. R. (2007), 'Distributed shape control of homogeneous swarms of autonomous underwater vehicles', *Autonomous Robots* **22**(1), 37–53.

Katada, Y. (2018), 'Evolutionary design method of probabilistic finite state machine for swarm robots aggregation', *Artificial Life and Robotics* **23**(4), 600–608.

Kato, S. & Jones, M. (2013), 'An extended family of circular distributions related to wrapped cauchy distributions via brownian motion', *Bernoulli* **19**(1), 154–171.

Kengyel, D., Hamann, H., Zahadat, P., Radspieler, G., Wotawa, F. & Schmickl, T. (2015), Potential of heterogeneity in collective behaviors: A case study on heterogeneous swarms, *in* 'International conference on principles and practice of multi-agent systems', Springer, pp. 201–217.

Khatib, O. (1986), Real-time obstacle avoidance for manipulators and mobile robots, *in* 'Autonomous robot vehicles', Springer, pp. 396–404.

Kolling, A., Walker, P., Chakraborty, N., Sycara, K. & Lewis, M. (2016), 'Human interaction with robot swarms: A survey', *IEEE Transactions on Human-Machine Systems* **46**(1), 9–26.

Krieger, M. J. & Billeter, J.-B. (2000), 'The call of duty: Self-organised task allocation in a population of up to twelve mobile robots', *Robotics and Autonomous Systems* **30**(1-2), 65–84.

Kube, C. R. & Bonabeau, E. (2000), 'Cooperative transport by ants and robots', *Robotics and autonomous systems* **30**(1-2), 85–101.

Labella, T. H., Dorigo, M. & Deneubourg, J.-L. (2006), 'Division of labor in a group of robots inspired by ants' foraging behavior', *ACM Transactions on Autonomous and Adaptive Systems (TAAS)* **1**(1), 4–25.

Langer, J. S. (1980), 'Instabilities and pattern formation in crystal growth', *Reviews of modern physics* **52**(1), 1.

Lerman, K. & Galstyan, A. (2002), 'Mathematical model of foraging in a group of robots: Effect of interference', *Autonomous robots* **13**(2), 127–141.

Li, L., Martinoli, A. & Abu-Mostafa, Y. S. (2004), 'Learning and measuring specialization in collaborative swarm systems', *Adaptive Behavior* **12**(3-4), 199–212.

Ligot, A. & Birattari, M. (2020), 'Simulation-only experiments to mimic the effects of the reality gap in the automatic design of robot swarms', *Swarm Intelligence* **14**(1), 1–24.

Liu, W., Winfield, A. F., Sa, J., Chen, J. & Dou, L. (2007), 'Towards energy optimization: Emergent task allocation in a swarm of foraging robots', *Adaptive behavior* **15**(3), 289–305.

Liu, Y., Passino, K. M. & Polycarpou, M. M. (2003), 'Stability analysis of m-dimensional asynchronous swarms with a fixed communication topology', *IEEE Transactions on automatic control* **48**(1), 76–95.

Magnenat, S., Rétornaz, P., Bonani, M., Longchamp, V. & Mondada, F. (2010), 'Aseba: A modular architecture for event-based control of complex robots', *IEEE/ASME transactions on mechatronics* **16**(2), 321–329.

Martinoli, A. & Easton, K. (2003), Modeling swarm robotic systems, *in* 'Experimental robotics VIII', Springer, pp. 297–306.

Martinoli, A., Easton, K. & Agassounon, W. (2004), 'Modeling swarm robotic systems: A case study in collaborative distributed manipulation', *The International Journal of Robotics Research* **23**(4-5), 415–436.

Masi, G. D., Prasetyo, J., Zakir, R., Mankovskii, N., Ferrante, E. & Tuci, E. (2021), 'Robot swarm democracy: the importance of informed individuals against zealots', *Swarm Intelligence* **15**(4), 315–338.

Maxim, P. M., Spears, W. M. & Spears, D. F. (2009), 'Robotic chain formations', *IFAC Proceedings Volumes* **42**(22), 19–24.

Meinhardt, H. (1982), 'Models of biological pattern formation', *New York* **118**.

Mermoud, G., Brugger, J. & Martinoli, A. (2009), Towards multi-level modeling of self-assembling intelligent micro-systems, *in* 'Proceedings of the 8th International Conference on Autonomous Agents and Multiagent Systems (AAMAS 2009)', Vol. 1, IFAAMAS, pp. 89–93.

Minsky, M. (1967), 'Computation: Finite and infinite machines prentice hall', *Inc., Engelwood Cliffs, NJ* .

Mnih, V., Kavukcuoglu, K., Silver, D., Rusu, A. A., Veness, J., Bellemare, M. G., Graves, A., Riedmiller, M., Fidjeland, A. K., Ostrovski, G. et al. (2015), 'Human-level control through deep reinforcement learning', *nature* **518**(7540), 529–533.

Mogilner, A. & Edelstein-Keshet, L. (1999), 'A non-local model for a swarm', *Journal of mathematical biology* **38**(6), 534–570.

Montes de Oca, M., Ferrante, E., Scheidler, A., Pinciroli, C., Birattari, M. & Dorigo, M. (2011), 'Majority-rule opinion dynamics with differential latency: a mechanism for self-organized collective decision-making', *Swarm Intelligence* **5**(3–4), 305–327.

Nauta, J., Khaluf, Y. & Simoens, P. (2020), 'Hybrid foraging in patchy environments using spatial memory', *Journal of the Royal Society Interface* **17**(166), 20200026.

Nauta, J., Simoens, P. & Khaluf, Y. (2022), 'Group size and resource fractality drive multimodal search strategies: A quantitative analysis on group foraging', *Physica A: Statistical Mechanics and its Applications* **590**, 126702.

Nouyan, S., Campo, A. & Dorigo, M. (2008), 'Path formation in a robot swarm', *Swarm Intelligence* **2**(1), 1–23.

O'Grady, R., Pinciroli, C., Christensen, A. L. & Dorigo, M. (2009), *Supervised group size regulation in a heterogeneous robotic swarm*, IRIDIA, Institut de Recherches Interdisciplinaires et de Développements en ....

Parrish, J. K. & Edelstein-Keshet, L. (1999), 'Complexity, pattern, and evolutionary trade-offs in animal aggregation', *Science* **284**(5411), 99–101.

Parrish, J. K., Viscido, S. V. & Grunbaum, D. (2002), 'Self-organized fish schools: an examination of emergent properties', *The biological bulletin* **202**(3), 296–305.

Payton, D., Daily, M., Estowski, R., Howard, M. & Lee, C. (2001), 'Pheromone robotics', *Autonomous Robots* **11**(3), 319–324.

Pinciroli, C. & Beltrame, G. (2016), Buzz: An extensible programming language for heterogeneous swarm robotics, *in* '2016 IEEE/RSJ International Conference on Intelligent Robots and Systems (IROS)', IEEE, pp. 3794–3800.

Pinciroli, C., O'GRADY, R., Christensen, A. L., Birattari, M. & Dorigo, M. (2013), 'Parallel formation of differently sized groups in a robotic swarm', *Journal of the Society of Instrument and Control Engineers* **52**(3), 213–226.

Pinciroli, C., Trianni, V., O'Grady, R., Pini, G., Brutschy, A., Brambilla, M., Mathews, N., Ferrante, E., Di Caro, G., Ducatelle, F., Birattari, M., Gambardella, L. & Dorigo, M. (2012), 'ARGoS: a modular, parallel, multi-engine simulator for multi-robot systems', *Swarm Intelligence* **6**(4), 271–295.

Pini, G., Brutschy, A., Birattari, M. & Dorigo, M. (2009), Interference reduction through task partitioning in a robotic swarm, *in* 'Sixth International Conference on Informatics in Control, Automation and Robotics–ICINCO', pp. 52–59.

Pini, G., Brutschy, A., Frison, M., Roli, A., Dorigo, M. & Birattari, M. (2011), 'Task partitioning in swarms of robots: an adaptive method for strategy selection', *Swarm Intelligence* **5**(3–4), 283–304.

Pitonakova, L., Giuliani, M., Pipe, A. & Winfield, A. (2018), Feature and performance comparison of the v-rep, gazebo and argos robot simulators, *in* 'Annual Conference Towards Autonomous Robotic Systems', Springer, pp. 357–368.

Prasetyo, J., De Masi, G. & Ferrante, E. (2019), 'Collective decision making in dynamic environments', *Swarm intelligence* **13**(3), 217–243.

Prasetyo, J., De Masi, G., Zakir, R., Alkilabi, M., Tuci, E. & Ferrante, E. (2021), A bio-inspired spatial defence strategy for collective decision making in self-organized swarms, *in* 'Proceedings of the Genetic and Evolutionary Computation Conference', pp. 49–56.

Priolo, A. (2013), 'Swarming algorithms for multi-robot systems'.

Quinn, M., Smith, L., Mayley, G. & Husbands, P. (2003), 'Evolving controllers for a homogeneous system of physical robots: Structured cooperation with minimal sensors', *Philosophical Transactions of the Royal Society of London. Series A: Mathematical, Physical and Engineering Sciences* **361**(1811), 2321–2343.

Reif, J. H. & Wang, H. (1999), 'Social potential fields: A distributed behavioral control for autonomous robots', *Robotics and Autonomous Systems* **27**(3), 171–194.

Reina, A., Cope, A. J., Nikolaidis, E., Marshall, J. A. & Sabo, C. (2017), 'Ark: Augmented reality for kilobots', *IEEE Robotics and Automation letters* **2**(3), 1755–1761.

Reynolds, C. W. (1987), Flocks, herds and schools: A distributed behavioral model, *in* 'Proceedings of the 14th annual conference on Computer graphics and interactive techniques', pp. 25–34.

Rubenstein, M., Ahler, C., Hoff, N., Cabrera, A. & Nagpal, R. (2014), 'Kilobot: A low cost robot with scalable operations designed for collective behaviors', *Robotics and Autonomous Systems* **62**(7), 966–975.
URL: *http://dx.doi.org/10.1016/j.robot.2013.08.006*

Rubenstein, M., Ahler, C. & Nagpal, R. (2012), Kilobot: A low cost scalable robot system for collective behaviors, *in* '2012 IEEE International Conference on Robotics and Automation', IEEE, pp. 3293–3298.

Şahin, E. (2004), Swarm robotics: From sources of inspiration to domains of application, *in* 'International workshop on swarm robotics', Springer, pp. 10–20.

Sahin, E., Girgin, S., Bayindir, L. & Turgut, A. (2008), 'Swarm intelligence: Introduction and applications', *Natural Computing Series, Springer Verlag, Berlin, Germany, chapter Swarm Robotics* .

Saska, M., Vonásek, V., Chudoba, J., Thomas, J., Loianno, G. & Kumar, V. (2016), 'Swarm distribution and deployment for cooperative surveillance by micro-aerial vehicles', *Journal of Intelligent & Robotic Systems* **84**(1), 469–492.

Schmickl, T., Möslinger, C. & Crailsheim, K. (2006), Collective perception in a robot swarm, *in* 'International Workshop on Swarm Robotics', Springer, pp. 144–157.

Schranz, M. et al. (n.d.), 'April 2020. swarm robotic behaviors and current applications', *Frontiers in Robotics and AI* **7**.

Seeley, T. D. (1982), 'Adaptive significance of the age polyethism schedule in honeybee colonies', *Behavioral ecology and sociobiology* **11**(4), 287–293.

Seeley, T. D. (2010), *Honeybee democracy*, Princeton University Press.

Silva, F., Urbano, P., Correia, L. & Christensen, A. L. (2015), 'odneat: An algorithm for decentralised online evolution of robotic controllers', *Evolutionary Computation* **23**(3), 421–449.

Sion, A., Reina, A., Birattari, M. & Tuci, E. (2022*a*), 'Controlling robot swarm aggregation through a minority of informed robots', *arXiv preprint arXiv:2205.03192* .

Sion, A., Reina, A., Birattari, M. & Tuci, E. (2022*b*), Impact of the update time on the aggregation of robotic swarms through informed robots, *in* 'SAB 2022: 16th International Conference on the Simulation of Adaptive Behavior'.

Slavkov, I., Carrillo-Zapata, D., Carranza, N., Diego, X., Jansson, F., Kaandorp, J., Hauert, S. & Sharpe, J. (2018), 'Morphogenesis in robot swarms', *Science Robotics* **3**(25).

Soysal, O., Bahçeci, E. & Şahin, E. (2007), 'Aggregation in swarm robotic systems: evolution and probabilistic control', *Turkish Journal of Electrical Engineering and Computer Sciences* **15**(2), 199–225.

Soysal, O. & Sahin, E. (2005), Probabilistic aggregation strategies in swarm robotic systems, *in* 'Proceedings 2005 IEEE Swarm Intelligence Symposium, 2005. SIS 2005.', IEEE, pp. 325–332.

Soysal, O. & Şahin, E. (2006), A macroscopic model for self-organized aggregation in swarm robotic systems, *in* 'International Workshop on Swarm Robotics', Springer, pp. 27–42.

Spears, W. M., Spears, D. F., Hamann, J. C. & Heil, R. (2004), 'Distributed, physics-based control of swarms of vehicles', *Autonomous robots* **17**(2), 137–162.

Sperati, V., Trianni, V. & Nolfi, S. (2011*a*), 'Self-organised path formation in a swarm of robots', *Swarm Intelligence* **5**(2), 97–119.

Sperati, V., Trianni, V. & Nolfi, S. (2011*b*), 'Self-organised path formation in a swarm of robots', *Swarm Intelligence* **5**(2), 97–119.

Stirling, T. & Floreano, D. (2010), Energy efficient swarm deployment for search in unknown environments, *in* 'International Conference on Swarm Intelligence', Springer, pp. 562–563.

Stroeymeyt, N., Franks, N. R. & Giurfa, M. (2011), 'Knowledgeable individuals lead collective decisions in ants', *Journal of Experimental Biology* **214**(18), 3046–3054.

Szopek, M., Schmickl, T., Thenius, R., Radspieler, G. & Crailsheim, K. (2013), 'Dynamics of collective decision making of honeybees in complex temperature fields', *PloS one* **8**(10), e76250.

Theraulaz, G., Bonabeau, E. & Denuebourg, J. (1998), 'Response threshold reinforcements and division of labour in insect societies', *Proceedings of the Royal Society of London. Series B: Biological Sciences* **265**(1393), 327–332.

Trianni, V., Groß, R., Labella, T., Şahin, E. & Dorigo, M. (2003), Evolving aggregation behaviors in a swarm of robots, *in* 'European Conference on Artificial Life', Springer, pp. 865–874.

Trianni, V. & Nolfi, S. (2011), 'Engineering the evolution of self-organizing behaviors in swarm robotics: A case study', *Artificial life* **17**(3), 183–202.

Tuci, E., Alkilabi, M. & Akanyety, O. (2018), 'Cooperative object transport in multi-robot systems: A review of the state-of-the-art', *Frontiers in Robotics and AI* **5**, 1–15.

Tuci, E. & Rabérin, A. (2015), 'On the design of generalist strategies for swarms of simulated robots engaged in a task-allocation scenario', *Swarm Intelligence* **9**(4), 267–290.

Uvarov, B. P. (1966), *Grasshoppers and Locusts: Behaviour, ecology, biogeography, population dynamics*, Vol. 2, Anti-Locust Research Centre.

Valentini, G., Antoun, A., Trabattoni, M., Wiandt, B., Tamura, Y., Hocquard, E., Trianni, V. & Dorigo, M. (2018), 'Kilogrid: a novel experimental environment for the kilobot robot', *Swarm Intelligence* **12**(3), 245–266.

Valentini, G., Ferrante, E. & Dorigo, M. (2017), 'The best-of-n problem in robot swarms: Formalization, state of the art, and novel perspectives', *Frontiers in Robotics and AI* **4**, 9.
URL: *https://www.frontiersin.org/article/10.3389/frobt.2017.00009*

Valentini, G., Ferrante, E., Hamann, H. & Dorigo, M. (2016*a*), 'Collective decision with 100 Kilobots: Speed versus accuracy in binary discrimination problems', *Autonomous Agents and Multi-Agent Systems* **30**(3), 553–580.

Valentini, G., Ferrante, E., Hamann, H. & Dorigo, M. (2016*b*), 'Collective decision with 100 kilobots: Speed versus accuracy in binary discrimination problems', *Autonomous Agents and Multi-Agent Systems* **30**(3), 553–580.

Van Havermaet, S., Simoens, P. & Khaluf, Y. (2022), An adaptive metric model for collective motion structures in dynamic environments, *in* 'Swarm Intelligence: 13th International Conference, ANTS 2022, Málaga, Spain, November 2–4, 2022, Proceedings', Springer, pp. 257–265.

Verhoeven, C. J., Bentum, M. J., Monna, G., Rotteveel, J. & Guo, J. (2011), 'On the origin of satellite swarms', *Acta Astronautica* **68**(7-8), 1392–1395.

Wang, H. & Rubenstein, M. (2020), 'Shape formation in homogeneous swarms using local task swapping', *IEEE Transactions on Robotics* **36**(3), 597–612.

Wang, H. & Rubenstein, M. (2021), 'Decentralized localization in homogeneous swarms considering real-world non-idealities', *IEEE Robotics and Automation Letters* **6**(4), 6765–6772.

Wolpert, D. H. & Tumer, K. (1999), 'An introduction to collective intelligence', *arXiv preprint cs/9908014* .

Yadav, S. L. & Sohal, A. (2017), 'Comparative study of different selection techniques in genetic algorithm', *International Journal of Engineering, Science and Mathematics* **6**(3).